# DAVID W. TAYLOR NAVAL SHIP RESEARCH AND DEVELOPMENT CENTER

Bethesda, Maryland 20084

## THE FRICTION AND WEAR OF COPPER IN HIGH-LOAD, LOW-SPEED, SMALL-AMPLITUDE RECIPROCATING SLIDING

by
Sidney A. Karpe

APPROVED FOR PUBLIC RELEASE; DISTRIBUTION UNLIMITED.

SHIP MATERIALS ENGINEERING DEPARTMENT
RESEARCH AND DEVELOPMENT REPORT



August 1982

DTNSRDC-82/048

## MAJOR DTNSRDC ORGANIZATIONAL COMPONENTS

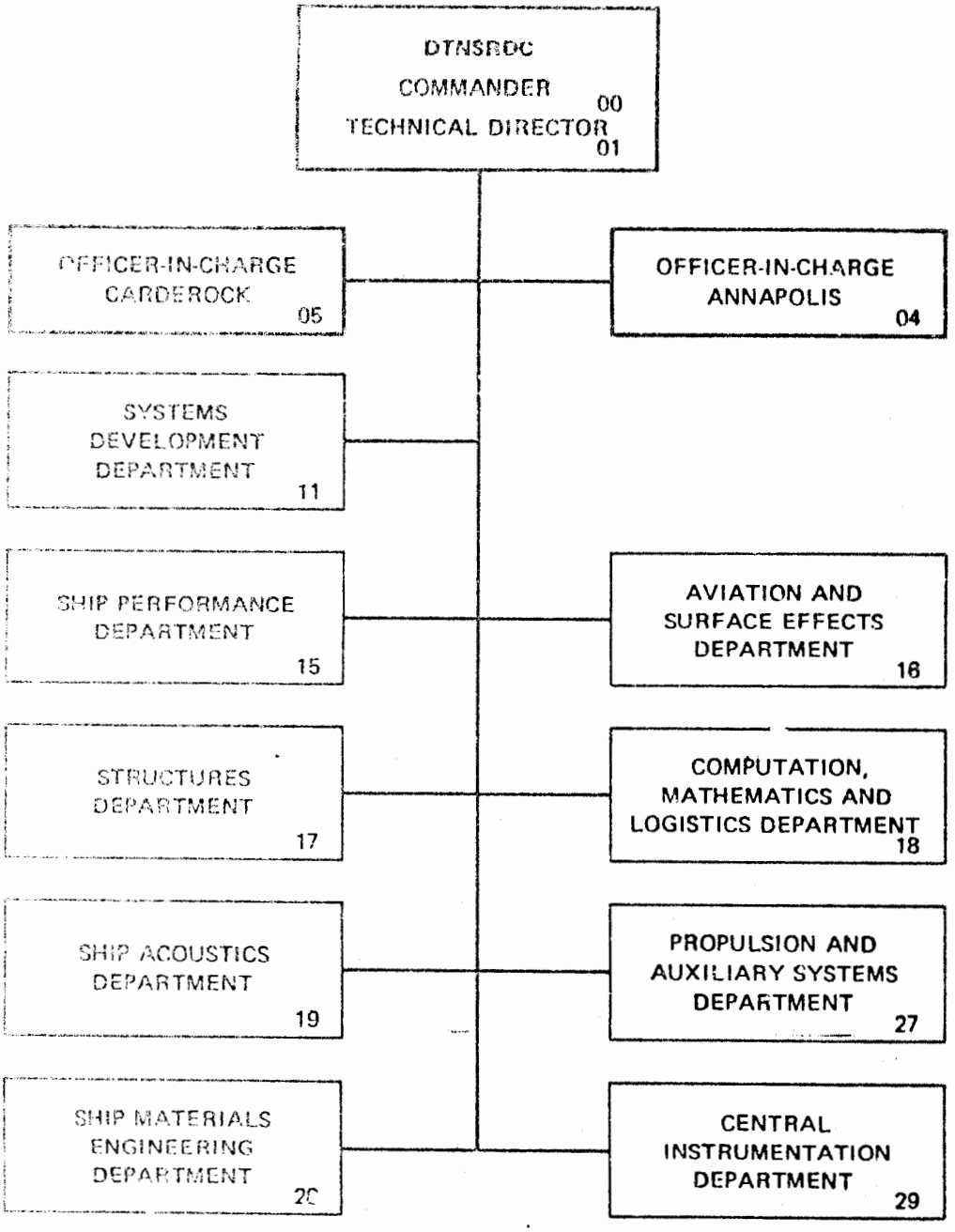

UNCLASSIFIED

SECURITY CLASSIFICATION OF THIS PAGE (When Data Entered)

## REPORT DOCUMENTATION PAGE

READ INSTRUCTIONS BEFORE COMPLETING FORM

| | |
|---|---|
| 1. REPORT NUMBER: DTNSRDC-82/048 | 2. GOVT ACCESSION NO.: AD-A119499 |
| 3. RECIPIENT'S CATALOG NUMBER: | |
| 4. TITLE (and Subtitle): THE FRICTION AND WEAR OF COPPER IN HIGH-LOAD, LOW-SPEED, SMALL-AMPLITUDE RECIPROCATING SLIDING | 5. TYPE OF REPORT & PERIOD COVERED: Research and Development Rept, Oct 1980 to Jun 1982 |
| | 6. PERFORMING ORG. REPORT NUMBER: |
| 7. AUTHOR(s): Sidney A. Karpe | 8. CONTRACT OR GRANT NUMBER(s): |
| 9. PERFORMING ORGANIZATION NAME AND ADDRESS: David Taylor Naval Ship R&D Center, Bethesda, MD 20084 | 10. PROGRAM ELEMENT, PROJECT, TASK AREA & WORK UNIT NUMBERS: Program Element 61152N, Task Area ZR 022-08-01, Work Units 2832-156 and 157 |
| 11. CONTROLLING OFFICE NAME AND ADDRESS: David Taylor Naval Ship R&D Center (Code 2832), Annapolis, MD 21402 | 12. REPORT DATE: August 1982 |
| | 13. NUMBER OF PAGES: 96 |
| 14. MONITORING AGENCY NAME & ADDRESS(if different from Controlling Office) | 15. SECURITY CLASS. (of this report): UNCLASSIFIED |
| | 15a. DECLASSIFICATION/DOWNGRADING SCHEDULE: |

16. DISTRIBUTION STATEMENT (of this Report)

APPROVED FOR PUBLIC RELEASE; DISTRIBUTION UNLIMITED.

17. DISTRIBUTION STATEMENT (of the abstract entered in Block 20, if different from Report)

18. SUPPLEMENTARY NOTES

19. KEY WORDS (Continue on reverse side if necessary and identify by block number)

| | | |
|---|---|---|
| Copper | Morphology | Reciprocating Sliding |
| Friction | Wear Severity Index | Subsurface Deformation |
| Wear | High-Load | Voids |
| Topography | Low-Speed | Microcracks |

20. ABSTRACT (Continue on reverse side if necessary and identify by block number)

There is a critical need that the mechanisms of wear in marine components sliding under marginally-lubricated conditions be elucidated. These conditions were simulated in a tribotester that was operated under conditions of high nominal pressure, low speed, and small-amplitude reciprocating sliding. High purity (99.9%) copper was selected as the rubbing member because of its

(continued on reverse side)

DD FORM 1 JAN 73 1473 EDITION OF 1 NOV 65 IS OBSOLETE S/N 0102-014-6601

UNCLASSIFIED

SECURITY CLASSIFICATION OF THIS PAGE (When Data Entered)

(Block 20 continued)

relatively simple microstructure and its widespread use as a base metal in many bearing alloys. The friction and wear of this metal, rubbing against various counterfaces in "inert" mineral oil, were determined. Topographical changes and subsurface deformation structures produced by sliding were determined.

The investigation produced information on the following: (1) The influence of topographical changes on the coefficient of friction (or frictional force); (2) The dependence of the depth of deformation on the coefficient of friction; (3) The mechanism of wear particle formation; and (4) The relationship between wear and the coefficient of friction. The results also suggested that the topographical changes produced by sliding may be more important than the properties of the material itself in determining wear resistance.

TABLE OF CONTENTS

LIST OF FIGURES

Page

## LIST OF ABBREVIATIONS

| | |
|---|---|
| BEI | Backscattering-electron image or backscattering photomicrograph |
| b | Burgers vector for copper |
| c | Number of cycles |
| d | Cell size |
| CPP | Controllable pitch propeller |
| DP 80 | Dual phase low-alloy, high-strength steel |
| DPN | Diamond Pyramid Hardness or Vickers Hardness Number |
| EDX | Energy Dispersive X-Ray Analysis |
| F | Frictional force |
| G | Shear modulus or the modulus of ridigity |
| H | Hardness of the material that is worn |
| (hkl) | Miller indices used to define atomic planes in a crystal |
| HY 100 | High-strength, low-carbon, medium chromium and nickel steel |
| Inconel 718 | Nickel-chromium based alloy |
| k | Wear constant, commonly called Archard wear coefficient |
| n | Wear severity index |
| OECD | Organization for Economic Cooperation and Development |
| OFHC | Oxygen-free high-conductivity copper |
| RA | Arithmetic average of surface roughness |
| s | Sliding distance |
| SEI | Secondary-electron image or secondary electron photomicrograph |
| SEM | Scanning electron microscope |
| V | Volume of wear |
| W | Applied load, axial load, or normal load |
| W-A | Warren-Averbach X-Ray diffraction method |
| $\epsilon$ | Strain |

| | |
|---|---|
| $\delta$ | Depth of heavily deformed region or layer |
| $\delta_m$ | Maximum depth of heavily deformed region or layer |
| $\delta_a$ | Average depth of heavily deformed region or layer |
| $\mu$ | Coefficient of friction |
| $\mu_o$ | Starting coefficient of friction |
| $\bar{\mu}$ | Mean coefficient of friction |
| $\bar{\mu}_4$ | Fourth power mean of the coefficient of friction |
| $\sigma_e$ | Effective stress |

UNITS OF MEASURE

| | |
|---|---|
| $\mathring{A}$ | Angstrom |
| cm | Centimeter |
| cp | Centipoise |
| Hz | Hertz |
| $^oK$ | Degrees Kelvin |
| $kg/mm^2$ | Kilogram force per millimeter square |
| $kg/m^3$ | Kilogram mass per cubic meter |
| m | Meter |
| mg | Milligram |
| mm | Millimeter |
| mm/sec | Millimeter per second |
| MPa | MegaPascal |
| N | Newton |
| $\mu$m | Micrometer |

## ABSTRACT

There is a critical need that the mechanisms of wear in marine components sliding under marginally-lubricated conditions be elucidated. These conditions were simulated in a tribotester that was operated under conditions of high nominal pressure, low speed, and small-amplitude reciprocating sliding. High purity (99.9%) copper was selected as the rubbing member because of its relatively simple microstructure and its widespread use as a base metal in many bearing alloys. The friction and wear of this metal, rubbing against various counterfaces in "inert" mineral oil, were determined. Topographical changes and subsurface deformation structures produced by sliding were determined.

The investigation produced information on the following: (1) The influence of topographical changes on the coefficient of friction (or frictional force); (2) The dependence of the depth of deformation on the coefficient of friction; (3) The mechanism of wear particle formation; and (4) The relationship between wear and the coefficient of friction. The results also suggested that the topographical changes produced by sliding may be more important than the properties of the material itself in determining wear resistance.



## ADMINISTRATIVE INFORMATION

This report covers work conducted under DTNSRDC In-House Independent Research, Program Element 61152N, Task Area ZR022-08-01, Work Units 2832-156 and 2832-157.

## ACKNOWLEDGEMENTS

The author is very much indebted for valuable discussion to many colleagues: Dr. F. E. Kennedy (Dartmouth College), Dr. N. Saka (Massachusetts Institute of Technology), Professor S. Weissmann (Rutgers University), and, particularly, R. G. Brown of DTNSRDC. I also thank Professor E. Rabinowicz (Massachusetts Institute of Technology), who designed the specimen contact configuration, and J. Alberti (formerly of DTNSRDC) for constructing the tribometer. The continuing personal and technical support of Dr. I. Kramer is deeply appreciated. The assistance of V. Surprenant (Dartmouth College) in preparing the metallographic specimens and members of the E.M.V. Associates (Rockville, MD) in obtaining the scanning electron micrographs is gratefully acknowledged.

## INTRODUCTION

Heavily-loaded low-speed sliding wear of metals is a tribological problem that investigators generally avoid. Yet, the payoff from being able of operate machinery in the regime can be large. One such case is the pitch-changing mechanism of controllable pitch propellers (CPP)* used in some of the Navy's ships.

The mechanism of wear in this regime is poorly understood. Wear particle formation, subsurface damage to the softer bearing member, the role of deformation-induced surface microstructural and topographical changes, and the influence of the coefficient of friction on wear and on the depth of heavily deformed regions remain uninvestigated. In some cases, wear problems are solved at great expense, while in others, excessive maintenance is accepted because solutions are not found. Existing technology cannot readily solve problems of friction and wear in the high-load, low-speed sliding regime.

The purpose of this investigation was therefore to investigate in detail the low-speed, high-load sliding behavior of metals, to elucidate the mechanisms of friction and wear, and to recommend methods of mitigating wear.

## BACKGROUND

A disturbing feature of the wear process is that in most practical cases the conditions at and below the sliding interface are extremely complex. Naturally, the tendency is to isolate a specific mechanism and then to overemphasize the role of that mechanism in the wear process. However, apart from the most exceptional circumstances, we do not know in detail what happens between two surfaces while wear is actually occurring.[1]** The best we can do is study wear at various stages and reconstruct a picture of the processes occurring.

### ANALYTICAL TREATMENTS OF WEAR

The simplest relationship between the volume of wear, V, produced in sliding a distance, s, was shown by Archard[2] to be:

$$V = k \frac{Ws}{H} \qquad (1)$$

---

*Abbreviations used are defined on page x.

**References are listed on page 83.

where

k = wear constant,* Archard wear coefficient

W = applied load

H = hardness of the material that is worn

This equation is equivalent to that derived by Holm,[3] and is similar to that deduced empirically by Burwell and Strang.[4]

The value of the wear coefficient used by Archard in the model is the probability that the adhesive (cold-welding) forces will be large enough to tear out a wear particle at a contact. For most material combinations the wear coefficient varies from $10^{-7}$ to $10^{-2}$. There is currently no theory capable of predicting the values of k, although attempts have been made in the past.[6]

Experiments conducted with a wide range of material combinations and operating conditions (loads and speeds) have shown that once steady-state surface conditions are established the wear rate is independent of the apparent area of contact.

Experiments have also determined that, for a wide range of conditions, the wear is proportional to the sliding distance, but exceptions to this rule may be found. Wear is proportional to the load is also in accordance with experimental results if a change in load does not change sliding conditions. Thus, the wear rate has been found to be proportional to the load in mild wear[6] and again in severe wear[7] after the load increase has changed the regime of wear. This rule, again, has many exceptions. Despite these limitations, the Archard relationship generally agrees with experimental evidence--i.e., wear increases with load and sliding distance (time), and is generally reduced by use of harder materials.

Starting around 1960, challenges to Archard's model began to appear. These new models were directly or indirectly based on the concept that what was generally regarded as adhesive wear was a fatigue process. Fatigue weakens materials, subsequently forming wear debris. In this fatigue model, the nondimensional wear coefficient represents approximately the reciprocal of the number of stress cycles required to produce a wear particle.[8]

---

*In severe wear, k may take a value $10^2$ to $10^4$ greater than that found in mild wear. Clearly, a constant of proportionality in a mathematical equation should be constant. To change materials would be to allow the constant to change, but to increase the load or the speed should not change the constant of proportionality, as admitted in the distinction between severe wear and mild wear.

Additional challenges to the adhesive wear model were made in the mid-1970's. These concerned the inability of the model to predict: (a) abrupt changes in wear; (b) formation of shell-, plate- or flake-type wear debris; (c) topography of worn surfaces, which is one of scratches and grooves, (d) failure of some alloys to show a decrease in wear with increasing hardness, and (e) large variations in the friction and wear behavior of metals that have only limited mutual solubility.

## CHANGING CONDITIONS DURING SLIDING

Although all possible external inputs before a test can be diligently controlled, conditions usually change during sliding. Wear by its very nature means change. The diversity of changes in sliding conditions and these changes' relative contributions and possible synergistic interactions under similar (or different) sliding situations are poorly understood.

Changes in conditions that may occur during sliding include:

- entrappment of wear debris;
- increase in roughness of the contacting surfaces;
- formation of transfer films on one or both surfaces;
- chemical or physical modifications such as structural changes, plastic deformation, and crack nucleation and growth;
- removal and formation of contaminant films, such as oxides and sulphides;
- softening and melting produced by frictional heat;
- reversal in the wear mode, whereby wear on one member ceases and wear on the other begins; and
- changes in lubricating conditions.

All of these factors, singly or synergystically, may change the response of the system to the wear process. One manifestation of such changes in sliding conditions is the change in the coefficient of friction ($\mu$). This change is generally large and readily detectable, although other times it is small and undetectable. In a recent paper, Blau[10] provided numerous examples where the coefficients of friction and wear change with time. The shape of the friction vs. sliding distance (i.e. number of cycles, time) curve is useful for identifying the various contributions to the process of wear in a given system. The factors responsible for the change in surface conditions must be clearly identified in describing wear behavior and providing solutions to reduce wear.

## WEAR REGIMES

There are two distinct wear regimes: mild and severe. Mild wear exhibits the following characteristics:

- sliding surfaces become polished;
- there is little subsurface damage;
- wear particles, if any, are round, small, and nonmetallic, such as sulfides or oxides;
- rubbing surfaces are electrically nonconductive (contact resistance is fairly high), where the lubricant film or other insulating nonmetallic films block current flow across the interface;
- little or no transfer of metal occurs between surfaces;
- the coefficient of friction is relatively small--about 0.1 or less, and
- wear is relatively light.

In contrast, severe wear has the following characteristics:

- worn surfaces are rough;
- subsurface damage is considerable;
- wear particles are relatively large, flake-like, and predominantly metallic;
- rubbing surfaces are electrically conducting (contact resistance falls to a low value);
- a large amount of metal is transferred between surfaces and can usually be observed with the unaided eye;
- the coefficient of friction is usually much greater than 0.1; and
- the wear may increase a hundred- or thousandfold over mild wear.

## RELATION OF COEFFICIENT OF FRICTION TO WEAR

In most situations where mild wear occurs, the friction coefficient is of the order of 0.1 or less.[9] In the high-load, low-speed, controllable pitch propeller application discussed in the introduction, wear was severe--visible wear and transfer of metal between surfaces occurred--when the coefficient of friction was greater than 0.12. In general, high wear accompanies high friction coefficients, but otherwise there appears to be little correlation between friction and wear.[11] The use of the coefficient of friction to compare different systems (material and operating inputs) as to their propensity to wear may be misleading, but if restricted to similar systems this comparison may be valid.

## CONTACT LOAD EFFECTS ON WEAR

At light loads, where nominal contact pressures are low, the wear particles generated become detached and may leave the contact interface with relative ease. At higher loads nominal contact pressures increase and the true area of contact approaches the size of the apparent or nominal contact area. A loose particle, once formed, cannot escape without producing more particles, which then increase roughness, friction coefficient, and subsurface damage.

## CURRENT STATE OF KNOWLEDGE

As Tabor[1] says, "There are no 'laws' of wear." On the whole, wear increases with load and with duration of sliding, but even here there are exceptions, and usually hard materials wear less than soft materials. Rowe[12] has remarked that "the general principles for improving service life are the same as they were 3,000 years ago: choose a smooth hard material, lubricate it effectively, and keep out the grit."

# OBJECTIVES AND APPROACH

## OBJECTIVES

Because of the current state of knowledge, the challenges made to the existing tribological models, the complexity of the wear process, and the competing theories of wear, a program was initiated at DTNSRDC to study friction and wear. The objectives of the study reported here were to investigate the following aspects of wear:

- microstructural changes produced by wear,
- subsurface damage produced by wear,
- topographical changes produced by wear,
- the influence of the topographical changes on the coefficient of friction,
- the relationship between the coefficient of friction and wear,
- mechanisms of wear particle formation, and
- the stresses and strains within the substructure of the heavily deformed regions.

## APPROACH

Instead of simply measuring the amount of wear under a series of loads, speeds, temperatures and environments, these experimental variables were fixed. The conditions selected were based on the conditions that exist in a CCP bearing where severe wear is known to occur. In this bearing, wear does not occur during pitch changes; it occurs when pitch is fixed and there is no apparent bearing movement, where small amplitude vibratory motion is produced because of the varying hydrodynamic load on the propeller blades.

However, three departures from the actual situation in the CPP bearing were made: (a) a high-purity copper was selected instead of the multi-phase bearing bronze; (b) an additive-free mineral oil was used instead of an additive-laden lubricating oil; and (c) high-purity copper sliding against itself was also tested.

The friction and wear characteristics of three material combinations have been determined by a tribometer, which can measure the coefficient of friction continuously. Experiments were conducted under a defined set of conditions, load, speed, amplitudes of sliding, contact configuration, environment, and initial contact topography. The weight lost by the materials after a period of sliding was determined. The evaluation conditions were selected so that there was no full fluid film between the rubbing contacts. The surface microstructural changes, subsurface deformation, and apparent topographical changes induced by wear were observed using a scanning electron microscope (SEM). The worn copper surface was also examined by microhardness and X-ray measurements. Each copper bearing specimen was heat-treated before the tests to relieve damage due to machining and to produce a known grain size and hardness.

## DEFINITION OF WEAR

For the purpose of this paper, wear is defined as the weight of material removed from the copper bearing surface by the mechanical interaction of this surface when placed under load against a counterface and set in motion. This definition of wear differs only slightly from the definition given by the Scientific Research Committee of the Organization for Economic Cooperation and Development (OECD): "the progressive loss of substance from the operating surface of a body occurring as a result of relative motion of the surface."[13]

## EXPERIMENTAL MATERIALS, TRIBOMETER, AND PROCEDURES

### BEARING SPECIMENS

#### Material Selection

High-purity copper (99.9% copper) commonly designated as oxygen-free high-conductivity copper (OFHC) was selected for the following reasons: (a) its ready availability; (b) its simple (single-phase) microstructure, which avoids complications associated with materials containing second phase particles; (c) its widespread use in both tribological and mechanical property studies which allows our results to be compared with those of other investigators; (d) its widespread use as a base metal in the formulation of bearing bronzes; (e) its susceptibility to heat treatment and working into such various structures as fully-worked, partially recrystallized, and fully recrystallized or annealed structures; and finally (f) the ease with which it allows the regions of near-surface deformation produced by sliding to be distinguished from the undeformed bulk structure and to be measured.

#### Heat Treatment, Fabrication, and Properties

The copper was received in 2.54-cm-diameter hard temper rod. The Knoop hardness and grain size of the specimens used after annealing for 2 hours at $700^{\circ}K$ are indicated by an arrow in Figure 1. The density of this metal at $293^{\circ}K$ is 8940 $kg/m^3$. The specimens were machined from the rod as received and then annealed in sealed capsules to the desired hardness and grain size. They were then lightly electropolished to remove any residual near-surface deformations that might have been introduced by maching and remained after annealing. The surface of the electropolished bearing is shown in Figure 2.

### COUNTERFACE SPECIMENS

#### Materials

Three types of metals were used as counterface specimens: (a) a low-carbon, medium chromium and nickel steel (HY 100), (b) a nickel-chromium based alloy (Inconel 718) and (c) high-purity copper. These metals hereafter are identified as (a) steel, (b) Inconel, and (c) copper.

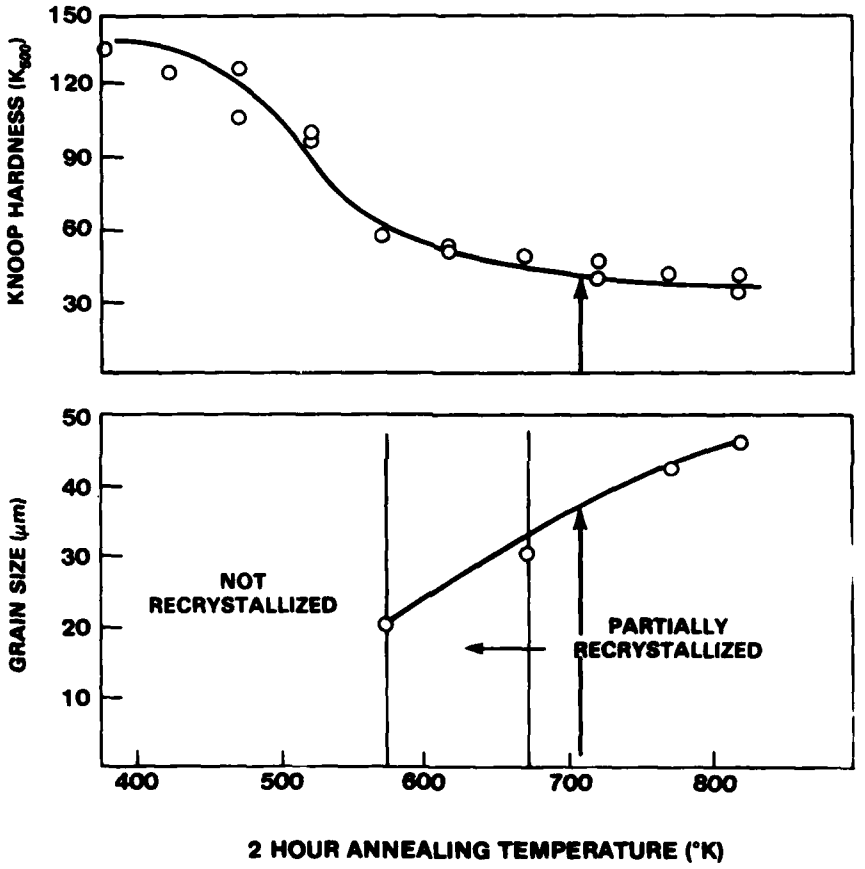


Figure 1 - Hardness, Grain Size (Shown by Arrows) and Annealing Conditions Used for Copper Bearing Specimen

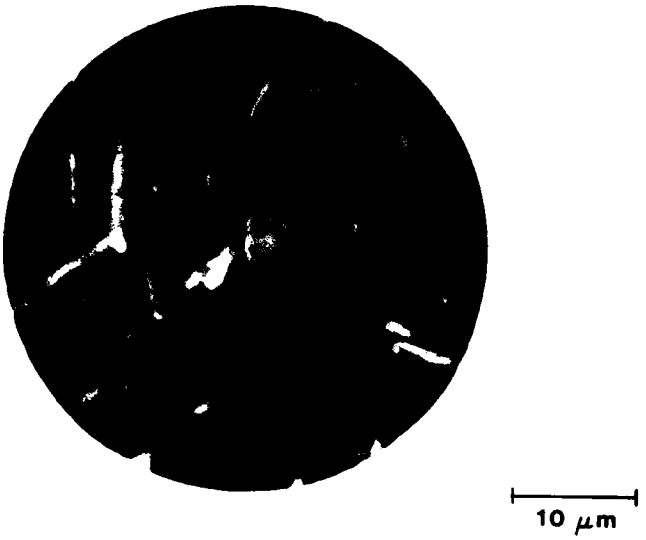


Figure 2 - Electropolished Bearing Surface

The steel and Inconel were selected for study because the steel is currently used in the CPP application and the Inconel had been suggested as a substitute for steel for structural reasons. The copper was selected to obtain a larger coefficient of friction and larger amount of wear than would be obtained by copper sliding against steel or Inconel.

### Fabrication

The steel and Inconel counterface specimens were machined from plate. The steel was used as received, whereas the Inconel was solution-annealed and aged. The copper counterface was fabricated using the same procedures used for the copper bearing specimen.

The bearing surfaces of the steel and Inconel were circumferentially ground to a relatively fine finish of better than 0.2 μm, RA. The surfaces were then lightly lapped to remove loose debris that might have been generated by grinding.

The Diamond Pyramid Hardness (DPN, or Vickers hardness) using a 29-N identation load was 2900 ± 300 MPa for the steel and 4100 ± 200 MPa for the Inconel. The copper counterface had the same hardness as the copper bearing specimen.

## SPECIMEN SHAPE AND DIMENSIONS

The copper bearing specimen had three projecting rectangular bearing surfaces (tips), each 1.02 by 0.76 mm. The sides of the projections sloped at an angle of 45 degrees. The projections were centered on a 19-mm-diameter circle and were spaced 120 degrees apart. They were about 0.76 mm high. The length, diameter, and tip dimensions of the bearing specimen are shown in Figure 3. Specimens were designed so that both sides could be used for separate evaluation of friction and wear.

The counterface was cylindrical with top and bottom surfaces ground flat and perpendicular to the cylindrical axis (see Figure 4).

## MINERAL OIL ENVIRONMENT

The contact interface between the bearing and counterface specimens was covered with a pharmaceutical-grade heavy napthenic oil, which will be called mineral oil. The mineral oil was filtered through a diatomaceous earth and silica gel filled column to remove active additives, such as an antioxidant known to be present.

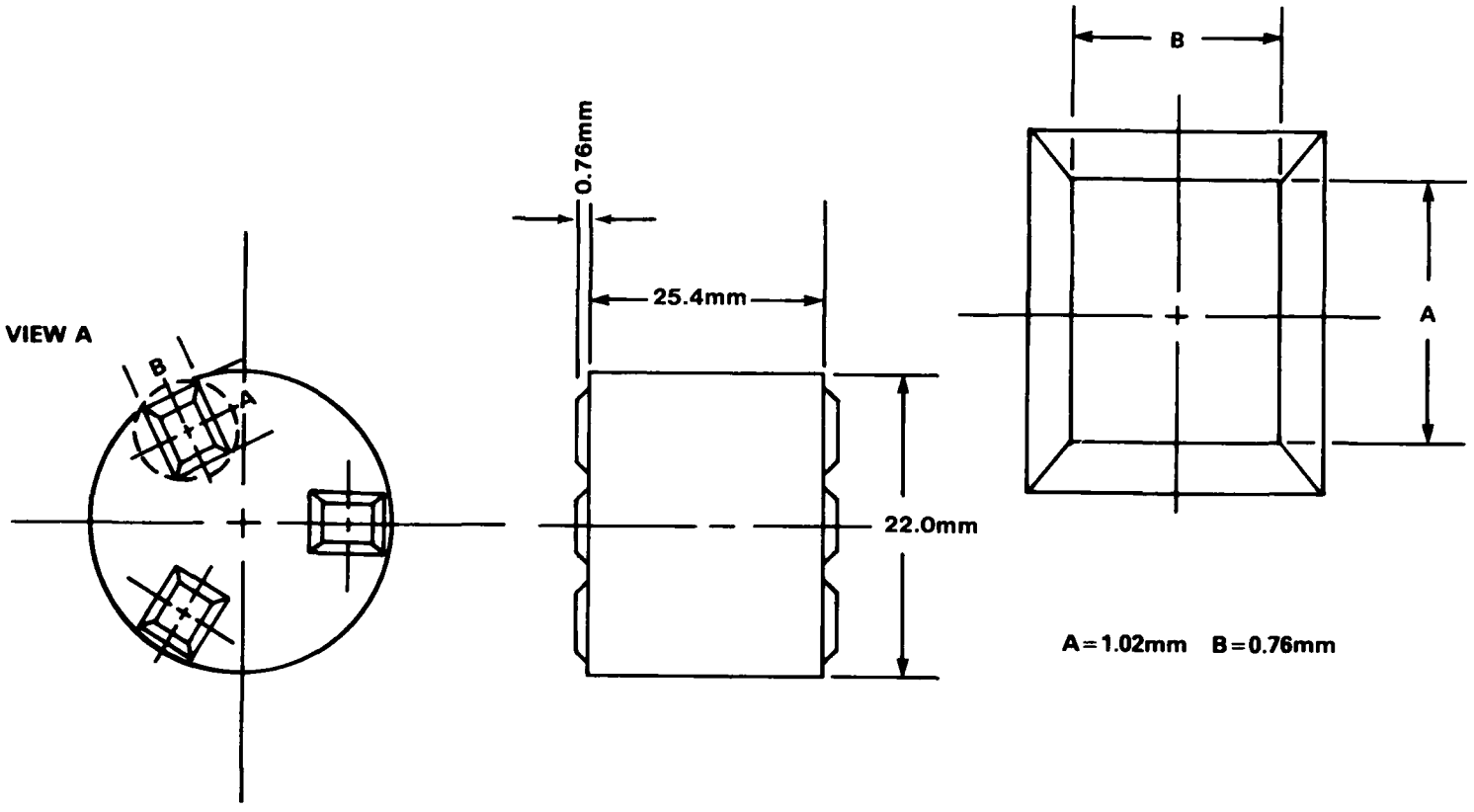


Figure 3 - Bearing Specimen

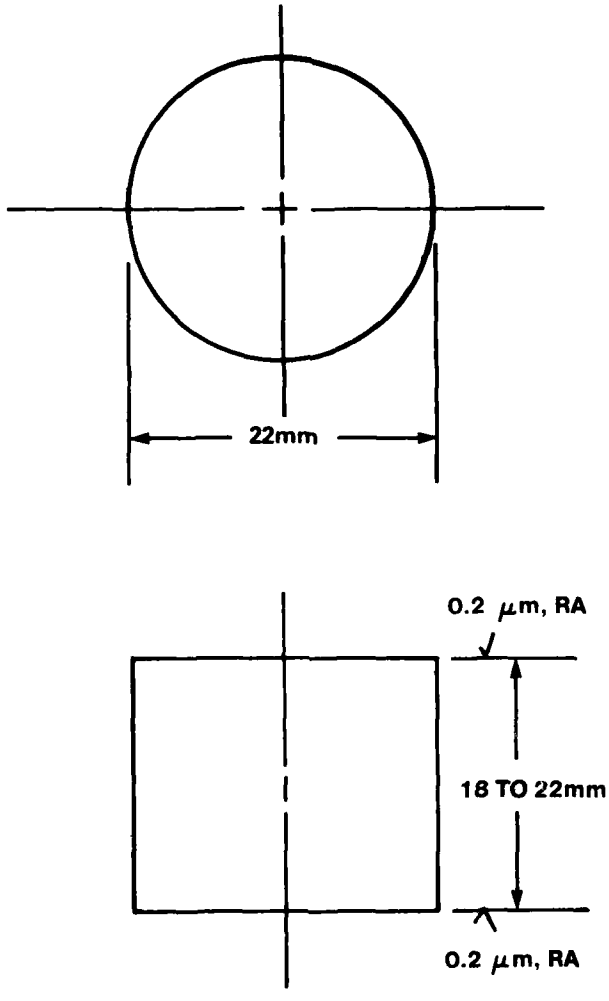


Figure 4 - Counterface Specimen

The oil typically has an absolute viscosity of 50 centipoise (cp) at 310°K and 8.5 cp at 372°K. The density at 298°K is 886.3 kg/m$^3$. The viscosity characteristics of the oil resemble a Navy Symbol 2135-grade lubricant.

The mineral oil was used for two reasons: to recreate an environment similar to that present in practice; and to reduce reactions between the highly active metal surfaces, wear particles, and transfer metal with gaseous species in the ambient air, such as oxygen and water vapor. I also recognized that the mineral oil may contain a small concentration of oxygen and also a trace of water that might play an active role in the wear process. In mild wear or boundary lubricated situations, this factor might well be important,[14] whereas in the severe regime its role is probably insignificant.

## HIGH-LOAD, LOW-SPEED, RECIPROCATING SLIDING TRIBOMETER

The tribometer is shown Figure 5. It was designated to evaluate the friction and wear of two specimens (the copper bearing and flat-faced counterface specimens) mounted end-to-end and aligned axially. One of the two test specimens is rigidly mounted to a load cell and the other to a fixture mounted on a precision spindle. A torque arm is mechanically fixed to the spindle. Cyclic motion is imparted to the spindle, via the torque arm, by an air motor with an adjustable center cam. A load cell positioned between the torque arm and the cam center measures the frictional torque, which can be converted to a frictional force (F) by dividing the torque value by the mean radius of frictional contact. A constant axial load (W) is applied to the specimens by an air cylinder. The signals from both the axial load cell and the torque arm load cell are continuously monitored by a two-channel Sanborn 321 recorder.* A typical strip-chart record showing the normal force and the cyclical frictional force produced by sliding is shown in Figure 6. The coefficient of friction ($\mu$) is obtained by dividing the normal load (W) into the friction force (F). The axial load cell is calibrated by a compression gage and the torque load cell by dead weight loading. Signals from microswitches

*Certain trade names and company products are identified in order to adequately specify our experimental procedure. In no case does such identification imply recommendation or endorsement by the Department of the Navy or the Naval service at large, nor does it imply that the products are necessarily the best available for the purpose.

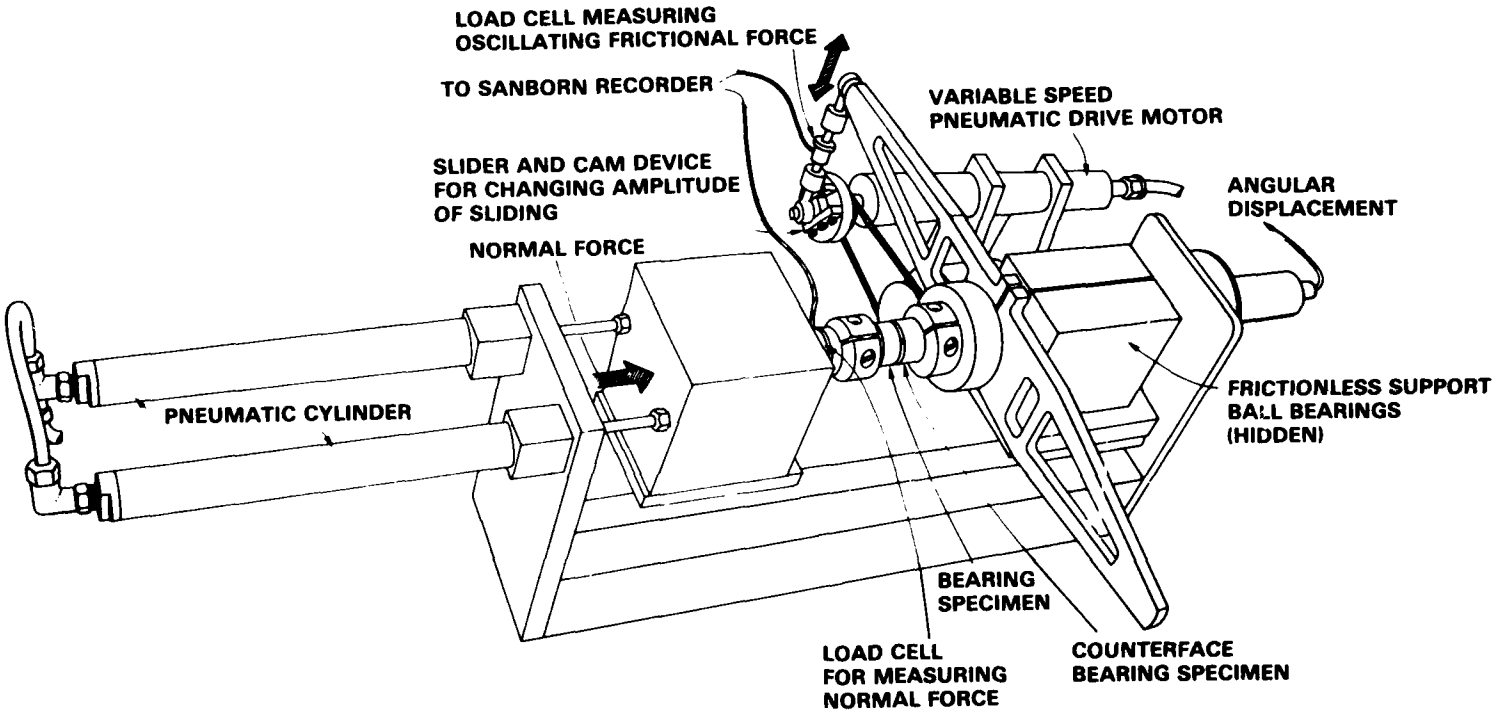


Figure 5 - High-Load, Low-Speed Reciprocating Sliding Tribometer

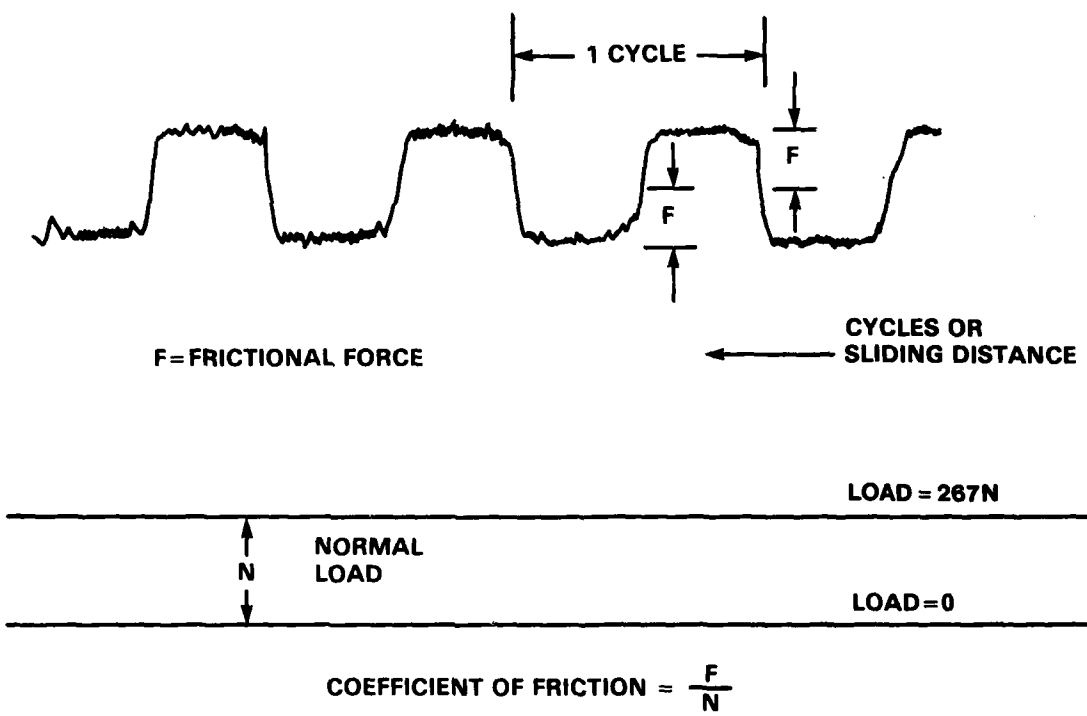


Figure 6 - Typical Strip Chart Record of Normal Load and Frictional Force vs. Distance Travelled

contacting the outer periphery of the cam are fed to a counter. The counter registers the number of cycles of sliding.

## TEST CONDITIONS

Tests were conducted under the following conditions: (a) normal load of 276 N, (b) mean sliding speed of 4 mm/sec, where the amplitude of oscillation is ±2 degrees with a frequency of 3 Hz. The total distance travelled per cycle by the copper bearing specimen relative to the counterface was 1.32 mm. The tests were conducted at room temperature. The contact interfaces were covered with mineral oil.

These test conditions are typical of the conditions experienced by an actual service-type bearing. The load used corresponded to the probable peak contact loading experienced in service. In other (unpublished) studies I have found that most, if not all, wear takes place at these loads. The nominal contact pressure, based on the rectangular dimensions of the copper tips, was about 115 MPa. The nominal pressure used in this study is comparable to the Hertzian contact stresses used by other investigators in the study of the severe wear of metals.[15,16] Although the loads used by these investigators, in many cases, seem relatively small--on the order of 10N--the geometrical arrangements used, i.e., flat-on-ring, pin-on-disk, or cross-cylinders, produce high initial contact stresses which can readily lead to a rough topography, high coefficients of friction, and high wear. It was not our intention in this study to use conditions that could yield severe wear, but rather to duplicate conditions that would be experienced in the CPP application.

## WEAR MEASUREMENTS

Specimens were weighed to determine wear because this method is accurate and simple. A Mettler HL52 electronic balance with a sensitivity of 0.01 mg was used to determine the weight loss of the copper bearing specimen and the weight loss (or gain) of the counterface specimen. The reproducibility of repeat weighings was 0.1 mg.

Before testing, the copper bearing specimen and its companion counterface were ultrasonically cleaned in boiling hexane, allowed to cool to room temperature, and then weighed. Weight measurements were taken until at least three consecutive weighings agreed at least to within 0.1 mg. After completing the test, the

specimens were removed from the tribometer, cleaned again, and weighed. The difference in weight before and after testing is the material lost because of wear. The wear volume of the copper bearing specimen may be determined by dividing the weight loss by the density of the copper.

## FRICTION AND WEAR TEST PROCEDURES

The three combinations of metals were tested for 50,000 cycles (66 m of sliding). During this period the frictional forces were continuously monitored. The coefficients of friction were then calculated. Each combination of metals was tested three times. A new copper bearing specimen and an unworn counterface surface were used for each test. A fresh spot on the counterface specimen was obtained for each test by rotating the counterface in its holder to a new location.

Friction and wear were also determined for shorter durations of sliding, for example, 100 cycles (0.132 m of sliding), 1000 cycles (1.32 m of sliding), and 10,000 cycles (13.2 m of sliding).

In some additional experiments, worn copper tip was slid against an unworn counterface, and friction versus time was monitored. In others, a test was begun, then stopped, and the specimens were separated but not removed from their holders for lengths of time ranging from 1 hour to 1 day. The specimens were returned to contact, the load reapplied, and sliding resumed. Upon resumption of test, the friction versus time was monitored as before. In other tests, the test was begun, then stopped, and the specimens were separated. The contact surfaces were lightly brushed to remove loose or weakly adhering wear particles, the specimens were then returned to contact, the load applied, and the test resumed.

## MICROHARDNESS MEASUREMENTS

The DPN values were determined using a 0.49-N indentation load in a Leitz Microhardness Testing Microscope. They were determined, on one tip of each copper bearing specimen slid, without interruption, for 100, 1,000, 10,000, and 50,000 cycles against steel or Inconel. At least five hardness determinations were made at random locations on each worn copper tip. No attempts were made to measure hardness of the copper transferred to the counterface, because indentation hardness of a relatively thin layer is affected by the properties of the underlying material.

Subsurface hardness of the deformed region in the copper was determined where the region was thick enough to allow a reliable measurement. If the region is thin, measurements of hardness taken too close to the free surface result in unreliable and generally low hardness values. Even for the thickest deformed region found in this study, a 0.49-N load gave indentations that were too large and too near the free surface to obtain meaningful values of hardness. Therefore a 0.15-N load was used to provide a smaller indentation further from the free surface. No hardness measurements were made on the copper bearing tip sliding against a copper counterface because the resultant surfaces were too rough.

## PARTICLE SIZE AND MICROSTRAIN MEASUREMENTS

The Warren-Averbach (W-A) method of X-ray diffraction was applied to the wear specimens to determine the particle size and the mean strain $\langle \varepsilon^2 \rangle^{1/2}$ from the line broadening of the X-ray profiles, which was caused by surface deformation during sliding. The line broadening represents convolution of the contributions of both particle size and microstrains; the W-A method, applying a Fourier analysis of the profiles, separates these two effects. The principle by which the two contributing factors--particle size (coherently reflecting domains) and microstrain--are separated is based on the fact that the particle size is independent on (hkl) planes, whereas the microstrain depends on the (hkl) planes studied. Thus, particularly in determining the microstrains, one selects the higher orders of a particular (hkl) reflection. In this case planes (111) and (222) were investigated and a Fourier analysis of the wear specimens according to the W-A method was done.

## DETERMINATIONS OF WORN COPPER TIP AND COUNTERFACE TOPOGRAPHY

The surface contact morphologies of the copper against steel and copper against Inconel wear specimens were viewed in the scanning electron microscope. Scanning electron photomicrographs of each of the three tips were obtained for 100, 1,000, 10,000, and 50,000 cycles. Scanning electron micrographs for the corresponding contact areas on the counterface were obtained at 10,000 and 50,000 cycles. Secondary electron images (SEI) were obtained throughout in the study of the topographical changes in the worn copper and counterface contact surface. Contact topography on the steel and Inconel at 100 and 1000 cycles could not be readily differentiated from the prepared, unworn surface.

## MATERIAL TRANSFER

Transfer of material between tip and counterface was determined by Energy Dispersive X-ray Analysis (EDX). For each scanning electron image obtained, an elemental spectrum was also obtained. This elemental spectrum provides information about the possible material transfer between the surfaces. For example, the high-purity copper contains only the peak absorption line of the copper, whereas the steel and Inconel counterfaces contain peak absorption lines for the elements iron, chromium, and nickel, but none for copper. In looking for transfer to either the steel or the Inconel, the presence of a copper absorption peak would indicate that metallic copper or its oxide had been transferred. The presence of iron, chromium, or nickel on the copper wear surface would suggest that material from the counterface had been transferred in metallic or nonmetallic form. The absence of an absorption peak for copper on the counterface or iron, chromium, or nickel on the copper surface does not necessarily indicate that no transfer has occurred, only that any amount transferred is too small for detection.

## METALLOGRAPHIC SECTIONING OF WORN COPPER TIPS

Metallographic sections of worn copper tips were made to observe the subsurface deformation produced by sliding. The size and depths of heavy deformation near the copper bearing surface were determined from both transverse (cut perpendicular to the direction of motion) and longitudinal (cut parallel to the direction of motion) cross-sections for specimens slid 100, 1,000, 10,000, and 50,000 cycles. One tip from each copper bearing specimen was sectioned longitudinally, and a second tip was sectioned transversely. Sectioning of a single tip both transversely and longitudinally was not possible because of size. Sections of the copper bearing tip were mounted, metallographically polished and lightly etched with 30 volume percent nitric acid to bring out regions of heavy near-surface deformation. The distinction could be made fairly easily between the deformed regions produced by wear and the bulk large-equiaxed grain structure of the fully annealed nondeformed copper when the material was viewed at high magnification in an optical or scanning electron microscope. Sections were viewed in the scanning electron microscope in both the back-scattering and secondary electron modes. For many sections the back-scattering photomicrographs (BEI) were obtained. The back-scattering photomicrographs appeared to highlight the deformation characteristics and crack formation better than the secondary electron micrographs.

## RESULTS AND DISCUSSION

### THE POWER RELATIONSHIP

Although it is generally accepted that wear, is to a first approximation proportional to the load, it is less commonly appreciated that a slight change in the coefficient of friction can produce drastic changes in wear. Tabor has consistently emphasized this fact.[1] In addition, wear is probably some exponential function of the coefficient of friction. The functional form can be dependent on the regime of sliding and may be specific for a given combination of sliding materials. For example, in the copper-steel system the relationship between wear and coefficient of friction may be written:

$$\text{wear} \quad \alpha \int_0^s \mu^n \, ds \tag{2}$$

where

n = wear severity index

$\mu$ = coefficient of friction produced by solid contact

s = sliding distance.

For hydrodynamic lubrication no solid contact occurs and ideally there is no wear. For boundary lubrication Litvinov and Mikhin[17] demonstrated that, for copper sliding on steel, as the coefficient of friction increases from 0.01 to 0.07, the wear intensity increases about two orders. The magnitude of the coefficient of friction may be related to the original surface finish of the steel. A replot of their data (on log-log paper where n is the slope of the line obtained) for wear intensity as a function of coefficient of friction shows that as the roughness or coefficient of friction increases, n approaches a value of 2.5. For very fine finishes or low coefficients of friction, n is a small number.

Stowers and Rabinowicz,[18] who studied copper sliding against steel and steel sliding against steel, found that in the severe wear regime, n was about 4. In another study, Rabinowicz[8] used a wide variety of metals in both unidirectional and reciprocating sliding, lubricated and unlubricated. He concluded that n fell between 4 and 5, but an accurate value of n could not be determined by this writer

because of the wide scatter of data. A plot of the wear data versus steady-state coefficient of friction obtained by Ruff and Blau[19] for the dry sliding of copper alloys and steels on steel also showed that the wear is proportional to about the fourth power of the friction coefficient. In the same paper the steady-state coefficient of friction for a dual phase (DP) 80, low alloy, high-strength steel was reported to have two values, 0.55 and 0.78, which were obtained under apparently the same conditions of sliding. The wear at the larger friction coefficient was four times greater. This is not surprising, because the fourth power of the larger coefficient of friction is four times larger than the fourth power of the smaller coefficients. I have determined friction and wear for a wide range of copper-based alloys sliding against many types of hard counterfaces at DTNSRDC (data not published). It was found that the wear in these systems was proportional to the fourth power of the quasi-steady-state coefficient of friction. In these studies a variety of commercially-available bronzes, such as cast and wrought aluminum bronzes, nickel-aluminum bronze, manganese-aluminum bronze and high-tin bronze were used.

FRICTION-SLIDING DURATION CURVES

Curves of friction vs. cycle time (or distance travelled) can be used (1) to identify the mechanisms of friction and mode of wear, (2) to calculate the fourth power mean of the friction coefficient, (3) to determine specific wear rates from shorter periods of sliding where large changes in the coefficient of friction may occur, and (4) to determine the work input and temperature rise.

In this study, friction-duration curves were used primarily to detect changes in the mode of sliding and to calculate the fourth power mean of the coefficient of friction.

The fourth power mean is given by the following equation

$$\bar{\mu}_4 = \sqrt[0.25]{\frac{\int_0^c \mu^4 \, dc}{c}} \qquad (3)$$

where c = number of cycles.

Because the wear and friction varied as the fourth power of the coefficient of friction, I chose to describe the data using this relationship. In this study the fourth power mean $\bar{\mu}_4$ and the mean coefficient of friction ($\bar{\mu}$) for the 50,000 cycle sliding duration were about equal. In a system where no transient states occur, i.e., for a constant coefficient of friction (steady-state), would equal $\bar{\mu}_4$, but for a large change in coefficient in time, $\bar{\mu}_4$ would provide the proper representation. For example, where copper slides against itself the short-term evaluation showed that $\bar{\mu}_4$ is greater than $\bar{\mu}$; whereas, where copper slides against steel or Inconel, and small changes in coefficient of friction occurred with increasing cycles, $\bar{\mu}_4 \approx \bar{\mu}$ throughout the duration of test. The relationships between $\bar{\mu}_4$ and $\bar{\mu}$ is shown in Figure 7.

WEAR RESULTS

The wear data obtained in this study are shown in Figure 8. The weight loss after 50,000 cycles (66 m) of sliding is plotted on log-log paper against the fourth power mean of the coefficient of friction. Because the fourth power mean was generally equivalent to the average coefficient, ($\bar{\mu}_4 \approx \bar{\mu}$), either coefficient of friction could be used. A line of slope 4 fit the data rather well, and agrees with other researchers findings previously discussed.[18,19] From my work the following relationship between wear and the coefficient friction was obtained.

$$\text{Wear (weight loss)} \propto \mu^4 \tag{4}$$

Included in Figure 8 is an order of magnitude estimate of the Archard wear coefficient (k) obtained from Equation (1). A specific value for this coefficient will not be provided because of the uncertainty in the value of the metal hardness. Most probably the fully-worked hardness of about 1370 MPa (140 kg/mm$^2$) would have been a more reasonable value to have used than the bulk hardness of 440 MPa (45 kg/mm$^2$), as wear is expected to occur in regions of heavy deformation where the hardness approaches or equals the fully strain-hardened value. Typical values of the coefficient of wear, k, for metal (on metals) or nonmetal (on metal) have been provided by Rabinowicz (Reference 5, Table 6.6, p. 164). The wear data of

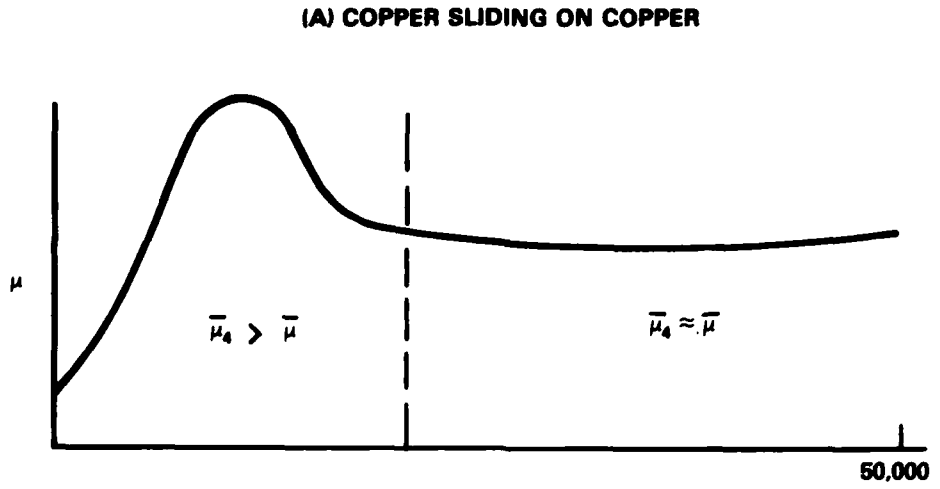


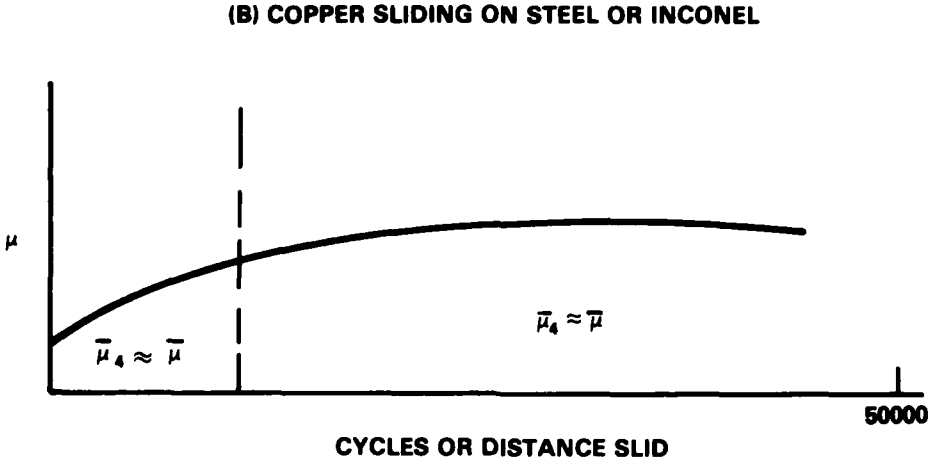


Figure 7 - Typical Curve of Friction vs. Number of Cycles Slid, Showing Relationship Between $\bar{\mu}_4$ and $\bar{\mu}$.

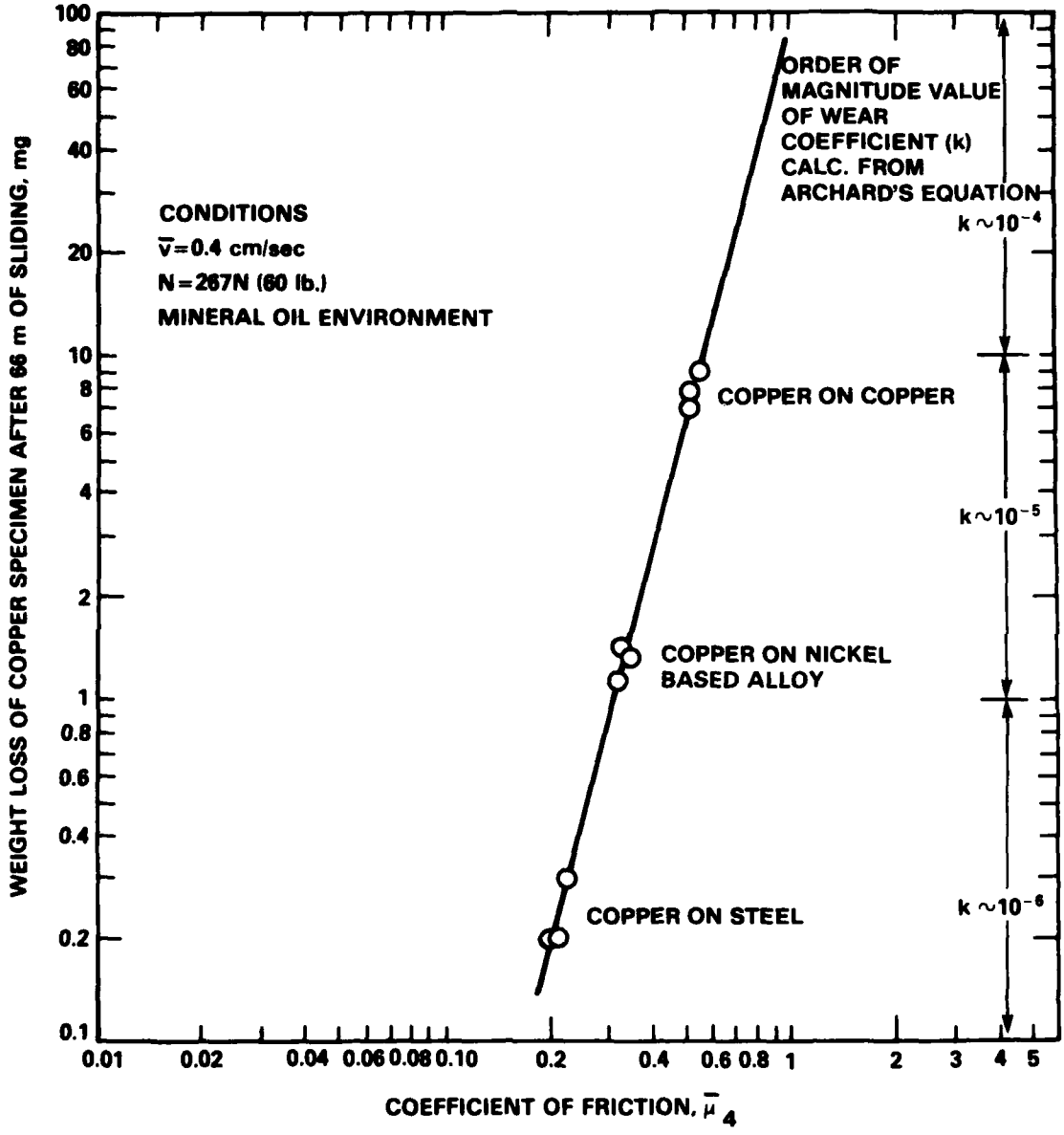


Figure 8 - Relationship Between Weight Loss of the Copper Bearing Specimen and Coefficient of Friction at 50,000 Cycles

of Figure 8 also show that the wear of copper sliding against steel was lower than copper sliding on Inconel, and that the highest wear occurred when copper was made to slide against copper.

Stages of Wear for Copper Sliding on Steel or Inconel

Although the curve of coefficient of friction vs. time gives a qualitative picture of the changing surface condition during sliding, it may or not not be useful in quantitatively distinguishing between the onset of one stage of sliding wear and the end of another. Three stages of wear based on the friction vs. test duration were assigned. The three stages are shown in Figure 9 and are identified as early stage, intermediate stage, and later stage. The transitions between the stages were arbitrarily selected. In the early stage the friction coefficient was relatively constant at 0.16 ± 0.03; this stage extended to about 10,000 cycles for copper against steel and to only 1,000 cycles for copper against Inconel. In the intermediate stage the coefficient of friction increased with duration of sliding; for example, for the copper against Inconel the friction coefficient increased to about 0.34 and for the copper against steel to about 0.24. This stage lasted about 20,000 cycles for copper against steel and 30,000 cycles for copper against Inconel. In the later stage the coefficient of friction stayed constant and continued up to 50,000 cycles and beyond in some evaluations where periods of sliding longer than 50,000 cycles were investigated.

The division of the wear process into three distinct stages (multistages) is not inconsistent with the experimental findings of Kerridge and Lancaster[7] and Kennedy and Voss.[20] The system that they chose is similar to the one used in this investigation--brass against a harder metal in which the debris produced is metallic. Kerridge and Lancaster[7] identified at least two distinct stages: the removal of metal from the wearing surface by transfer, and the formation of wear debris from the transferred layer on the opposing member. Kennedy and Voss[20] showed that the wear process appeared to proceed i : three stages: an initial or surface preparation stage, a second stage during which a transfer film was formed, and a steady-state stage.

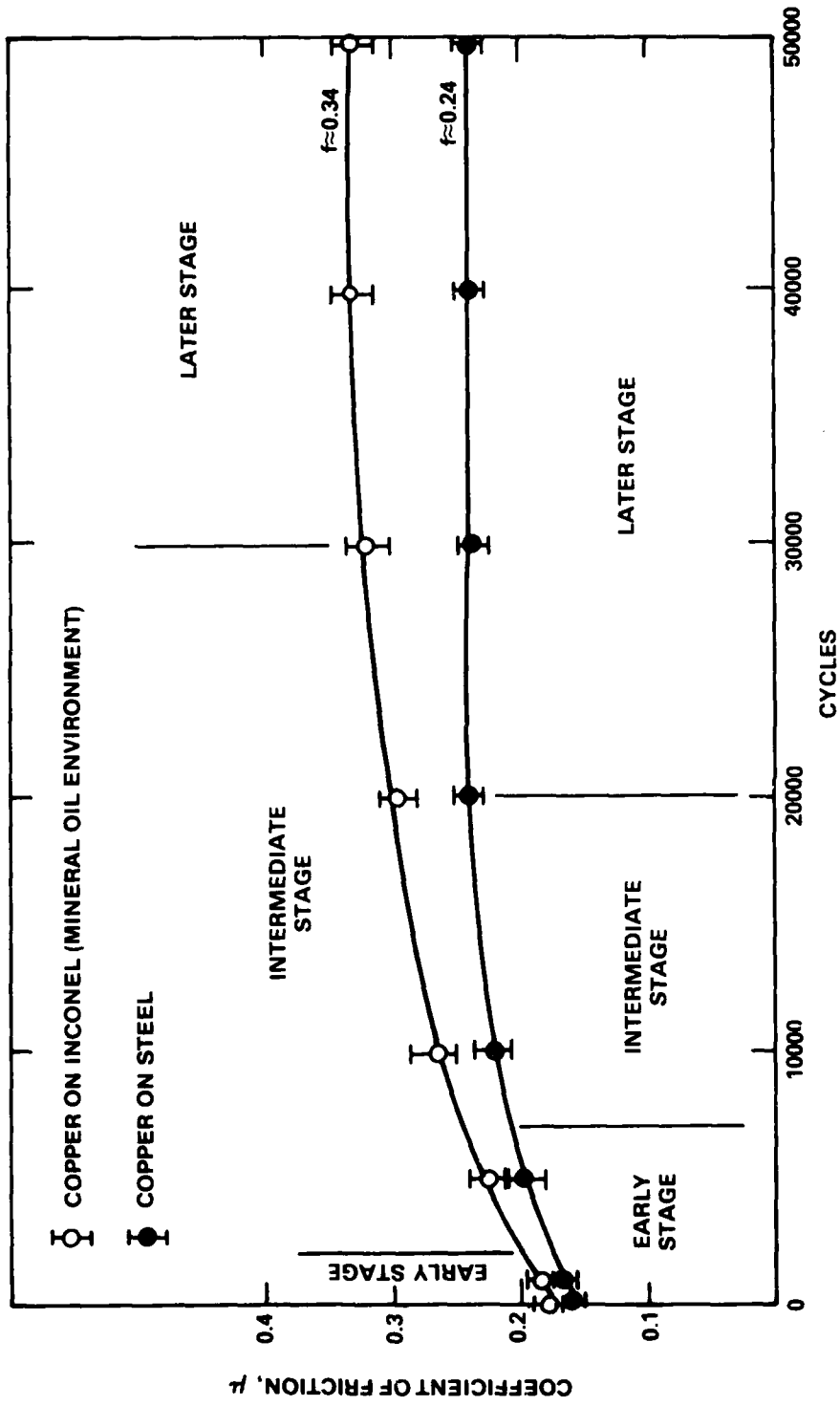


Figure 9 - Coefficient of Friction vs. Number of Cycles for Copper Sliding on Steel or Inconel and the Stages of Sliding

### Coefficient of Friction During the Early Stage

The coefficient of friction observed in the early stage of sliding is similar to that reported by Suh and Sin,[21] who attribute it to asperity deformation. They also reported that the value of the coefficient of friction in this state is independent of the materials tested, the test environment, and the surface roughness. The values reported here and by Suh and Sin[21] are similar because the initial topographies had about the same characteristics. If a much rougher counterface were made to slide against copper, the early stage coefficient of friction would be larger than that reported in this study. The initial coefficient of friction may also be increased by use of a softer member that has been highly polished and fully strain-hardened. Thus the same initial constant values obtained in this study and reference[21] are probably an artifact based on the test conditions.

## MORPHOLOGICAL CHANGES AND METAL TRANSFER

### Early Stage

The original surface of copper becomes smooth and assumes a polished appearance during early stage wear, as shown in Figures 10 and 11. Toward the completion of this stage there is an increasing amount of grooving.

Although the dominant mode of surface modification near the completion of the early stage was smoothing, we observed that for copper sliding against Inconel at 1000 cycles, a relatively small localized region of fragmentation and roughening had formed in one of the copper tips, as shown in Figure 12. This region of relatively heavy fragmentation had the same characteristic surface morphology found in the subsequent stages of sliding. This figure shows that the localized fragmentation of the surface contained platelike wear particles, cracks, tears, and metal removal. The severity of damage in this region may be attributed both to the strain-hardening of the copper and to the load concentration and high localized stress produced by nonuniform contact. Another consequence of load concentration was increased localized frictional forces.

For copper sliding against steel, the early stage of polishing, smoothing, and slight grooving seemed to last to about 10,000 cycles. At this time one of the copper tips developed a localized region of heavy deformation and wear, as shown in Figure 13. The localized high intensity of deformation in one of the copper tips is clearly evident in Figure 14, a magnified view of Figure 13. In Figure 14

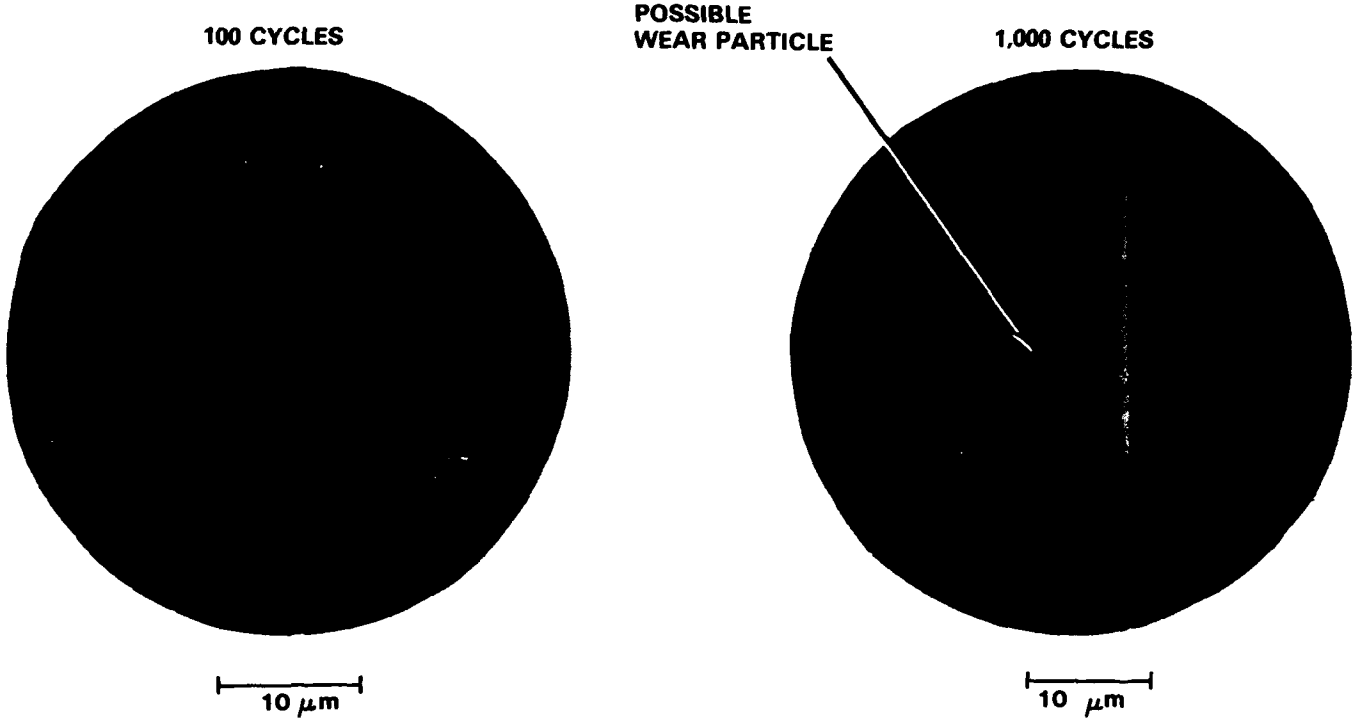


Figure 10 - Copper Bearing Surface Produced in Early Stage of Sliding on Steel. Initial Copper Topography Becomes Smoother (100 Cycles), Then Begins to Show Increased Grooving (1000 Cycles)

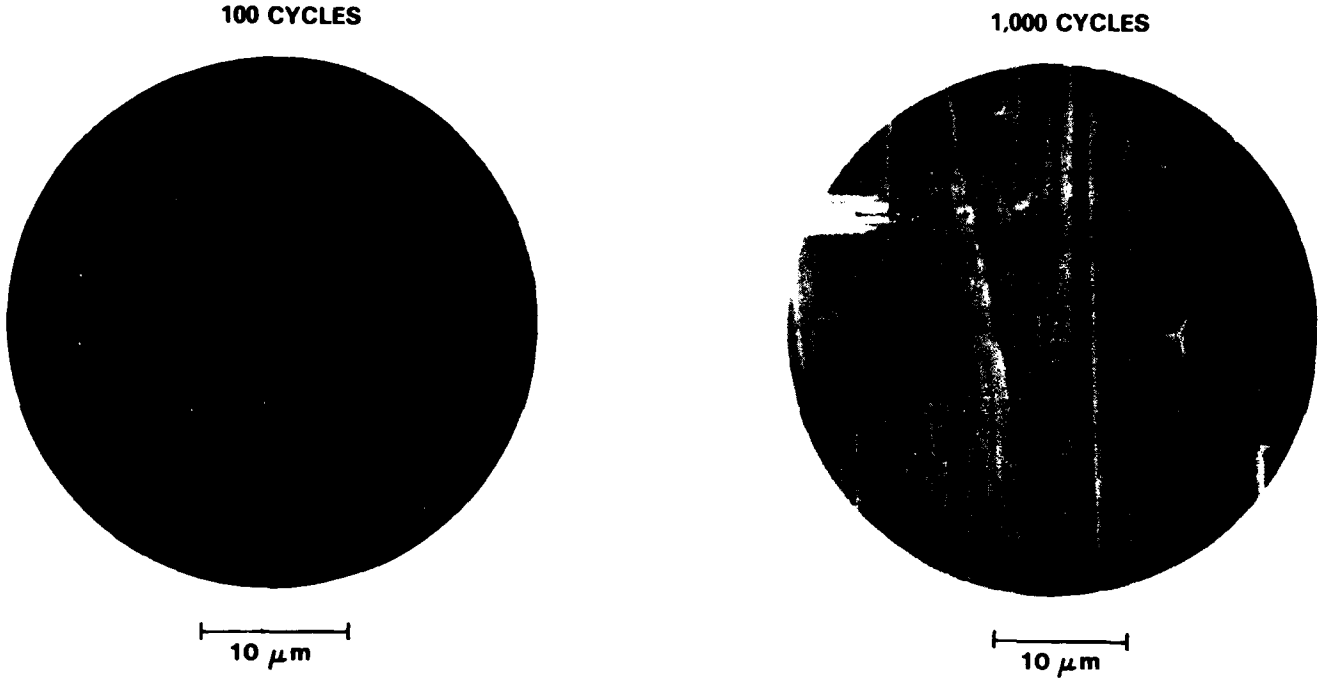


Figure 11 - Copper Bearing Surface Produced in Early Stage of Sliding on Inconel. Initial Copper Topography Becomes Smoother (100 Cycles) Then Begins to Show Increased Grooving (1000 Cycles)

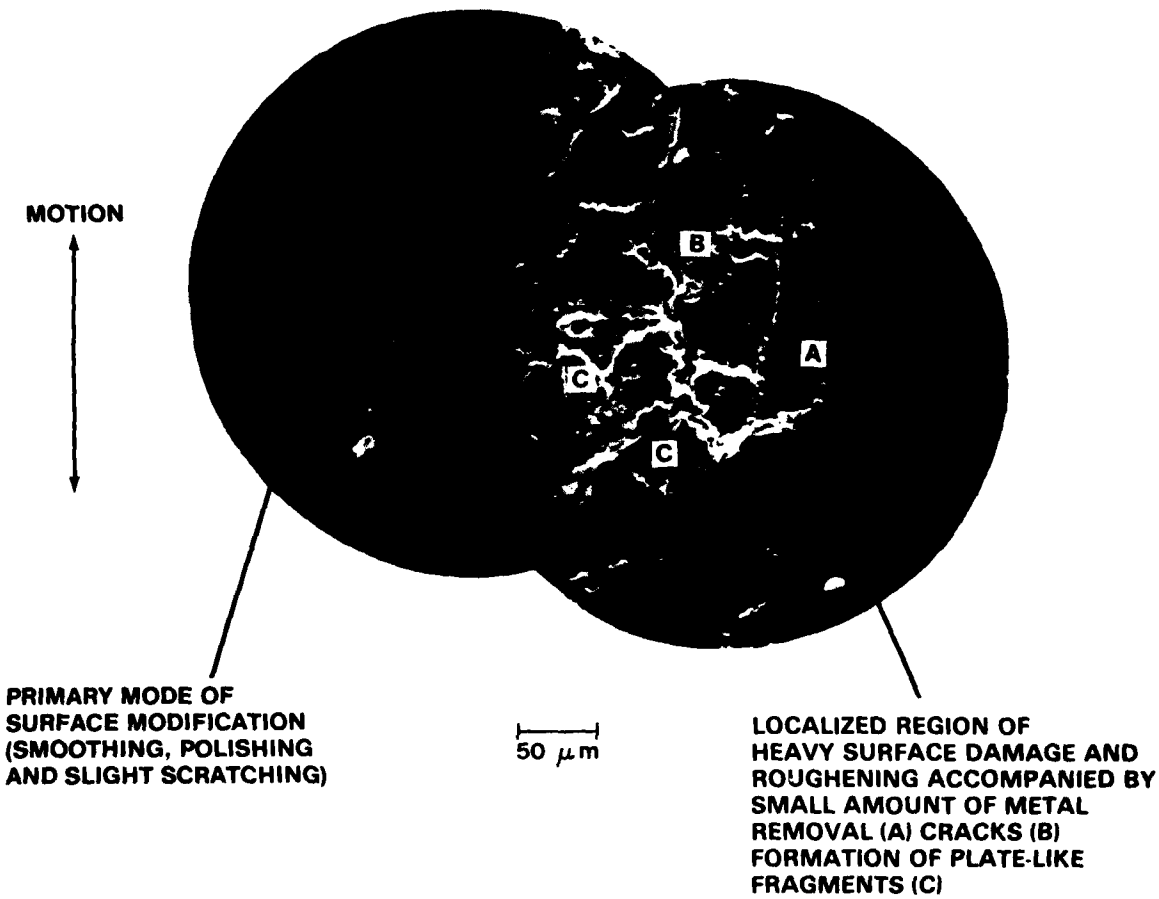


Figure 12 - Localized Heavy Damage on Copper Tip Toward End of Early Stage Sliding on Inconel, Even Though the Dominant Mode of Surface Deformation is Smoothing, Polishing and Light Grooving

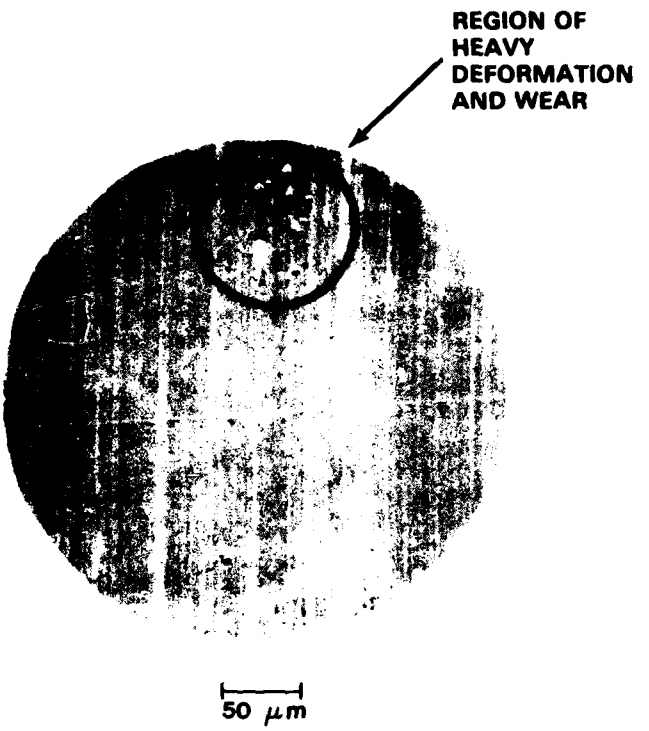


Figure 13 - Heavily Deformed Region in Copper Tip at the End of Early Stage Sliding on Steel

the plateaus and ridges appear to be highly strained, cracks have formed at the edges of the deformed ridges, a plateau has been fragmented and material removed, and very thin coiled-up wear particles have been generated. The reasons for the localized severity of surface damage are the same as those just mentioned for the copper sliding against Inconel. In the early stage of sliding there was no discernible transfer of copper to the hard counterfaces, although on some samples the EDX spectrum did pick up a slight trace of iron (probably iron oxide) on some of the copper wear tips. Neither the copper specimens nor the hard counterfaces lost measurable amount of weight. Atomic absorption spectrophotometry of wear debris collected during this stage revealed trace amounts of iron, but no apparent copper, chromium, or nickel.

Intermediate Stage

Sliding in the intermediate stage is characterized by ever increasing surface damage. The surface morphologies at the beginning of this stage resembled those in the early stage, but the morphologies developed toward the end resembled the later stage morphology. Damage to the copper sliding on the Inconel was much more severe than that observed for the copper sliding on steel. Figure 15 shows the topography of a copper tip worn against steel and a tip worn against Inconel, both after 10,000 cycles. The surface of the copper worn against Inconel is distinctly more worn, and also shows localized fragmentation and tearing of the uppermost layers of the copper.

The most striking difference between intermediate and early stage wear was the noticeable transfer of copper counterface. On the steel counterface, the transferred copper resided primarily within the initial grinding troughs and within scratches produced by hard particles during the course of sliding (see Figure 16). A copper map of the steel counterface in Figure 16 shows the location of such transfer. The height of metal transfer above the general level of topography was apparently slight. In comparison, the transfer of copper to the Inconel counterface was confined to localized discrete spots (see Figure 17). These spots generally appeared large, standing proud of the general level of the underlying topography. Some copper was also transferred within the initial surface depressions and scratches produced by sliding, but the the height of this transfer above the general level of topography was small.


Figure 14 - Magnified View of High Intensity Deformation Circled in Figure 13. Note Cracks, Plateaus, Metal Removal, and Thin Copper Wear Particles

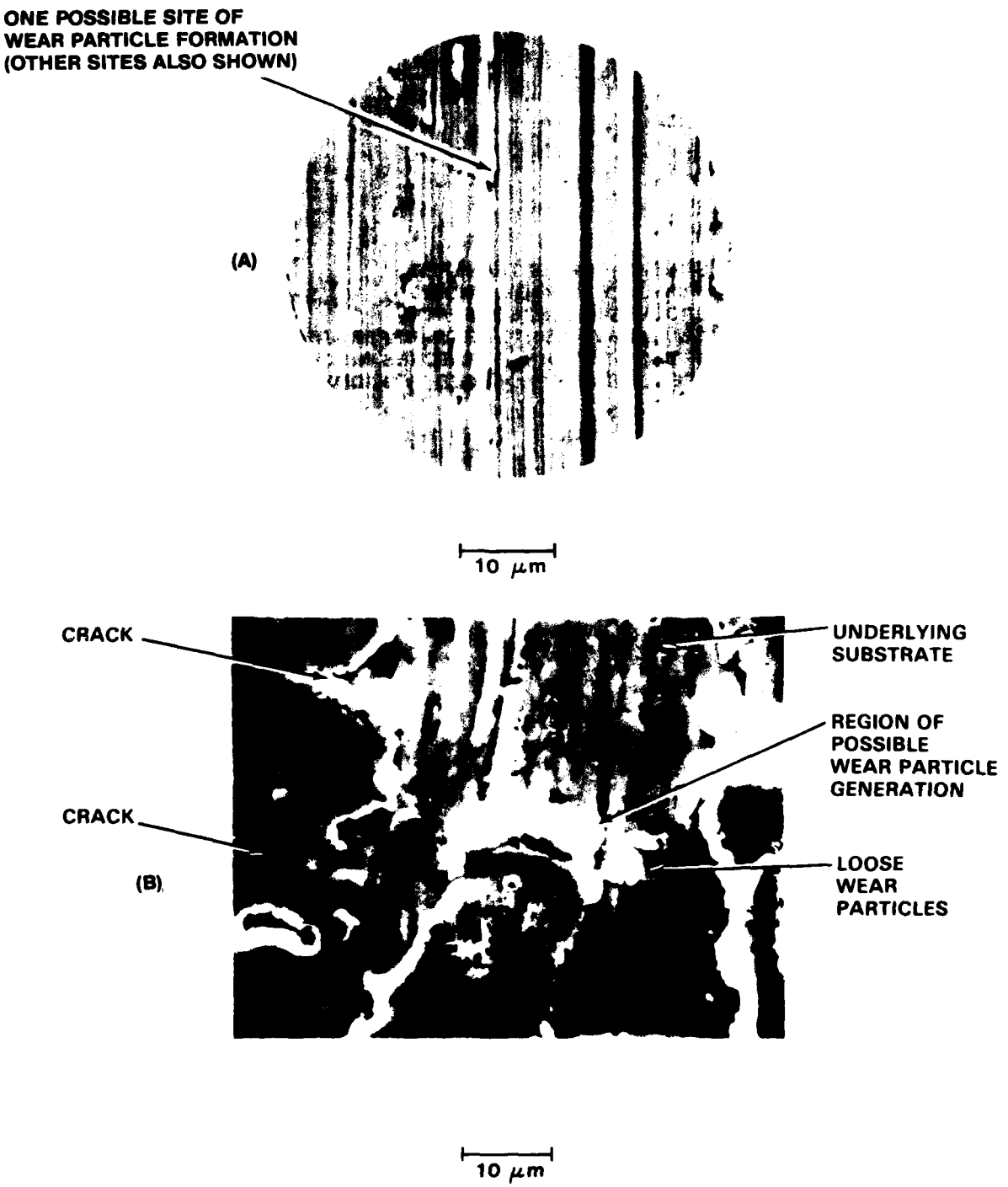


Figure 15 - During the Intermediate Stage of Sliding (at 10,000 Cycles), Damage to (A) Copper on Steel is Less Severe Than to (B) Copper on Inconel

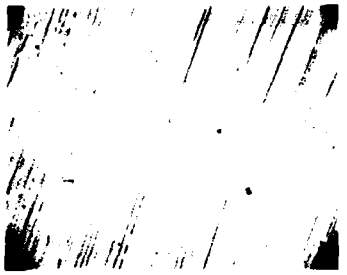

SITES OF COPPER TRANSFER PRIMARILY AMONG GRINDING GROOVES IN STEEL SURFACE (SMALLER AMOUNTS OF TRANSFER ARE SEEN TO OCCUR IN SCRATCHES WHICH ARE PROBABLY PRODUCED BY SLIDING)

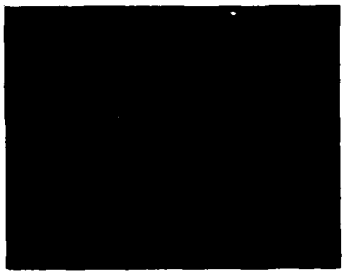

(EDX) MAP FOR COPPER

100 $\mu$m

SITES OF COPPER TRANSFER AT HIGHER MAGNIFICATION

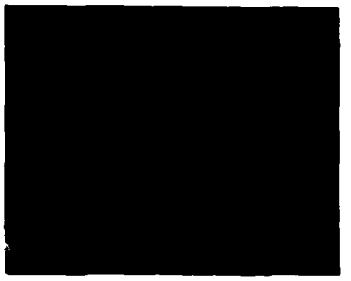

(EDX) MAP FOR COPPER

10 $\mu$m

Figure 16 - Steel Counterface in the Intermediate Stage of Sliding Showing Copper Transfer

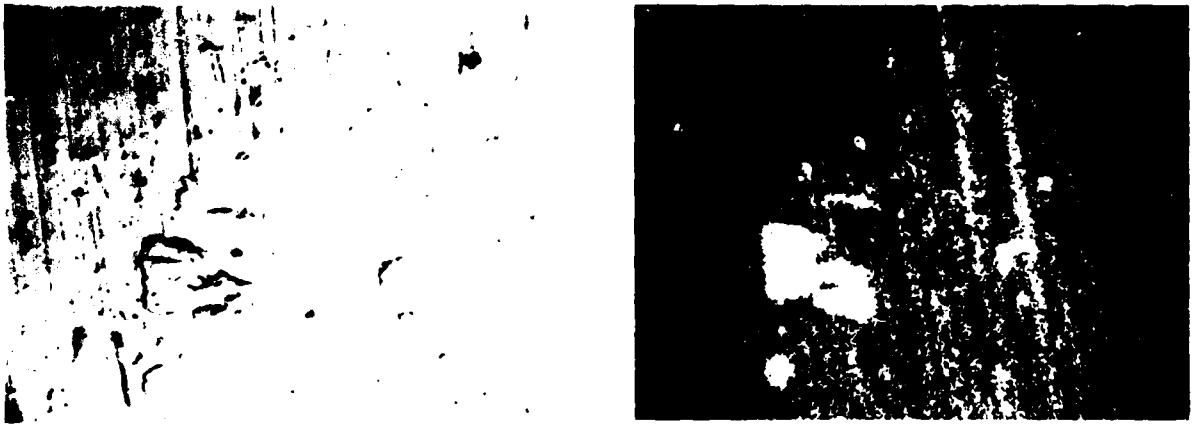


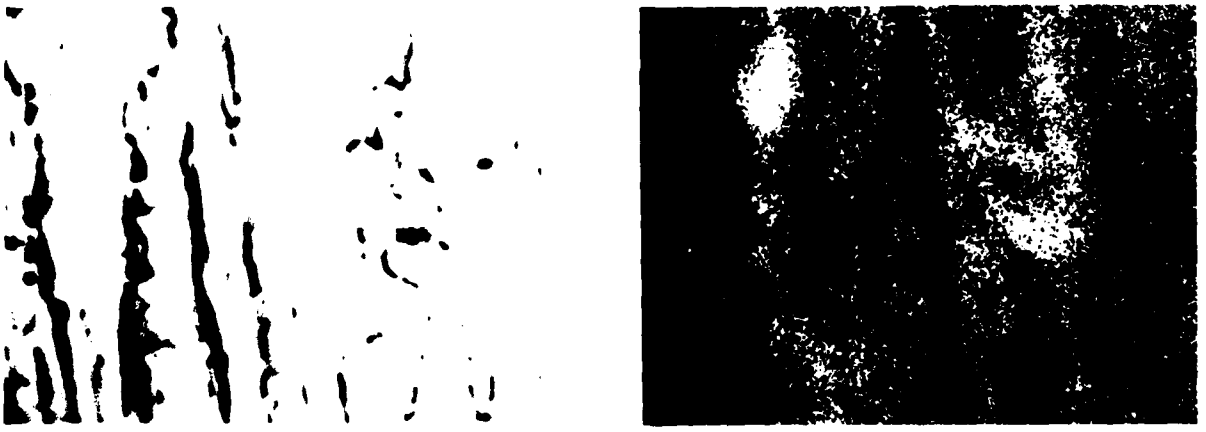


Figure 17 - Inconel Counterface in the Intermediate Stage of Sliding Showing Copper Transfer

The coefficient of friction in the intermediate stage increased from the base value of the early stage to a value of about 0.24 for copper sliding on steel and 0.34 for copper sliding on Inconel. The increase in both the degree of surface damage and the coefficient of friction was probably caused by this transfer. In the early stage the coefficient of friction and surface damage may be related principally to the surface asperity deformation of the copper bearing and may remain essentially constant. In the intermediate stage, however, the increase in coefficient of friction and severity of deformation may be related to the grooving or plowing of the copper surface by the transferred metal (the transfer patch). The further the transfer metal protrudes above the general level of topography, the greater its propensity to penetrate the copper bearing surface, grow, plow, and increase wear. The growth of the transfer patch probably occurs by adhesion or mechanical means. A closer examination of the Inconel counterface revealed that copper had been transferred into holes of the counterface (mechanical pitting) produced by the repetitive rubbing action. Hole formation in the Inconel counterface is shown in Figure 18. These holes are most likely produced by the removal of the hard Laves phase from this alloy. Unlike the transfer into the original grinding grooves of the steel counterface, where flow was not completely constrained, the copper transferred into the holes of the Inconel counterface was prevented almost completely from flowing plastically. The restraint on flow is illustrated in Figure 19. This finding suggests that the size and shape of the depressions in the counterface determine the strength of the attachment of the transfer metal and its height and flow characteristics. If the transfer metal is kept from flowing by the surrounding counterface metal, its effective hardness is considerably raised over its own nominal hardness. Such an increase in hardness would then increase its propensity to penetrate, plow, and grow.

Later Stage

The worn surface morphologies produced in later stage wear, as Figure 20 shows, were similar to those obtained in the intermediate stage. Here again the scale of damage appeared to be greater for copper rubbing on Inconel than for copper on steel.

This copper-Inconel sliding combination also produced many large platelike wear particles. One such particle which presumably had been back-transferred to

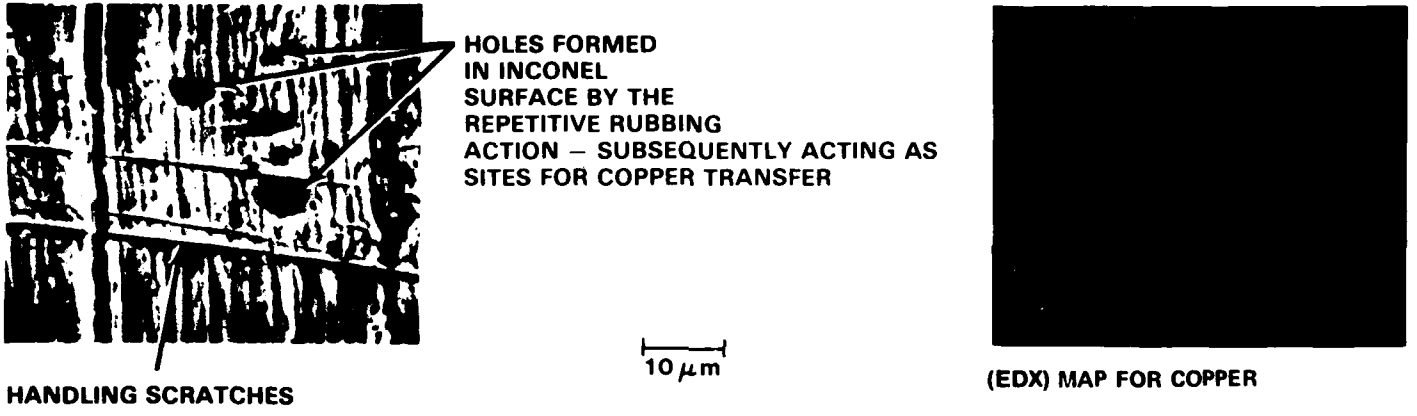


Figure 18 - Holes Produced in Inconel Surface by Sliding

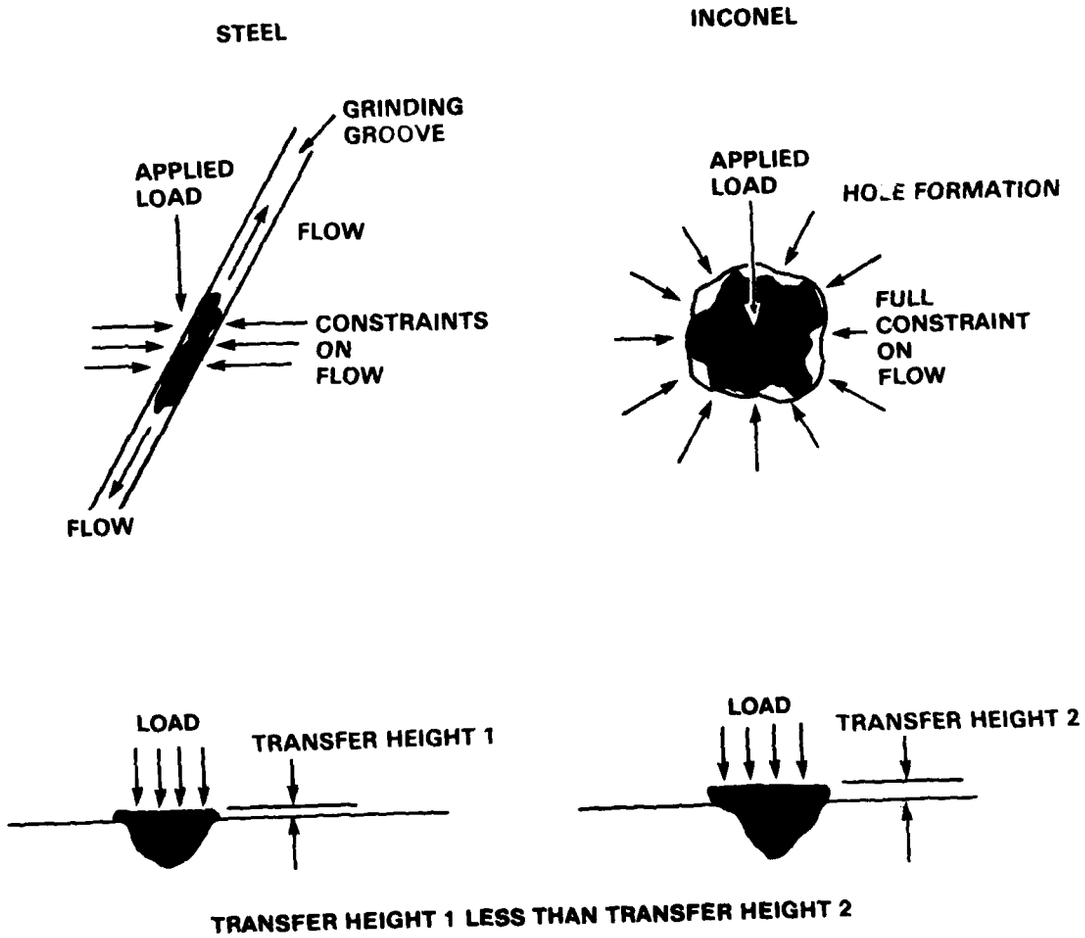


Figure 19 - Constraints on Copper Flow to Steel and Inconel and Resultant Height of Transferred Copper

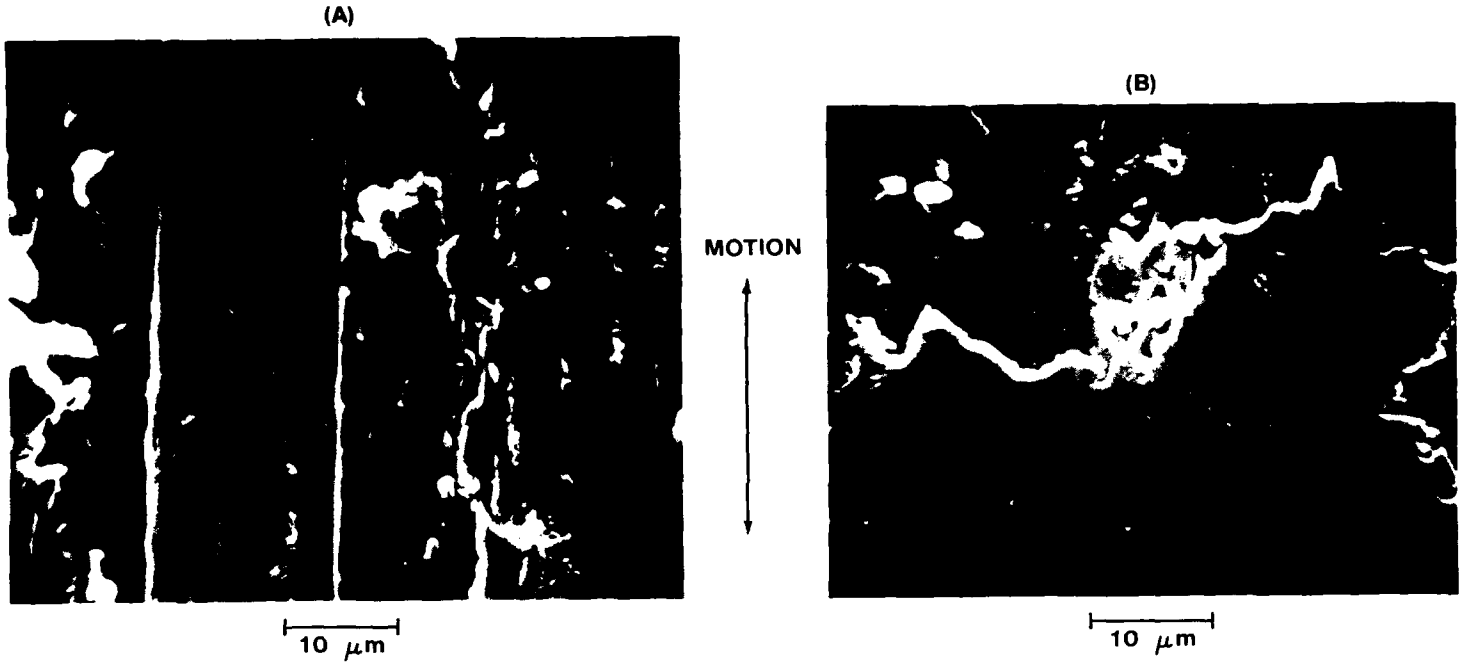


Figure 20 - Worn Copper Bearing Surface Produced By Later Stage Sliding (50,000 Cycles). (A) Copper on Steel; (B) Copper on Inconel

the copper surface and had been in rubbing contact with the counterface, is shown in Figure 20. This figure also shows quite vividly the heavy grooving of the worn surface and the break-up of the load-carrying plateaus by surface fragmentation. The cyclic deterioration of the sliding surface, which produces sheet- or platelike wear particles by a mechanism of crack initiation and growth, has been described by Suh.[15,24]

In the later stage, the pattern of transfer was similar to that observed earlier, as shown in Figures 21 and 22. The copper transferred to the steel counterface was more uniform and dense, and still apparently flat, whereas that transferred to the Inconel was still discrete, and consisted of large particles standing above the general level of topographical features. The contrast in contact morphology was even more stark when the two counterfaces were examined at lower magnification in the scanning electron microscope. The lower magnification increases the field of view and better represents the morphologies (see Figures 23 and 24). In the copper-steel sliding combination the morphology was relatively flat or smooth and uniform, whereas the copper-Inconel morphology was rough or chunky and discrete. Many large grooves can be found in the corresponding copper wear tip. The relatively flat transfer topography on the steel counterface indicates less penetration and consequently less plowing of the copper bearing surface, thereby lessening friction and severity of wear. Material transfer from the copper surface to the steel counterface in both the intermediate and later wear stages did not agree with adhesion or cold-welding theory. Transfer seemed to occur by plastic flow into the surface depressions initially present in the counterface or into depressions generated during sliding. Although no cross-sectional counterface micrographs were obtained in this investigation because of the difficulty in sectioning the small contact area used, Tabor has provided such a micrograph (Howell[23]). The micrograph was obtained for the copper sliding against steel. It has been repeatedly used to support the adhesion (cold-welding) theory of friction. This micrograph (taper section) is shown in Figure 25. Acutally, however, the figure shows that transfer occurs by plastic flow into the surface depression of the steel counterface. Also to be noted is that the larger the depression, the larger the amount of metal transferred.

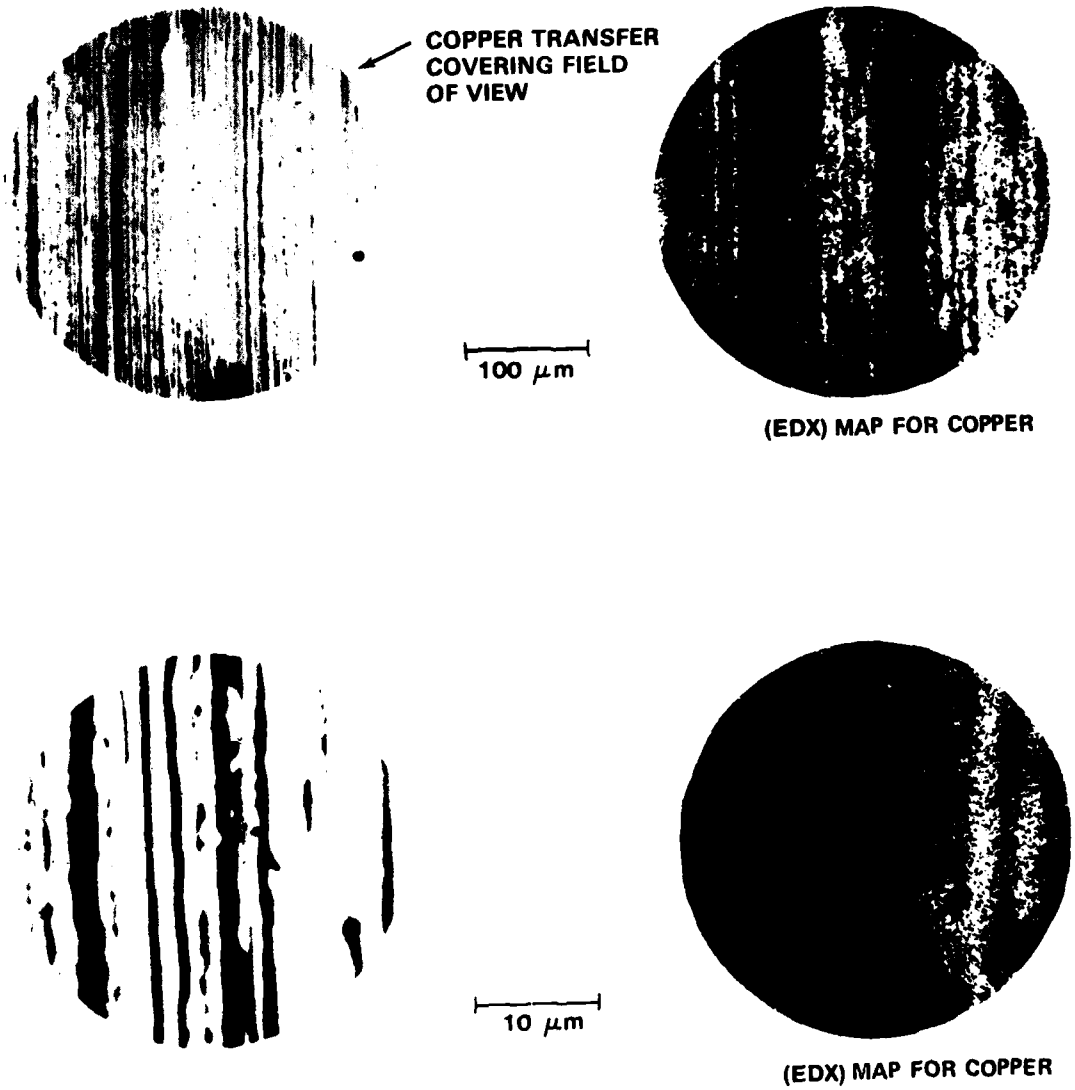


Figure 21 - Copper Transferred to Steel Counterface in Later Stage Sliding

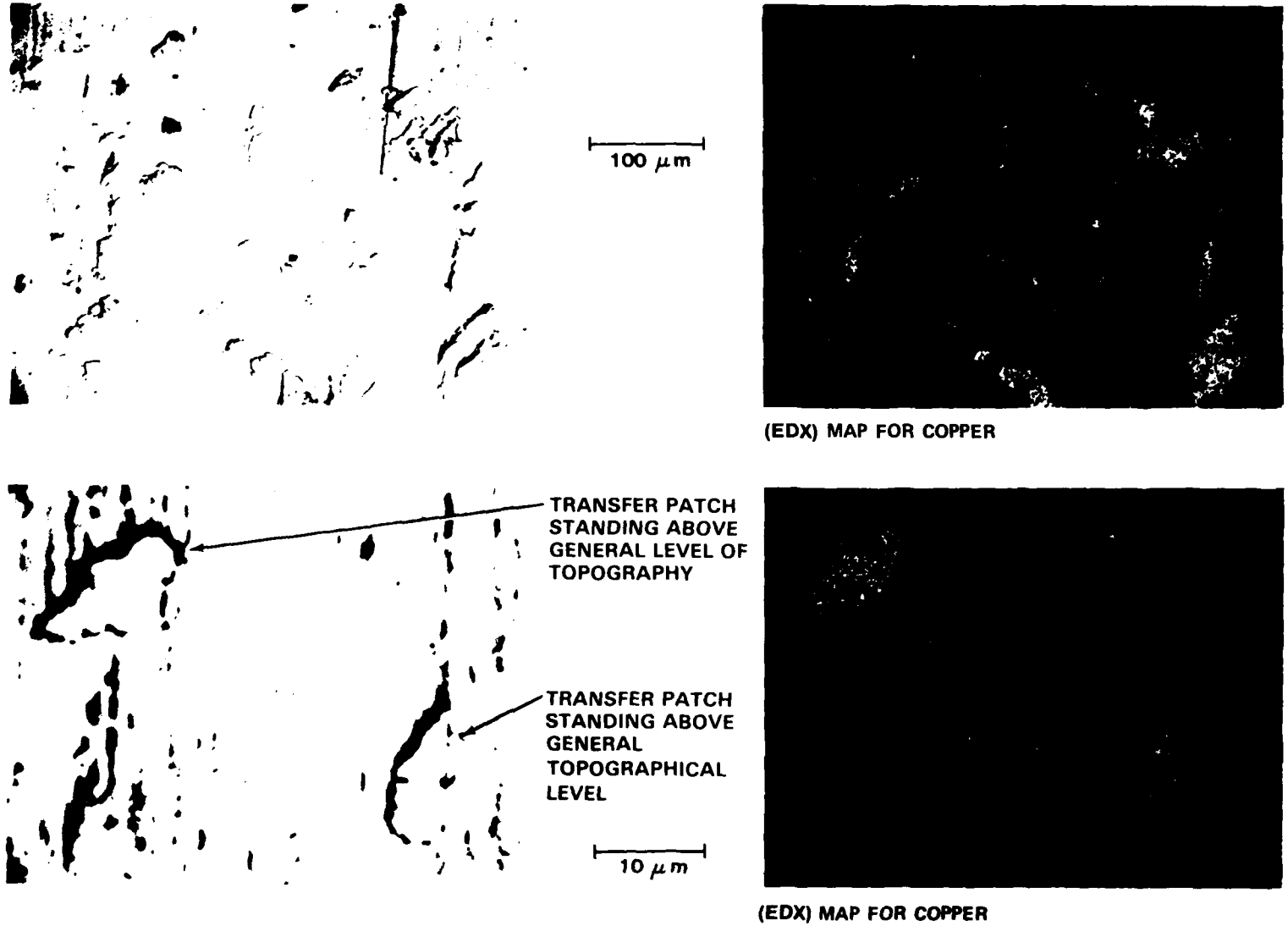


Figure 22 - Copper Transferred to Inconel Counterface in Later Stage Sliding

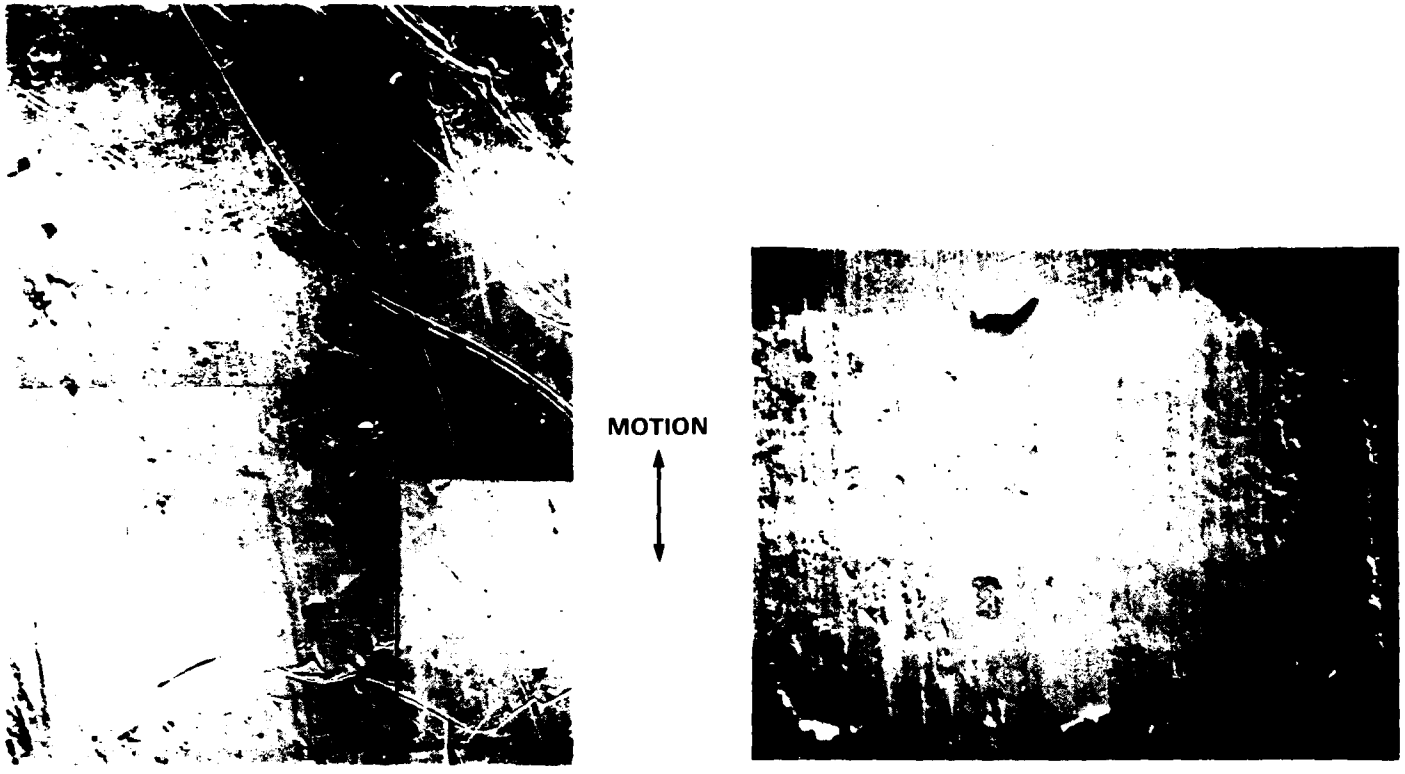


Figure 23 - Contact Topographies Produced by Later Stage Sliding of Copper on Steel. Copper Transferred to Counterface is Uniform, Dense, and Apparently Flat; Damage to the Copper Bearing Surface Appears to be Relatively Minor

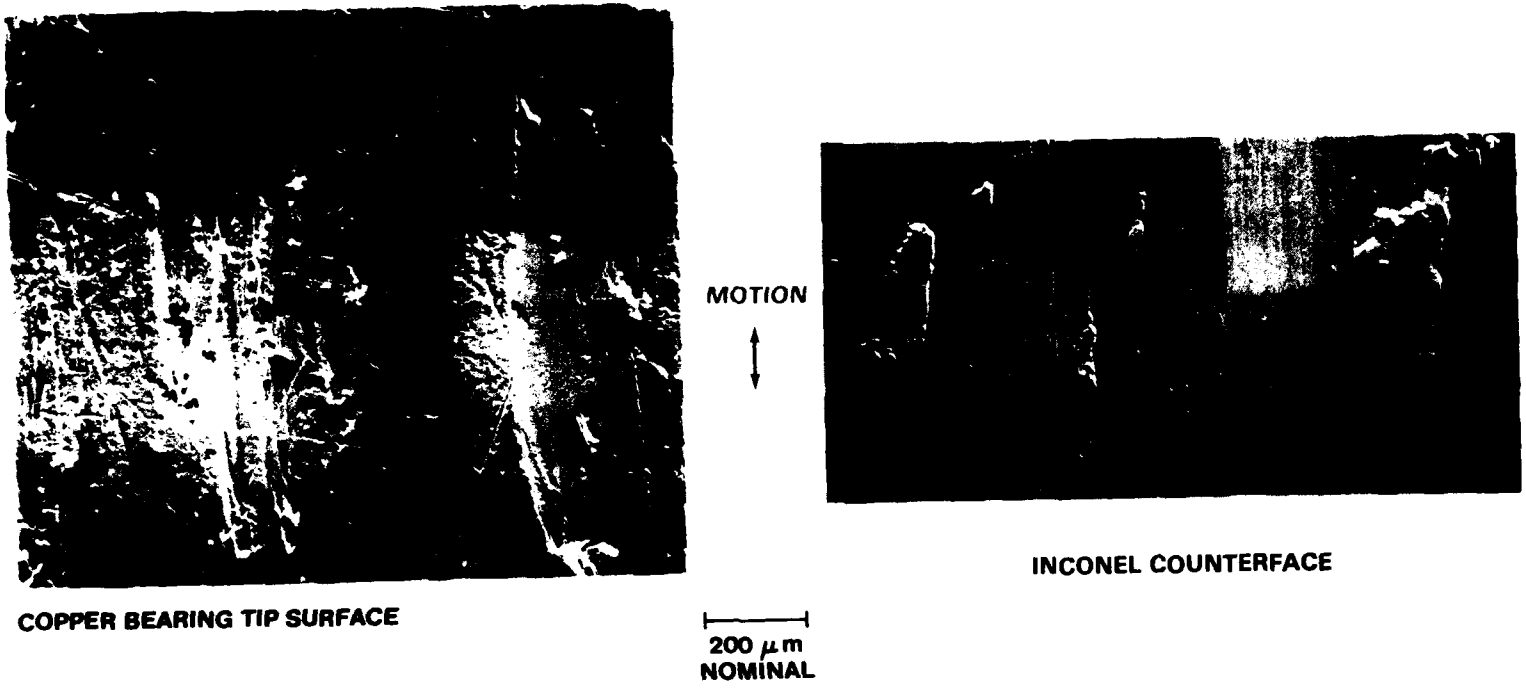


Figure 24 - Contact Topographies Produced By Later Stage Sliding of Copper on Inconel. Copper Transferred to Counterface is Rough, Chunky, and Discrete, with Corresponding Damage to Copper Bearing Surface

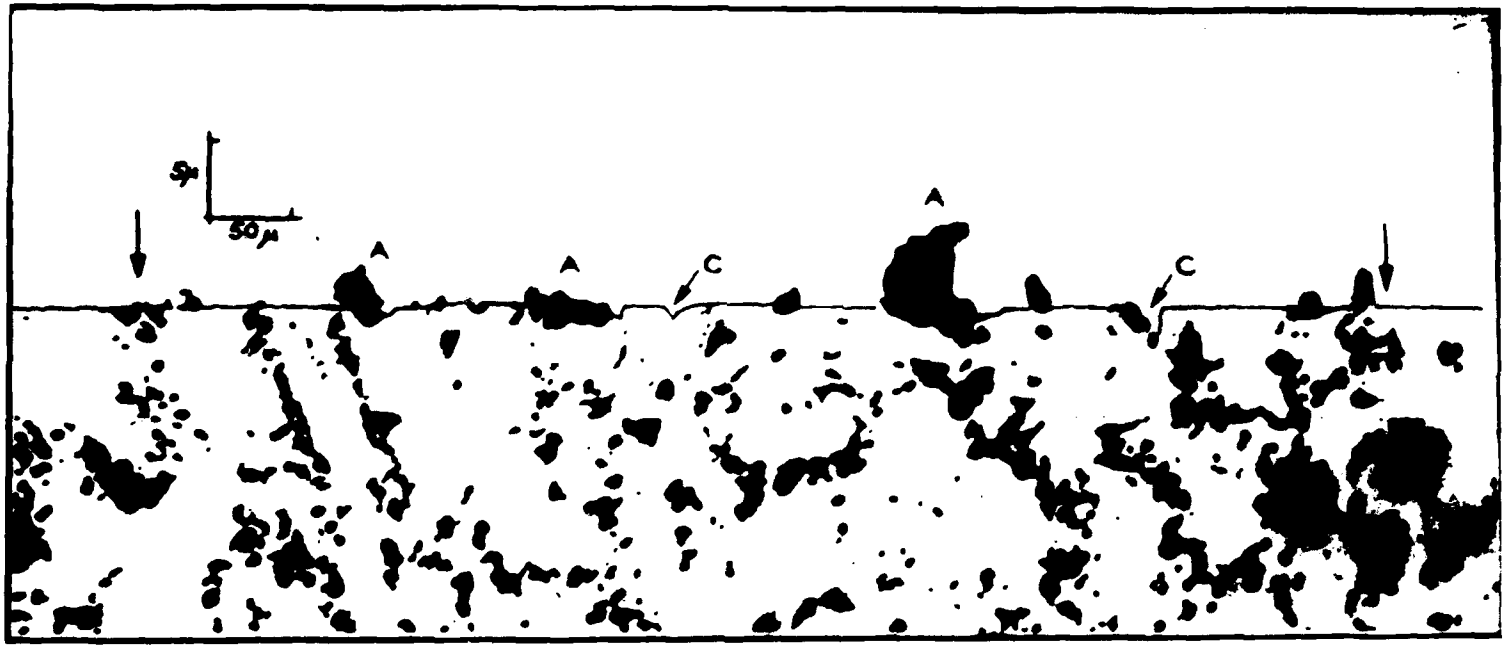


Figure 25 - Taper Section of Steel Surface Showing Transfer of Copper Into Surface Depressions. (In Howell Ref. 23; Reprinted Courtesy of John Wiley and Sons, New York)

STAGES OF WEAR FOR COPPER SLIDING ON COPPER

Copper sliding on itself is typical of a prow or wedge-forming wear mechanism where gross "adhesion," interpenetration and plowing occur. This is not unlike the mechanisms of wear occurring in the other sliding combinations studied in this investigation, where the build-up of transfer patches by agglomeration of wear particles leads to interpenetration and plowing. The prow or wedge formation wear mechanism has been described by several investigators.[24-27] Briefly, it is a severe wear process characterized by a build-up of a work-hardened transfer patch which grows against the direction of sliding by continuous plastic shearing, or plowing. The work-hardened transfer patch can be transferred back and forth in the contact interface or can be removed whole or in fragments as loose wear debris.

Copper sliding on copper was not analyzed in detail because (a) it has been described by numerous investigators, and (b) would not be used in practice. It was tested because it would give both high wear and high friction and also would serve to illustrate the asperity deformation and plowing aspects of wear.

The coefficient of friction versus time curve for copper sliding on copper is shown in Figure 26. It has been arbitrarily divided into two stages, an intermediate stage and a later stage. The intermediate stage may be further subdivided into two stages, which would include a surface preparation or early stage. The early stage was suppressed because of the high nominal contact pressure, the inability of the counterface to support the relatively thin superficial oxide, the type of motion, and the short length of rubbing contact. In other experiments (not reported here) heavily tarnished specimens having presumably a thick oxide or sulphide layer, were used. In these tests, the number of cycles of early stage sliding occupied a significant portion of sliding time. The role of oxides or other natural non-metallic films on the metal combinations in keeping the process within a regime of relatively low coefficient of friction and wear should not be overlooked. In fact, the tenacity of the natural oxide in withstanding repeated surface traction in experiments using copper sliding on the relatively hard steel or Inconel counterfaces should not be ignored, even if initial transfer is by mechanical entrapment within the surface depressions of the hard counterface.

A few relatively short duration sliding experiments were conducted with copper sliding on copper in order to obtain a picture of the early stage contact conditions developed. In the initial stages of sliding, about 100 cycles, once the oxide or

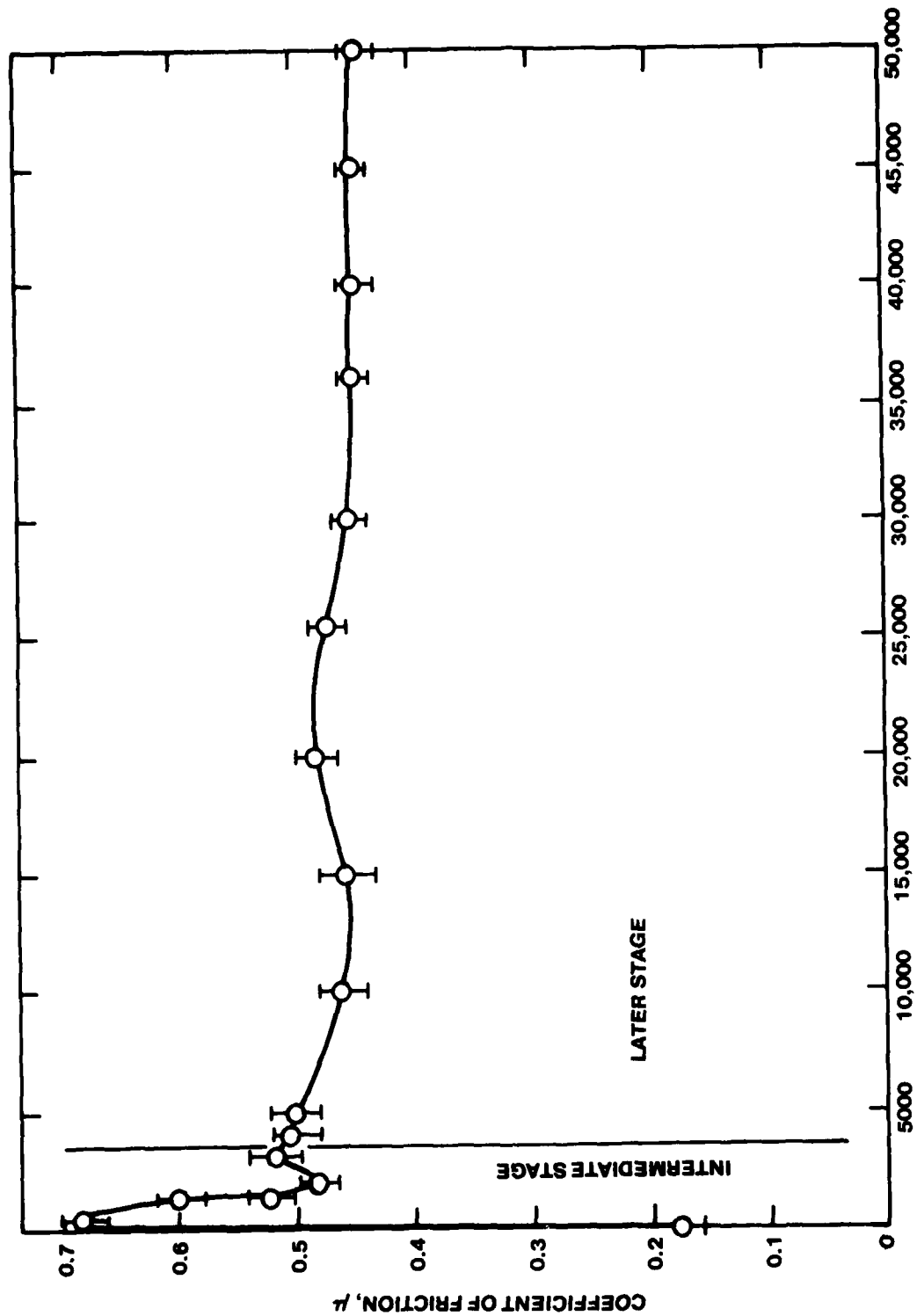


Figure 26 - Coefficient of Friction vs. Duration of Sliding for Copper Sliding on Copper

other nonmetallic film was broken, the copper contacts became extensively strained and hardened, with gross penetration, and plowing of the harder surfaces into the relatively soft subsurface metal. This penetration and plowing is shown in Figure 27. The coefficient of friction on sliding rose to its maximum of about 0.75 and was accompanied bv high wear. On further sliding to about 3000 cycles the contact geometry became more conforming and was accompanied by less plowing or interpenetration, as shown in Figure 28. Here large flakelike particles were formed by asperity shear deformation, as shown in Figure 29. The coefficient of friction in this time period decreased from its maximum value to about 0.52. On continuation of sliding the coefficient of friction decreased to a relatively low and steady value of about 0.40 (10,000 cycles). Here the contact geometry was fully conforming and the wear was lowest. A subsurface section obtained at 10,000 cycles is shown in the optical photomicrograph of Figure 30. In this figure the maximum height of grooving is about 30 μm. The groove height is larger than the maximum depth of subsurface deformation, 25 μm, seen throughout the micrograph. The fourth power mean of the coefficient of friction for the 10,000-cycle run was 0.48, whereas the mean coefficient was 0.45. The micrograph of Figure 30 also shows sheetlike wear particles.

## DEPTH OF DEFORMATION BELOW THE FREE SURFACE OF THE COPPER

### Early Stage

In the very early stage of sliding (100 cycles) the asperities of the copper bearing surfaces were deformed. The deformed metal flowed into the recesses, or valleys, originally present. Figure 31 is a longitudinal section typical of the very early stage of sliding. it shows the flow of metal from the high spots into the recesses; the black areas remaining within the recess are voids. The surface asperities in this stage were readily able to flow and relieve the contact stress imposed on them. The capacity of these high spots to be easily deformed and thus accommodate large strains is explained as follows: the contact loading provided a hydrostatic component to the state of stress; the copper was not fully strain hardened; and space for the metal from high spots to flow into was available. Later in this stage (1000 cycles), the asperities were almost completely flattened, and a well developed, relatively uniform, thin and probably work-hardened layer was

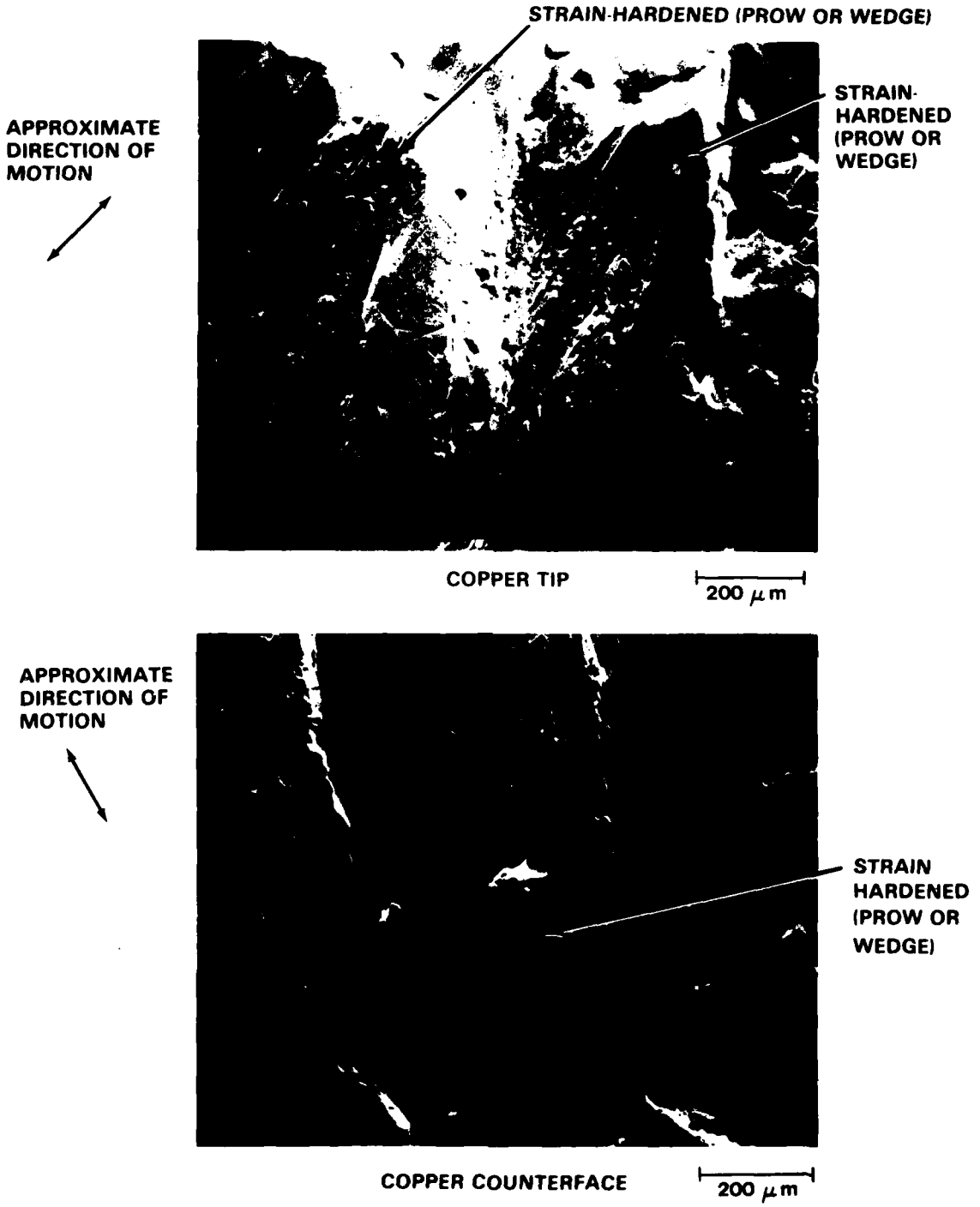


Figure 27 - Interpenetration of Contact Surface During the Very Early Stage (About 100 Cycles) of Copper Sliding on Copper

200 μm COPPER COUNTERFACE

200 μm COPPER TIP

Figure 28 - By About 3000 Cycles, Contact Geometry of Copper Sliding on Copper is More Conforming, and There is Less Plowing and Interpenetration of Contact Surfaces than Earlier. Circled Area is Further Magnified in Figure 29.


Figure 29 - Copper Bearing Surface After 3000 Cycles Sliding on Copper Shows Large Flakelike Particles Formed by Asperity Shear Deformations (Magnified View of Circled Area in Figure 28)

observed. A longitudinal section obtained during this period of sliding is shown in Figure 32. Figures 31 and 32 are typical of micrographs of copper sliding against both steel and Inconel. The coefficient of friction in this period (100 to 1000 cycles) reamined fairly constant for both systems, and there was no apparent metal removal by wear particle formation or transfer. The depth of the heavily deformed region in this stage ranged from about 2 to 4 μm. The nature of the subsurface changes in the early stage of sliding was the same for copper sliding against either steel or Inconel. At this stage, the deformed regions in the copper bearing surface result from the deformation of the asperities, and the resultant depth of this deformation would take on characteristic dimensions of the initial surface relief. The subsurface may also be deformed by high spots of the counterface plowing the softer copper surface. The contribution of counterface plowing to subsurface deformation was minimized in this study by the use of relatively smooth, hard counterfaces. The depth of deformation from plowing was expected to be about 0.1 μm. In essence, the depth of deformation observed during the early stage of sliding probably depends on the scale of the initial roughness of the copper bearing surface and also on the method used in surface preparation (see Figure 33).

Intermediate Stage

In the intermediate stage (10,000 cycles) of sliding on steel, both surface roughening and wear of copper increased (Figures 34 and 35). The surface roughening was associated with metal removal (Figure 34) and with the formation of ridges or narrow plateaus (Figure 35). Between the ridges are undulations or grooves produced by the plowing or grooving action of the protruding counterface transfer metal. The heavily deformed regions in Figure 34 and the deformation layer in Figure 35 contain what appear to be many voids, coalesced voids, and microcracks that are of various sizes and depths from the free surface. The maximum depth of deformation (the defect layer) was about 6 μm when the coefficient of friction was about 0.21. These sections should be compared to the morphological nature of the copper wear tip shown in Figure 15 for copper sliding against steel. The surface view provides a clearer visualization of the forms of the free surface topography shown in the subsurface sections of Figure 35. Subsurface morphology and depth of deformation for copper sliding on Inconel during the intermediate stage was similar to that for copper sliding on steel in the later stage, except that the deformed regions were more


Figure 30 - Optical
Tip After 10,000
Height of
Defor

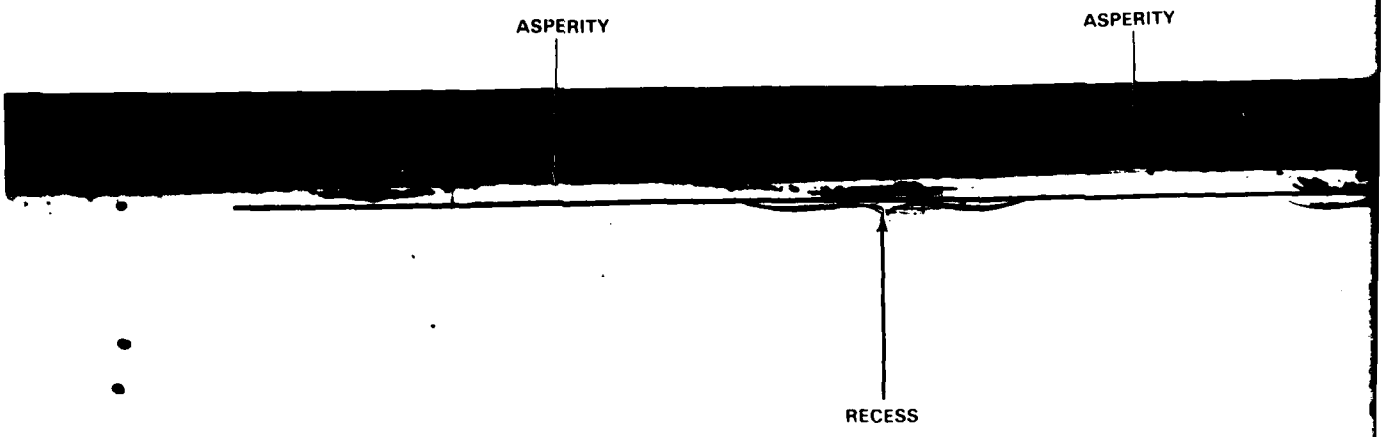


Figure 31 - Lo
Showing
Deforma
Recess

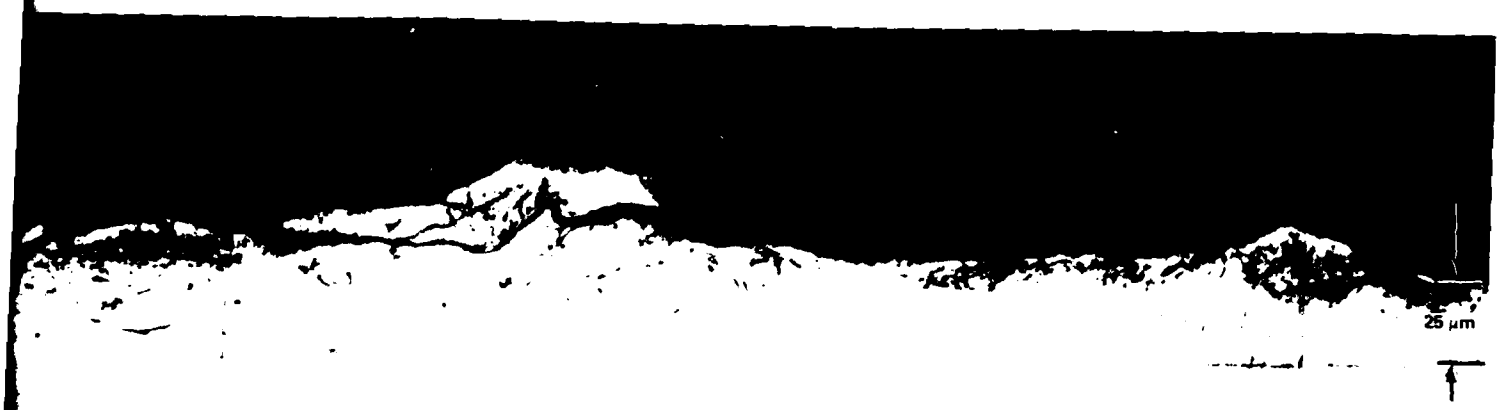


Figure 30 - Optical Micrograph of Transverse Section of a Copper Tip After 10,000 Cycles Sliding on Copper, Showing Maximum Height of Groove, Maximum Depth of Plastic Deformation, and Sheetlike Particles

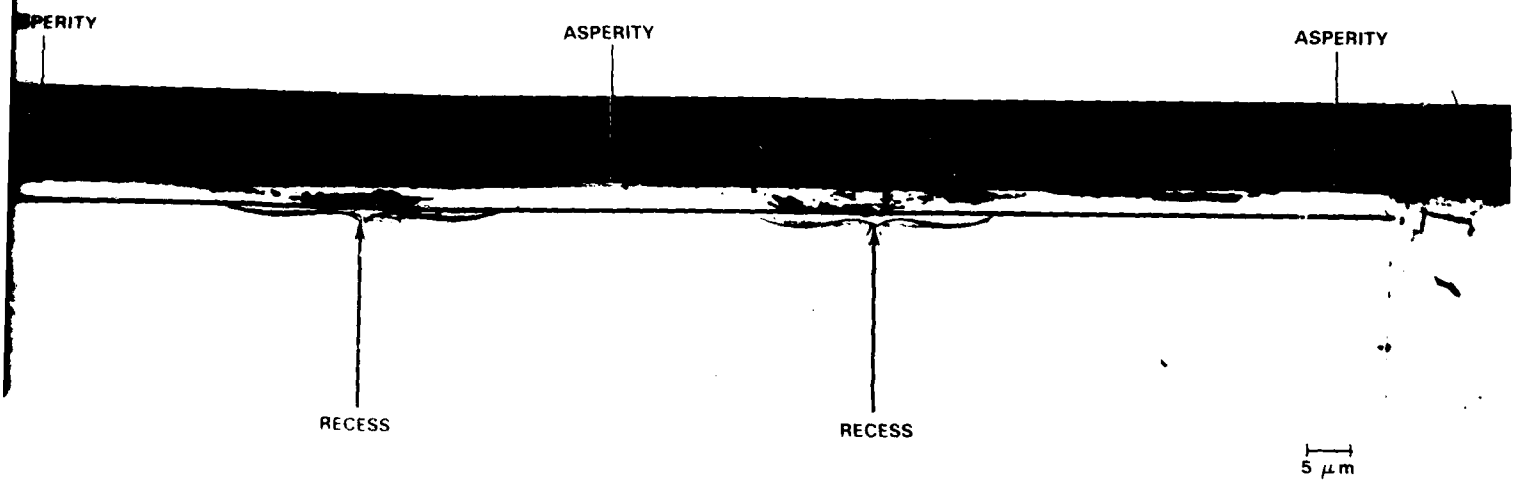


Figure 31 - Longitudinal Section (BEI) of Copper Bearing Showing Flow of Metal by Asperity (High Spot) Deformation Into and Across Sirface Relief Recesses During Very Early Stage Sliding

Figure 32 - Longi
a Well-Develo
Work-Har

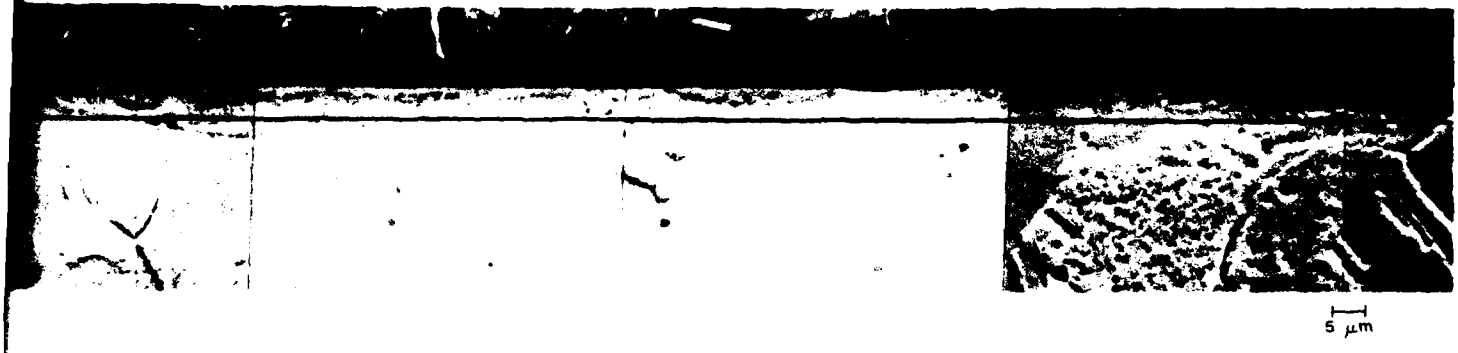


Figure 32 - Longitudinal Section (SEI) of Copper Bearing Showing a Well-Developed, Relatively Uniform, Thin, and Probably Work-Hardened Layer Produced During the Latter Part of Early Stage Sliding

widely spaced and slightly deeper. The depth of the heavily deformed region below the surface was about 8 μm, and the coefficient of friction about 0.24. No micrographs were obtained of subsurface deformation structures toward the end of the intermediate stage for the two combinations of sliding metals. However, the subsurface deformation was probably similar to that in the later stage of sliding.

Later Stage

In the later stage (50,000 cycles) the maximum depth of deformation for copper sliding on steel was about 9 μm. Figures 36, 37, and 38 clearly show the severe subsurface deformations associated with sliding under concentrated contact. Figure 38 is a secondary-electron image of Figure 37, and was included to show the general topographical nature of the deformed layer. Figure 38 better delineates the microcrack locations and sizes within the regions of heavy deformation and shows that the layer contains many microcracks of various sizes and at different depths, i.e., some are at the surface while others are below the worn free surface. Figure 36 shows a few shell-type wear particles lying on the surface and a particle about to separate (fracture) from the parent metal. This separation may be facilitated by the entrapment of wear debris in the plane of fracture. The subsurface damage to copper sliding on Inconel was similar to that found in copper sliding on steel, although the maximum depth of deformation, as shown in Figures 39 and 40, was much larger. The depth of deformation was about 14 μm, and the coefficient of friction was 0.34. This maximum value for the coefficient of friction for copper sliding on Inconel was larger than the maximum value of 0.24 for copper sliding on steel. Figure 40 also shows the separation of a large shell-like particle having a characteristic dimension similar to that observed for the platelike particle shown in Figure 20. The regions of heavy deformation in the copper bearing surface after sliding against Inconel are generally larger and more widely spaced than the regions found for copper sliding against steel, as can be seen by comparing Figures 36 and 40 (magnifications are not identical).

The deformed regions observed in the transverse sections were approximately semicircular, with the widths of deformation roughly corresponding to the transfer-patch width (compare Figures 40 and 41). In general, the distribution of both width and depth of the region of heavy deformation was narrower in copper sliding on steel than in copper sliding on Inconel (Figures 35, 36, and 40). This distribution was caused by the discrete nature of contact, and it was clearly evident in the

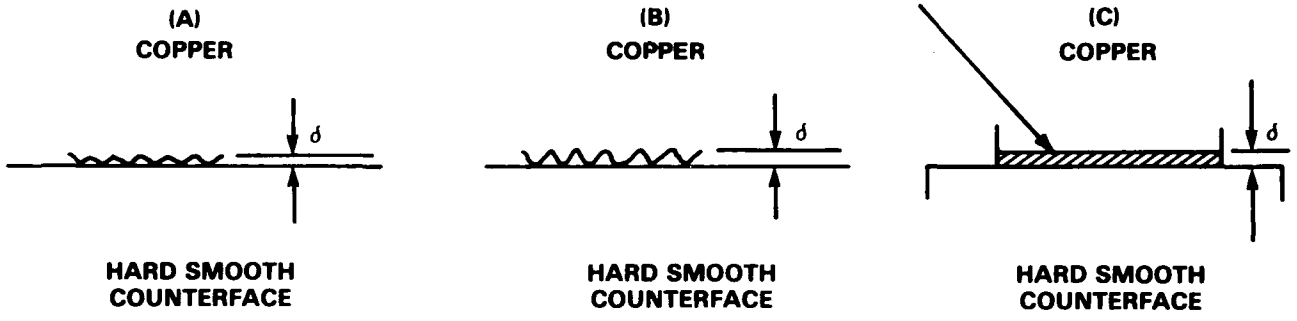


Figure 33 - Scale of Subsurface Deformation ($\delta$) in Copper Bearing That Might be Expected From Initial Bearing Surface Finish and Method of Sample Preparation. (A) Smooth Finish; (B) Rough Finish; (C) Defect Layer Produced by Initial Polishing

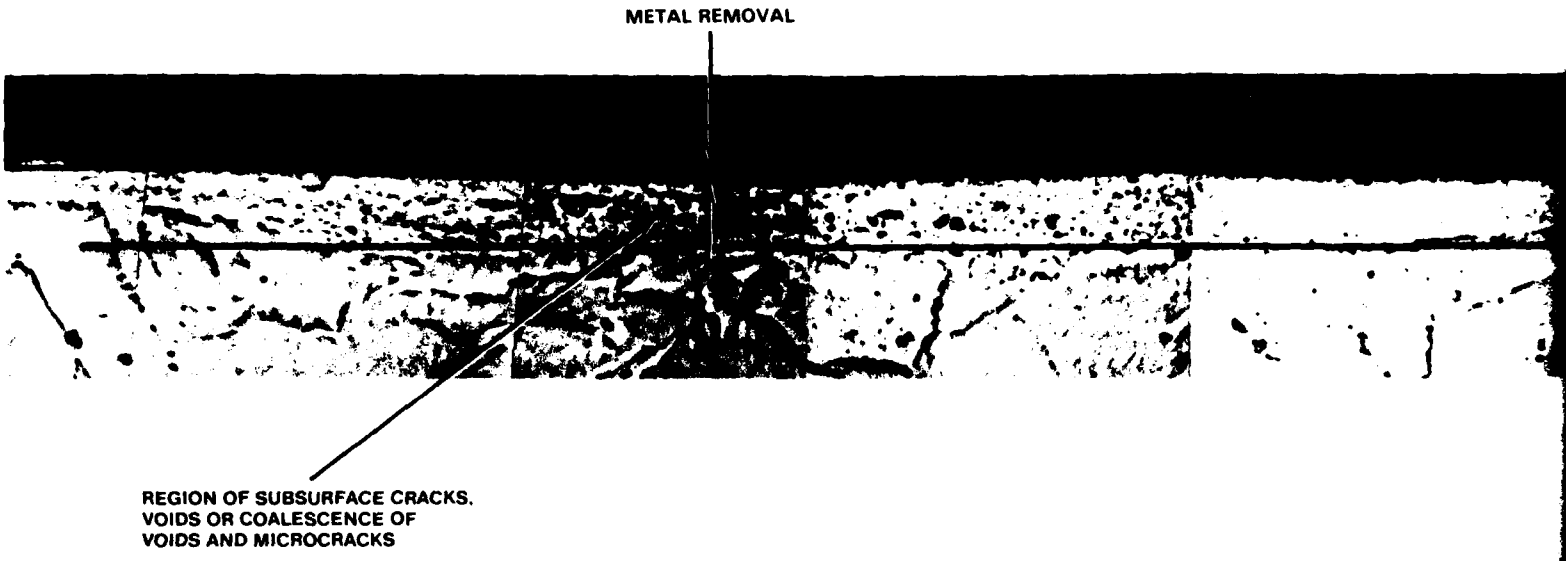


Figure 34 - I
Inter
Cont

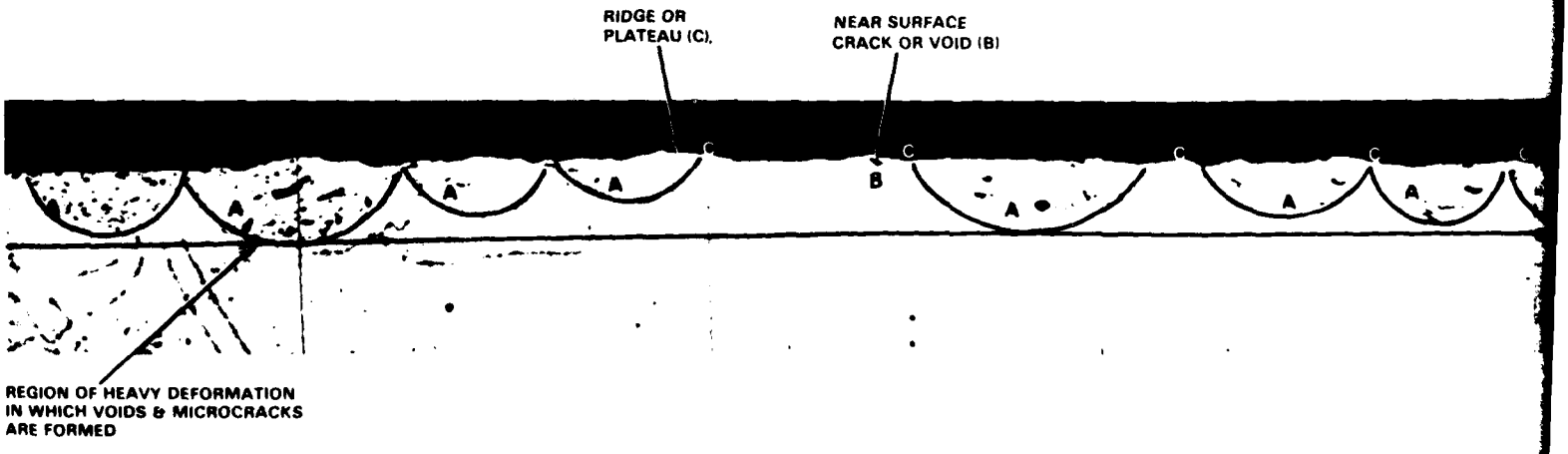


Figure 35 - Tr
mediate S
Nature
Deforme
(B) Nea

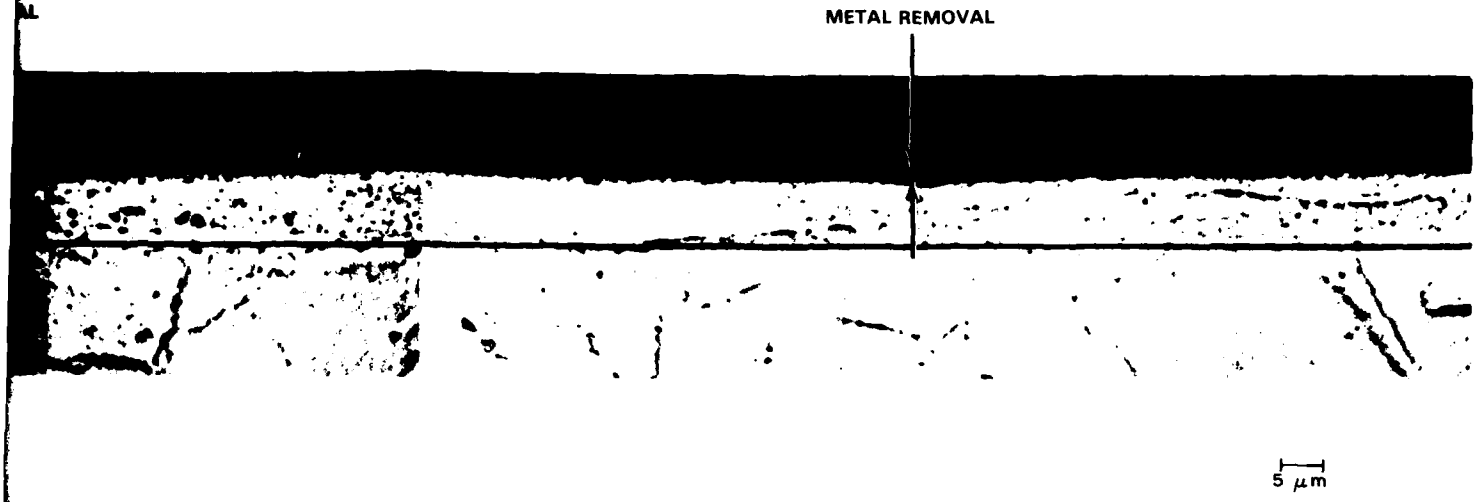


Figure 34 - Longitudinal Section (BEI) of Copper Bearing at Intermediate Stage of Sliding on Steel, That Contains Voids and Void Coalescence, Microcracks and Areas of Metal Removal

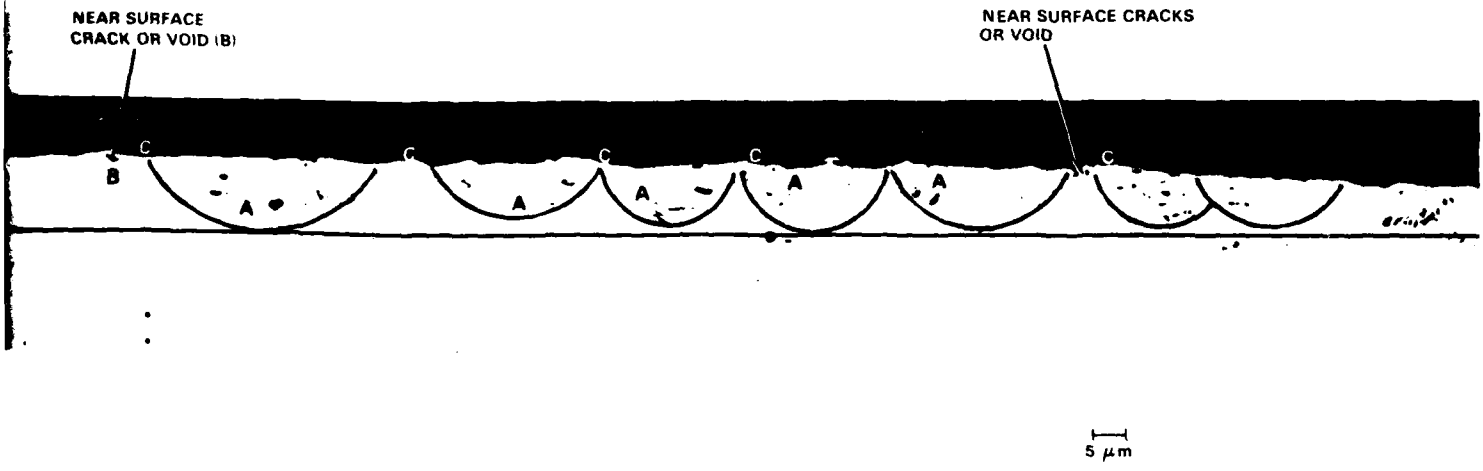


Figure 35 - Transverse Section (BEI) of Copper Bearing at Intermediate Stage of Sliding on Steel Showing the Discrete Nature of Contact and Regions of Heavy Deformation. Deformed Regions Contain (A) Voids or Microcracks, (B) Near-Surface Cracks and (C) Ridges or Plateaus

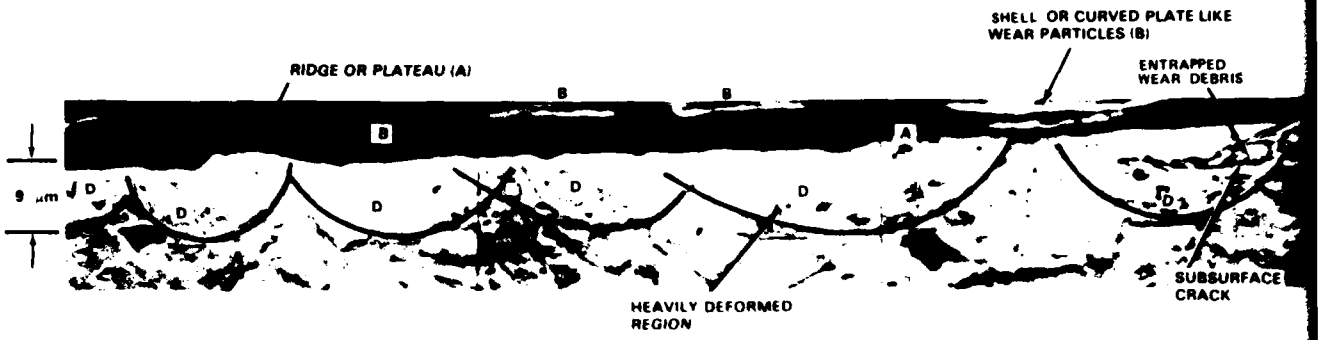


Figure 36 - T
of Sli
(A) R
Part
tat


Figure 37 - Lon
Sliding on
Contai

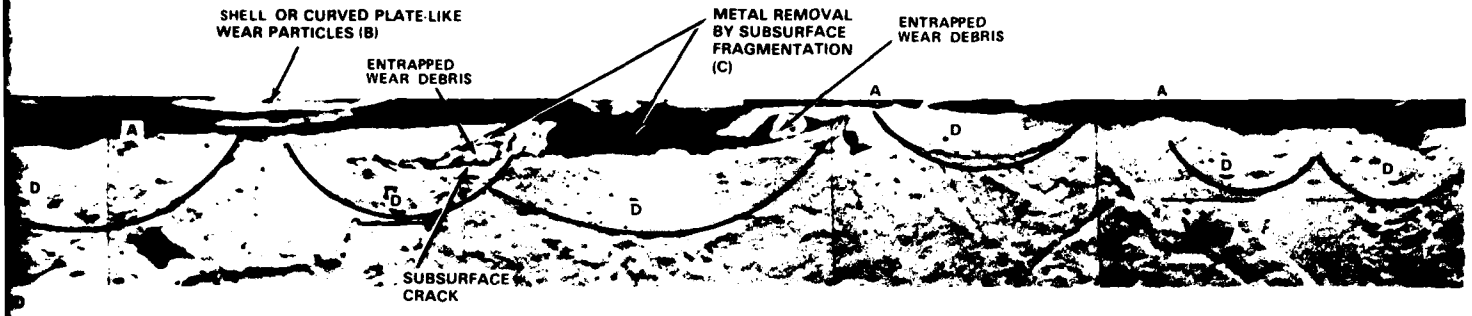


Figure 36 - Transverse Section (SEI) of Copper Bearing at Later Stage of Sliding on Steel, Showing Heavily Deformed Regions. (A) Ridges or Plateaus, (B) Shell- or Platelike Wear Particles, (C) Metal Removal by Subsurface Fragmentation, and (D) Regions of Very Heavy Deformation

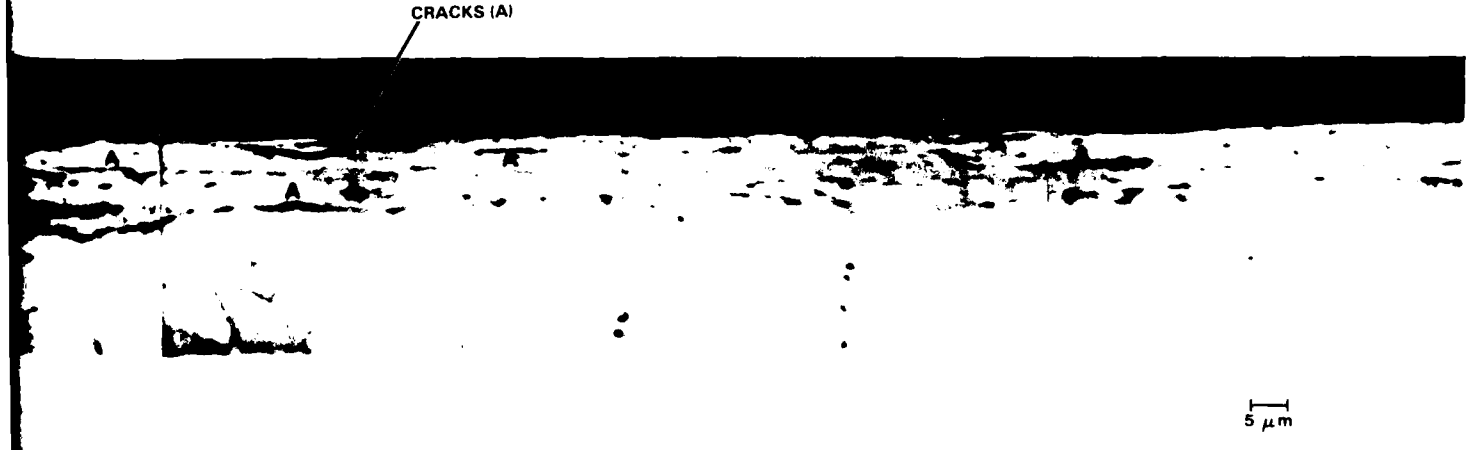


Figure 37 - Longitudinal Section (BEI) of Copper Bearing in Later Stage of Sliding on Steel, Showing That Heavily Deformed Layer of Figure 36 Contains Many Cracks Oriented Parallel to and at Various Depths From the Surface


LONGITUDINAL SECTION (PARALLEL TO DIRECTION OF MOTION)

Figure 38 - L
Stage on St

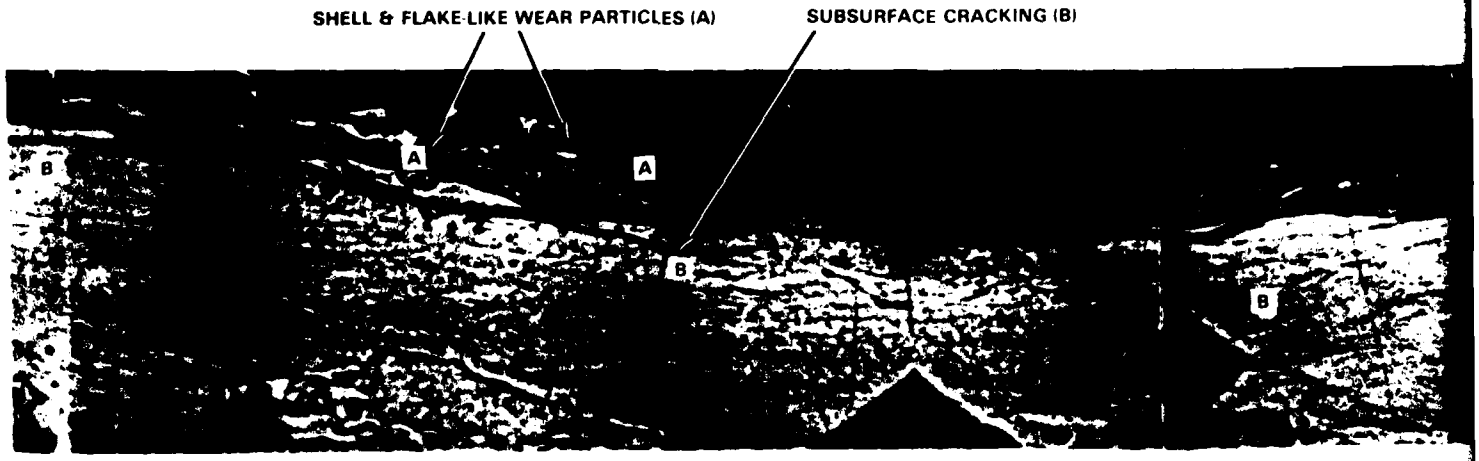


Figure 39 -
Stage of S

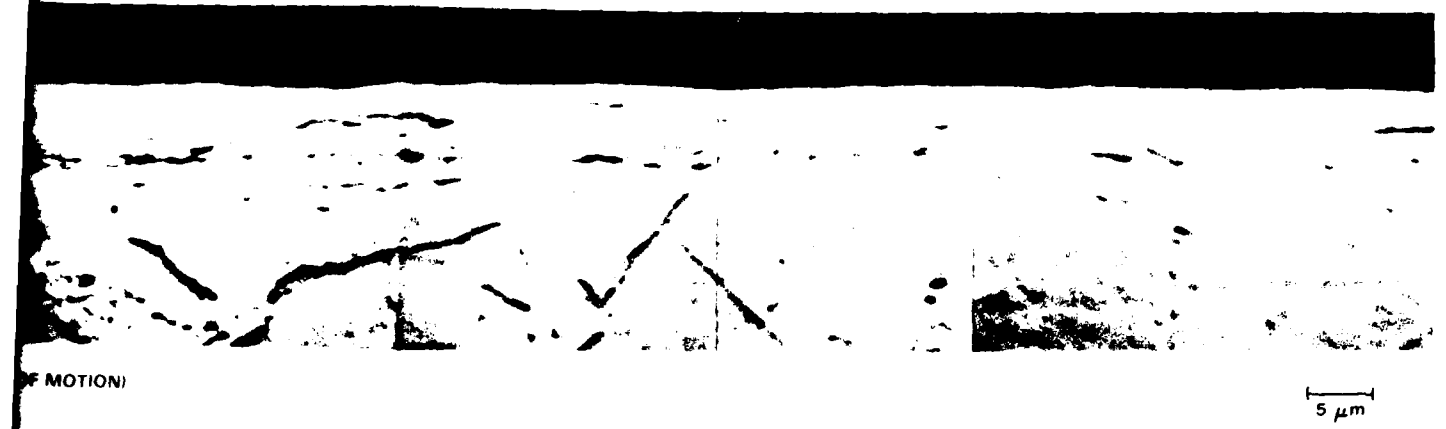


Figure 38 - Longitudinal Section (SEI) of Copper Bearing at Later Stage on Steel, Showing Morphology of Heavily Deformed Layer

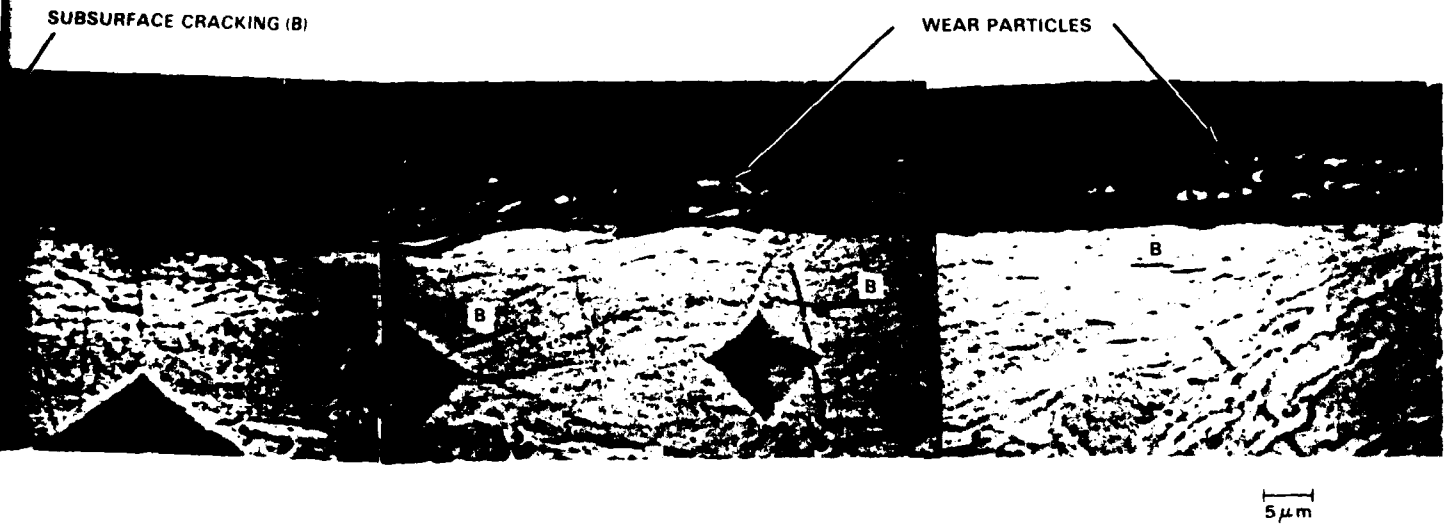


Figure 39 - Longitudinal Section (BEI) of Copper Bearing at Later Stage of Sliding on Inconel, Showing Heavily Deformed Region. (A) Many Shell- and Flakelike Particles and (B) Subsurface Cracking

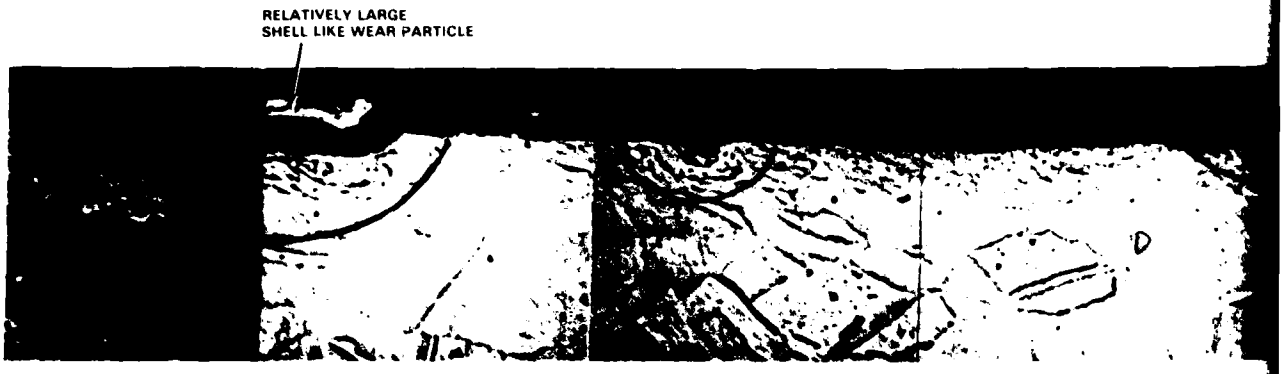


Figure 40 - Tra
on In
Sh

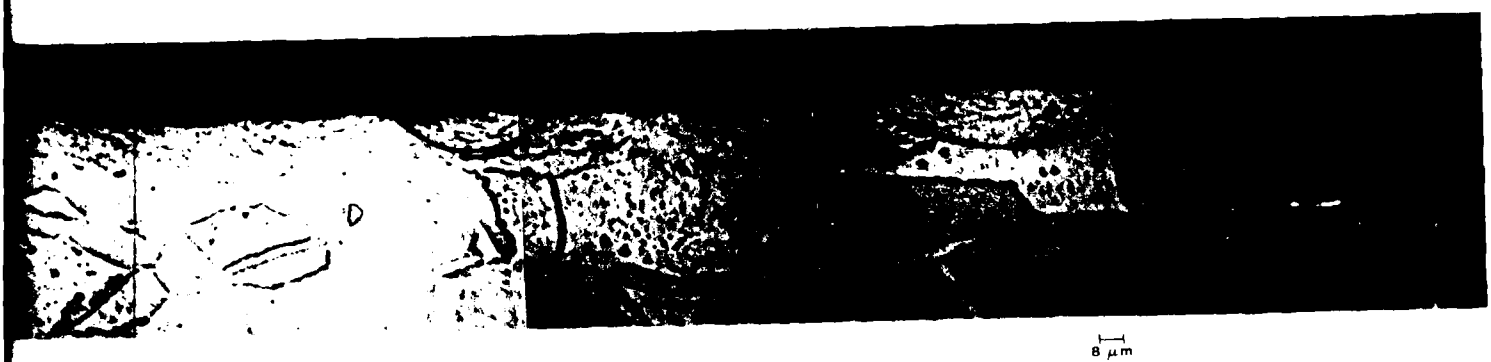


Figure 40 - Transverse Section (BEI) of Copper Bearing at Later Stage of Sliding on Inconel, Showing Heavily Deformed Regions. Relatively Large Shell-Like Wear Particle has Separated From the Surface.


Figure 41 - Copper Transfer to Inconel Counterface Showing That the Transfer Patch Widths in Later Stage Wear Roughly Correspond to the Widths of Deformed Regions Shown in Figure 40

intermediate and later stages of sliding, where a greater degree of nonconformity of contact resulted from metal transfer. Because of the variation in depths of deformation produced by nonuniform contact, load concentration, and strain, longitudinal sectioning is less reliable than transverse sectioning for obtaining the maximum depth of deformation ($\delta_m$).

## RELATIONSHIP OF DEPTH OF DEFORMATION ($\delta_m$) TO COEFFICIENT OF FRICTION ($\mu$)

A plot of the maximum depth of the very highly deformed regions ($\delta_m$) as a function of the coefficient of friction ($\mu$) is shown in Figure 42. The maximum depth of deformation below a free surface was selected because it can be identified using the height of the largest nonconformities produced by transfer, and it probably better represents the most recently developed deformed regions. Of course, the criteria used by the observer in various studies for identifying the depth of this heavily deformed region can differ greatly, and these criteria will greatly affect any comparison of values among studies. Figure 42 shows that the maximum depth of deformation increases with increase in the coefficient of friction. From these data both a linear relationship and a second power relationship between the depth of heavy deformation and the measured coefficient of friction can be derived as shown. Developing the proper functional relationship would require more data, particularly in the low friction area ($\mu<0.1$). A similar trend showing the increase in the average depth of heavy deformation with increasing coefficient for other copper-base metals is presented in Figure 43. Data in the figure were replotted from Blau[16], Table 1, for copper-zinc and copper-nickel alloys. Data for steels sliding on steel also appear to follow the same trend (Blau[16], Table 1). One exception to the general trend was found in a copper-aluminum system, where an increase in the aluminum content from 3.2 or 3.5 weight percent to 7 weight percent showed a larger depth of deformation with a smaller coefficient of friction. This exception probably resulted from a change in either the mode of deformation or the nature of wear. Also included in Figure 43 are data obtained from the present study and from Ives[28] for copper sliding on steel.

In general, results of this and other studies have shown that either the maximum or the average depth of deformation increases with an increase in the coefficient of friction.

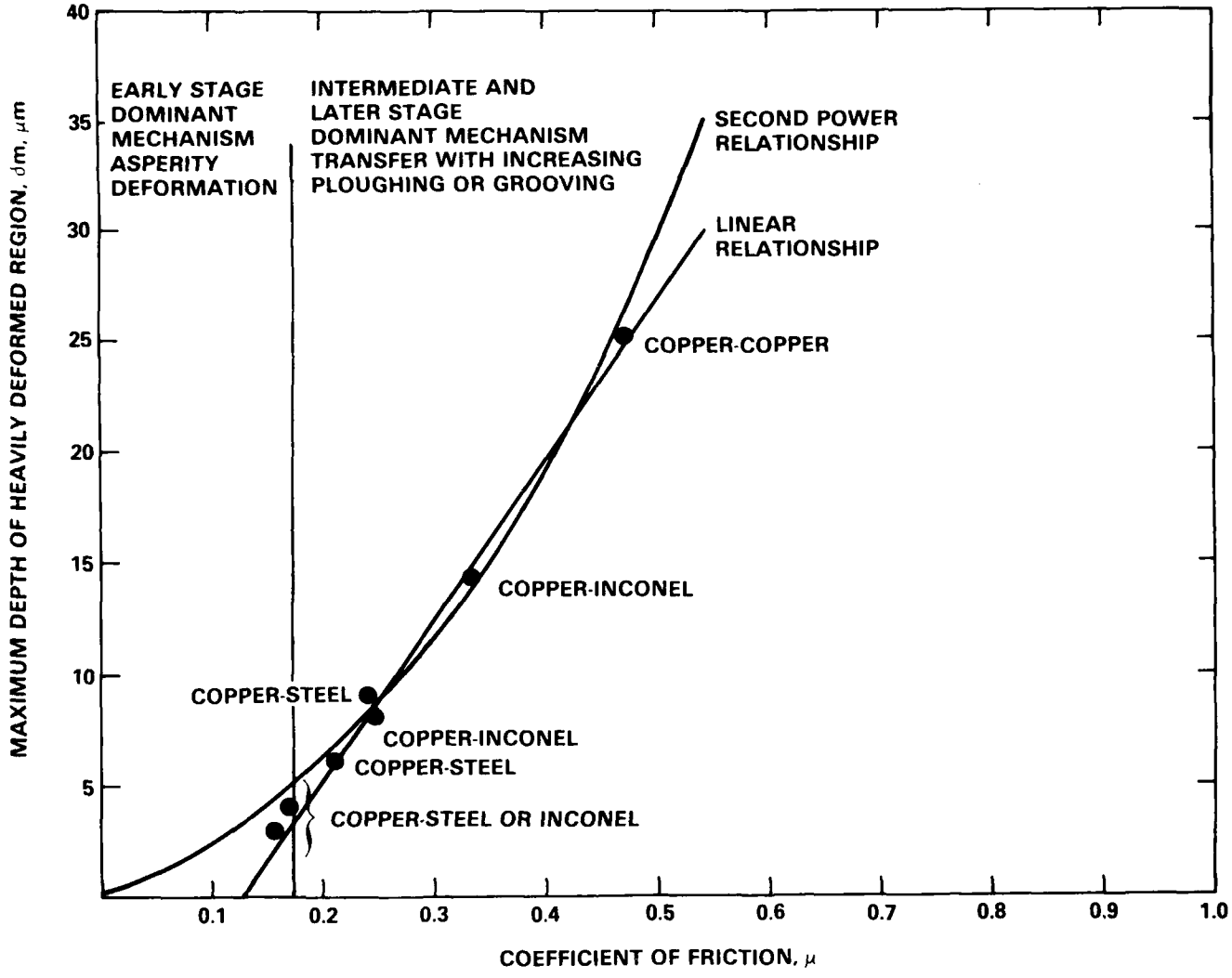


Figure 42 - Maximum Depth of Very Heavily Deformed Region ($\delta_m$) as a Function of the Coefficient of Friction ($\mu$)

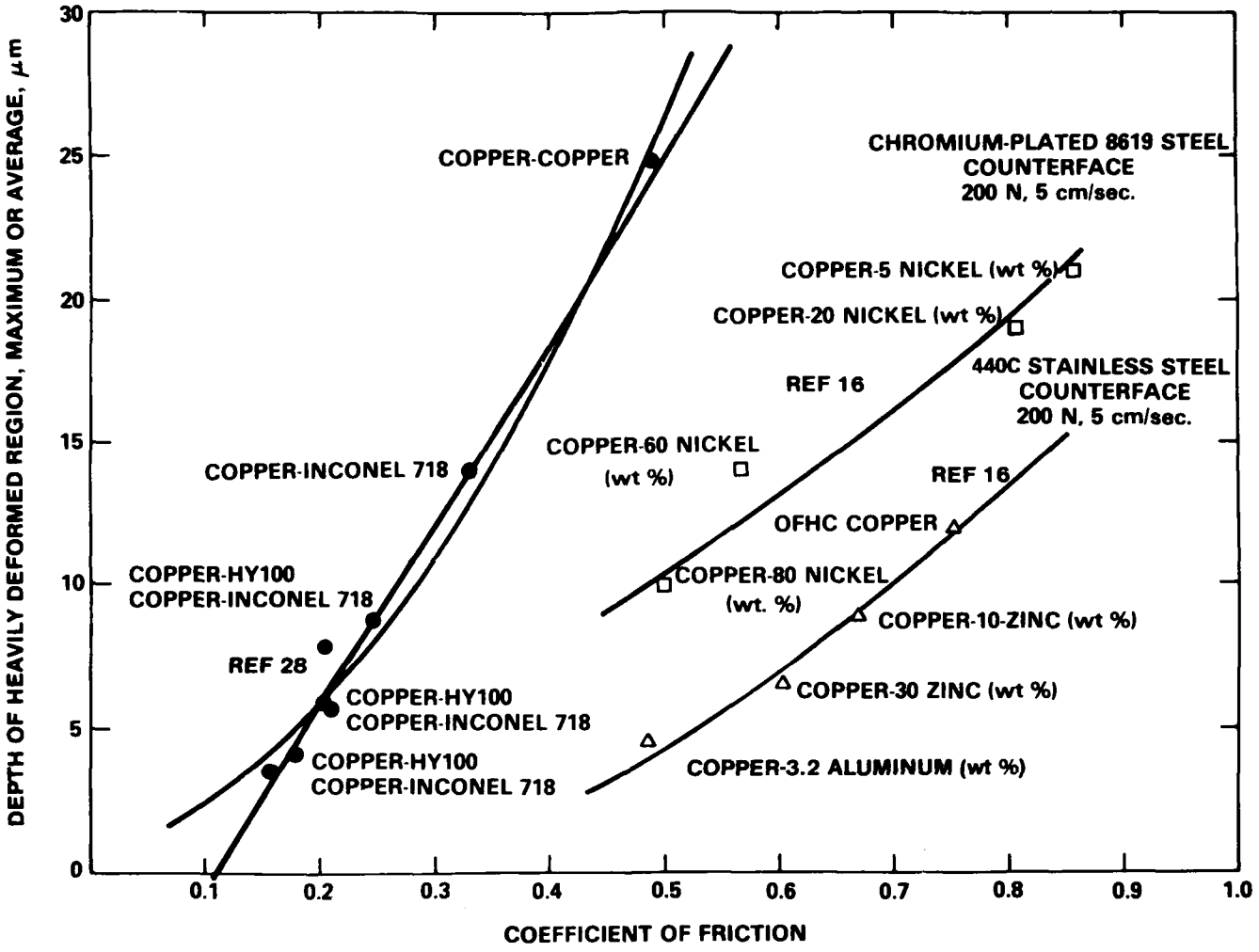


Figure 43 - Maximum Depth ( $\delta_m$ ) or Average Depth ( $\delta_a$ ) of Heavily Deformed Region as a Function of Coefficient of Friction. Data from this Investigation, Blau[16] (Table 1, p.191) and Ives[23]

## CRACK LOCATION, DISTRIBUTION AND MICROCRACK GROWTH

A review of all cross sections obtained in this investigation suggested that the prevalent location for crack (or defect) formation is below the rubbing surface. This result was not unexpected, because contacts were concentrated so that the maximum shear strain would be located below the surface and because a hydrostatic compression stress field was superimposed, which would inhibit near-surface void formation, void coalescence, and microcrack formation. The nonuniformity in crack sizes, i.e., length, depth, and distribution, when viewed in the longitudinal cross sections, might be explained by the fact that this section is only one of many that could have been taken through a heavily deformed region. The observer actually sees cracks that are at different distances from the location of maximum subsurface stress. When viewed in this section the cracks were orientated parallel to the sliding surface (see Figure 38, for example). In the transverse sections the cracks appeared as curved segments (arcs) and seemed to follow the deformation flow paths toward the free surface. Here again, the cracks in these sections were nonuniform in both depth and length. This is explained by the fact that in a wear test the localized concentrated load is changing both in time and space with changes in contact topography-- an explanation that is equally applicable to the nonuniformity in crack distribution seen in the longitudinal sections. When a crack in the transverse section propagates to the contact surface, it acts as a precursor for the formation of a shell-type (commonly called platelike) wear particle (shown in Figures 36 and 40). In this regard, models provided by Suh and coworkers[15] and Hirth and Rigney[29] for crack propagation parallel to the surface (as seen in longitudinal sections) only partially describe the three-dimensional nature of crack growth leading to platelike wear particles. To completely separate the particle from its parent metal, tensile forces would be required. Tensile force may be provided by the surface tractions produced at the sliding interface by the rubbing contact. The effective force for separation probably need not be very large, because of the many "large" subsurface cracks or defects present near the worn or free surfaces and the semi-brittle nature of the heavily deformed metal.

## CONTACT GEOMETRY AND LOAD DISTRIBUTION PRODUCED BY SLIDING

In the early stage of wear the dominant mode of deformation led to a smoother and more conforming geometry, but the forces that produced this conformity also strain-hardened the bearing surface. As a consequence, the contact loading and

stresses were more uniformly distributed. The wear and friction coefficient were low. Paradoxically, however, if the geometry was "too" conforming, a localized concentrated contact sometimes caused a large affected region of intense high load and stress to develop. This resulted from the inability of the soft contact metal to readily flow (because it had no place to go) to relieve the imposed load build up. In addition, if a wear particle formed in this circumstance, its ability to escape the conforming contact geometry was very limited, and a relatively large localized region of high wear ensued. Other plausible explanations advanced for this paradox are (1) that very smooth surfaces lose the ability to store contaminants or wear debris because they lack the valleys found between the relatively large asperities of a rough surface and (2) that smooth surfaces may result in higher molecular interaction forces, because more area of the two surfaces is in close proximity, where the greater attractive forces can contribute to wear.

In the intermediate and later wear stages (where the copper surface cannot sustain much deformation before fracture) metal transfer occurred. As a result of the transfer and its growth, the surfaces became rougher (plowing produced grooves) which further increased nonconformity of contact. The nonconformity of contact increased both the tendency for load to concentrate and the associated growth of the zone of high localized stress. These concentrations in load enhanced the possibility for high localized strain and large-scale fragmentation, which is accompanied by the formation of large platelike wear particles. The wear and the coefficient of friction increased.

## MICROHARDNESS MEASUREMENTS

To obtain a measure of the extent of plastic deformation and strain-hardening which had occurred, microhardness measurements were used. The general trend observed for copper sliding of both steel and Inconel was an increase in surface hardness with test duration (Figure 44). Because of the discrete nature of contact, a cumulative distribution functional relationship for percent of work-hardened surface is operative.

### Early Stage

The relatively low hardness observed in this stage is attributed to (a) the thinness of the work-hardened layer formed, which probably results from the

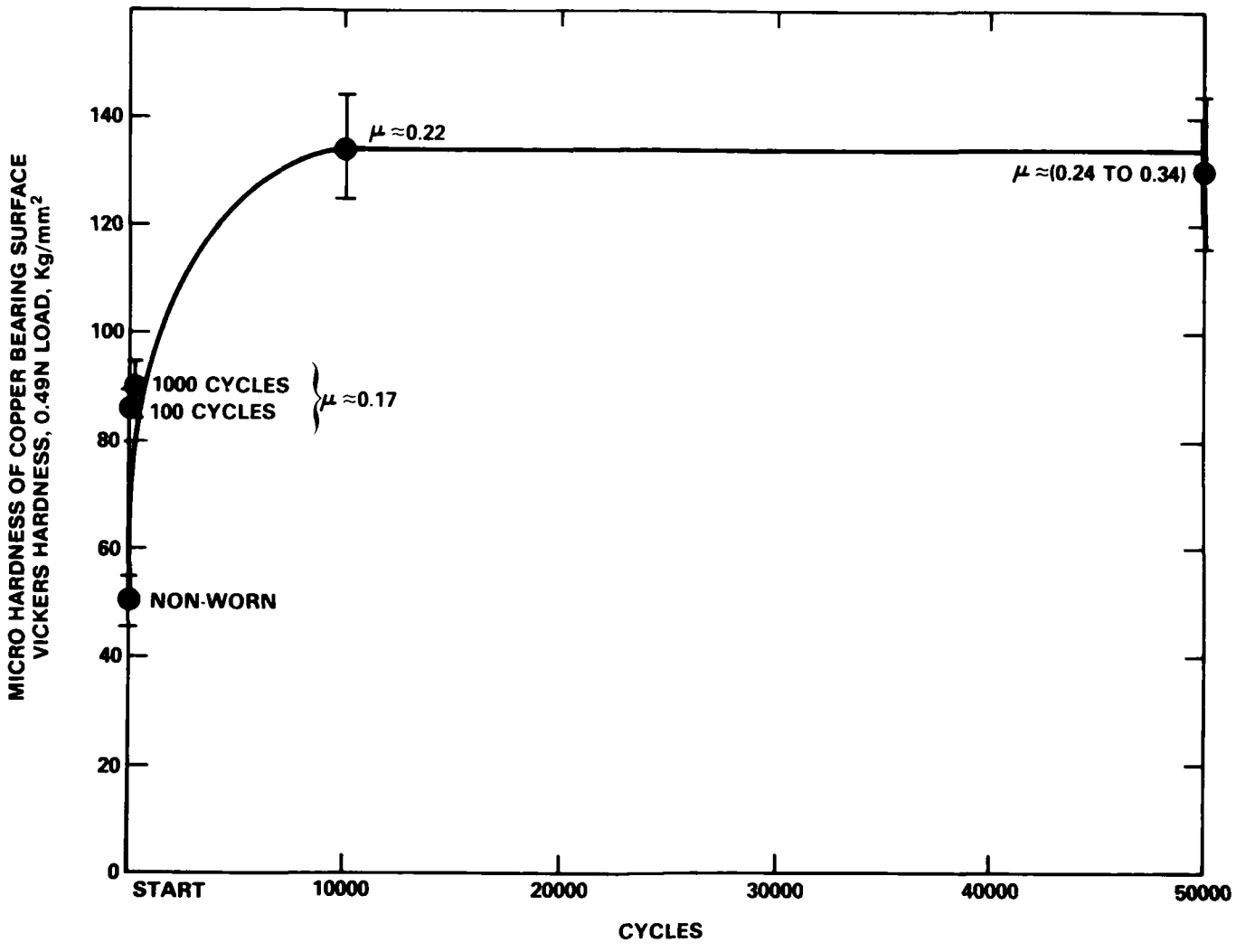


Figure 44 - Change in Copper Bearing Surface Microhardness With Sliding Distance and Surface Conditions for Copper Sliding Against Steel or Inconel

relatively low coefficient of friction, (b) the lack of complete sliding contact between the copper tip and the counterface, and (c) the voids trapped below the rubbing surface.

Intermediate Stage

A relatively thick layer of deformed metal was formed, the voids were essentially eliminated, and the tip was placed in "complete" rubbing contact. The surface damage in this stage, although similar to that in the later stage, was not as severe. As a consequence the least variable and highest nominal hardness was obtained.

Later Stage

In this stage the surface was severely fragmented and there was a larger scatter in hardness than in the intermediate stage. The highest hardness was equivalent to that measured in the intermediate stage and was representative of the hardness of a fully work-hardened piece of copper, about 1380 MPa (about 140 $kg/min^2$) Vickers Hardness at 0.49-N indentation load. In this stage hardness values were lower where large platelike particles had been removed. The hardness of about 1130 MPa in these areas was still much higher than of the unworn sample or the surfaces produced during the early stage of sliding. In all hardness measurements readings were highest where the largest amount of grooving had taken place. This observation suggested that the grooving produces both the largest amount of work-hardening and the largest depth of hardening.

Subsurface Microhardness Measurements

The only hardness value believed numerically reliable and characteristic of the heavily deformed subsurface region of the copper tip was obtained from a relatively thick region produced by copper sliding against Inconel for 50,000 cycles. The hardness values in this region were of the same order as the highest hardness determined by direct measurements of surface hardness. The increase in hardness (as indicated by smaller indentations) from the bulk undeformed metal toward the heavily deformed region is shown in Figure 45 for copper sliding on Inconel. A similar trend was observed for copper sliding on steel.

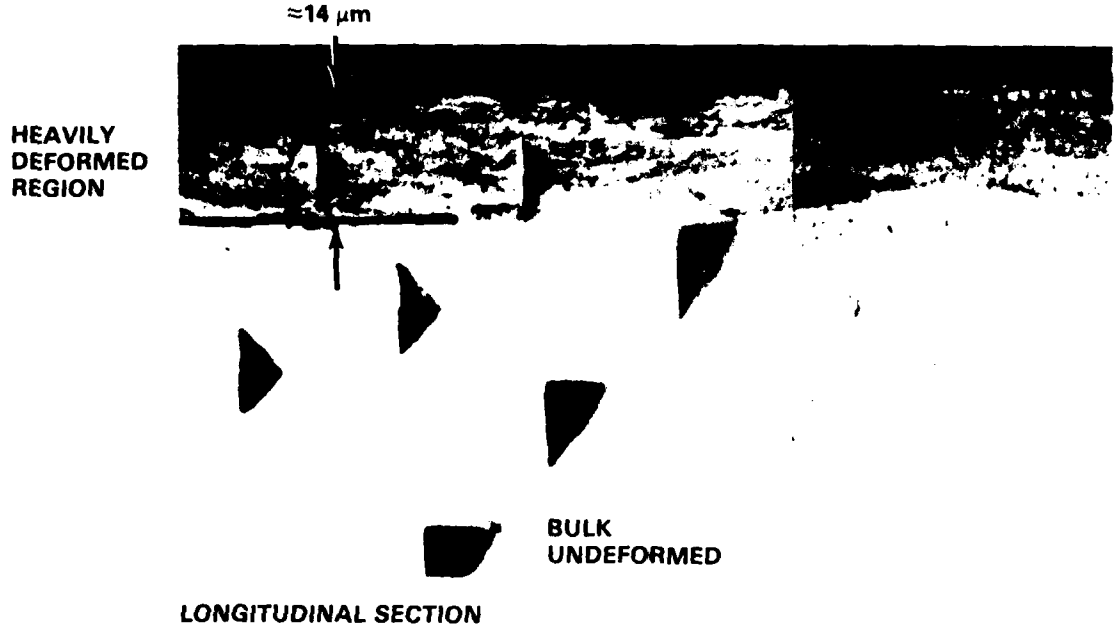


Figure 45 - Longitudinal Section of Copper Bearing at Later Stage of Sliding on Inconel, Showing Region Below the Rubbing Surface (Small Indentation Size Corresponds to Higher Hardness)

## X-RAY EXAMINATION OF WORN COPPER SURFACES

X-ray examination was used to follow the surface deformation produced in the copper bearing specimen during sliding. The X-ray technique indicated the degree of straining and the characteristic dimensions of the coherently reflecting domains, or cells produced by heavy deformation. The size of the cells obtained from X-ray experiments ranged from about 300 Å to 500 Å, with an average near 400 Å. These values are consistent with the experimental observation of Van Dijck's,[30] which showed a worn surface of copper consists of small grains or cells of about 250 to 600 Å. The dimensions of this cell can be scaled approximately to the effective stress used in developing the cell.[31] The effective stress and cell size are related by the following equation:

$$\sigma_e = \frac{Gb}{d} \tag{5}$$

where

$\sigma_e$ = effective stress

G = shear modulus or the modulus of rigidity

b = Burgers vector for copper = 2.6 Å

d = cell size in Å

Since the X-ray technique averages over the whole worn tip and does not concentrate on the most heavily-worked zones, the minimum cell size should be a more representative value for defining the stresses occurring within the heavily-deformed regions of copper. Using a value of 300 Å, stresses on the order of the ultimate strength of the copper were found to exist within the heavily-deformed region. It is therefore not surprising that, in this zone, many microcracks formed and subsequently grew and met the free surface, forming wear particles.

## SUBSTRUCTURE WITHIN THE ZONES OF HEAVY DEFORMATION

The substructure of the heavily-deformed region, as revealed by X-ray measurements and other reported data for worn copper, suggests that it is cellular[28,31] structure containing a high dislocation density and very large localized

microstrains. The cell structure is typical of the microstructures developed in metals subjected to high stress and large strains at relatively low temperatures. The cell structure can present many suitable regions for void formation, void coalescence, and microcrack formation, with or without second-phase inclusions. The X-ray measurements revealed very high microstrain gradient across the cells, or coherently reflecting domains.

## MECHANISMS OF WEAR PARTICLE FORMATION

At least five possible sources of wear particle formation and debris generation sites were identified. They are

(1) particles generated as a direct consequence of asperity deformation, which are flake-like (Figures 28 and 29).

(2) Particles that are produced by the following steps: (a) a groove is produced (b) a ridge forms at the side of the groove, (c) the ridge contacts the counterface and load is transferred, (d) the ridge deforms, causing the ridge metal to flow both in the direction of motion and perpendicular to it (material will flow into the nearest free space (the groove) to the side and beneath the top edge of the deforming ridge), (e) if the groove is relatively deep and wide and the metal produced by the ridge deformation is work-hardened, the deformed edge of the plateau formed will receive marginal support from the underlying substrate or groove bottom and will therefore break off after repeated load application. This second type of wear particle formation is similar to that proposed by Koba and Cook.[32] Although they proposed this mechanism for the early stage of wear, I observed it in all stages (see Figures 10, 15, and 46). Similar particles may be produced as a direct result of plowing (Figure 47). Ives[28] called this possible source of wear particles grooving lips.

(3) Shell-, plate-, or sheetlike particles produced by repetitive concentrated load sliding on surfaces that may be plateaus, ridges on original contact surface (see Figures 20, 26, 30, and 40).

(4) Transfer of metal to counterface depressions by plastic flow, where it becomes mechanically interlocked, and is subsequently separated from the parent metal by sliding (Figures 16, 17, and 22).

(5) Fragmentation of the transfer patch or, possibly, removal of a patch in its entirety (Figure 48).

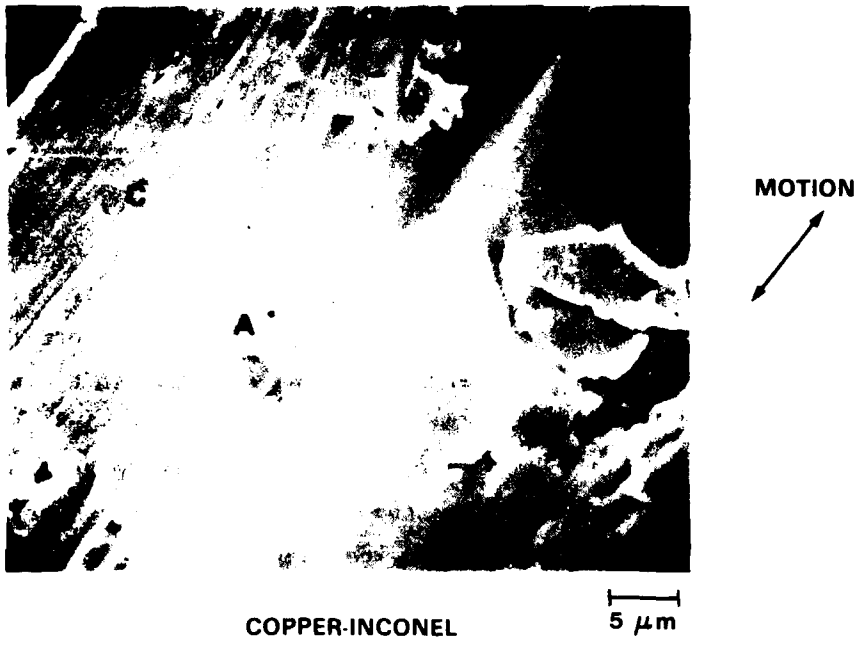


Figure 46 - Worn Copper Bearing Surface at Late Stage of Sliding on Inconel, Showing Mechanisms of Wear Particle Formation. (A) Edge Particle, (B) Groove, and (C) Deformed Ridge or Plateau

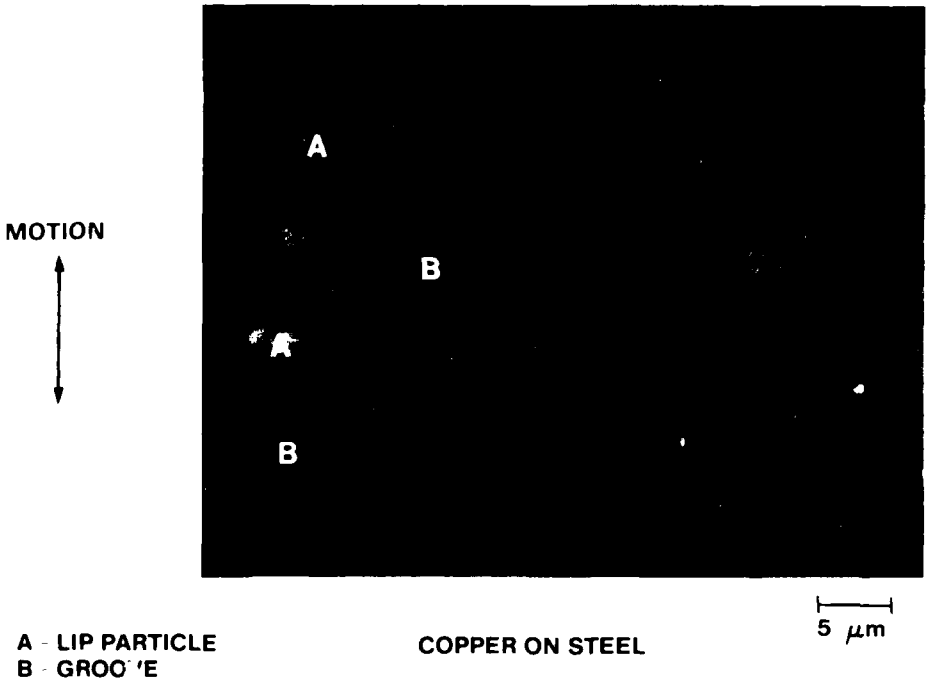


Figure 47 - Lip Particle Formation on Copper Bearing as a Direct Result of Ploughing and Grooving

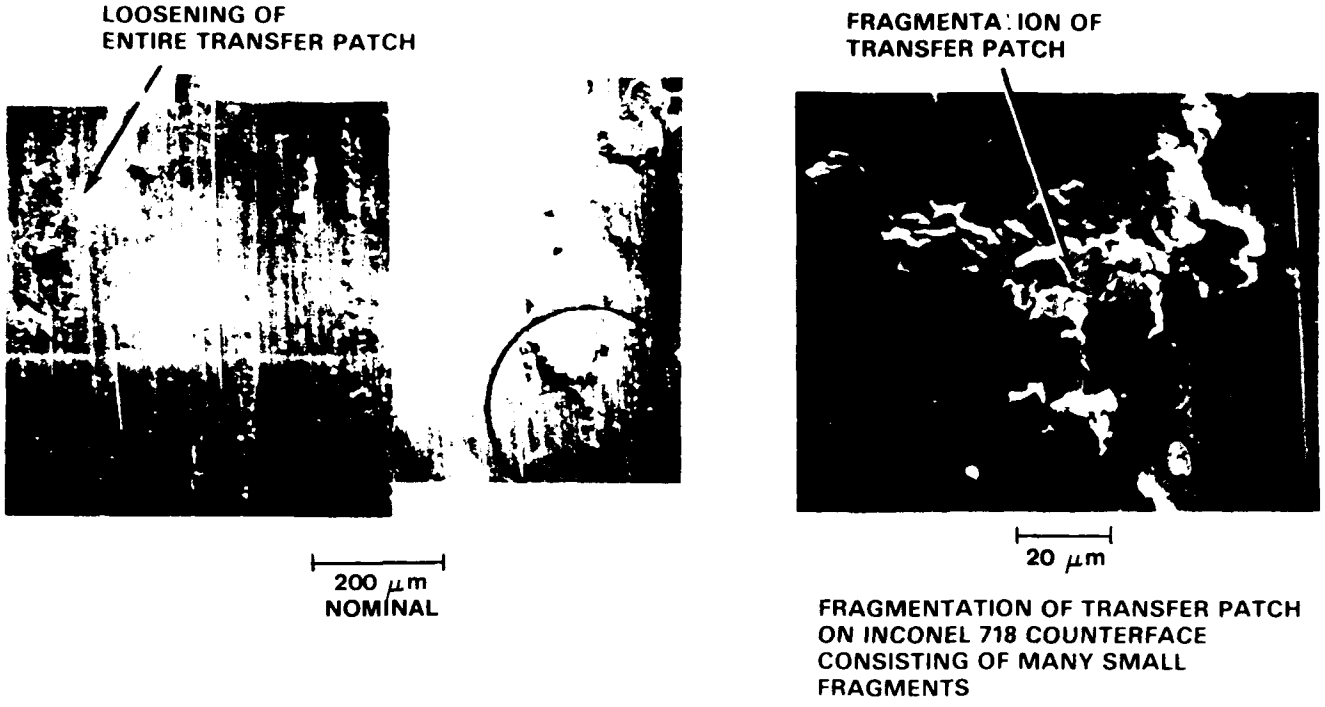


Figure 48 - Fragmentation of a Transfer Patch and Possible Removal of a Patch in its Entirety

Examination of collected wear debris in the SEM revealed particles having a wide range in morphologies. No evidence of the microchip formation characteristic of abrasive wear was found.

## COEFFICIENT OF FRICTION VS. DURATION OF SLIDING - FURTHER OBSERVATIONS

The coefficients of friction vs. duration of sliding for this investigation are plotted in Figures 9 and 26. The shape of the friction curve shown in Figure 9 held when two dissimilar metals were slid against each other. This behavior is completely contrary to that reported by Suh and Sin,[21] whose friction-time data were obtained in a crossed-cylinder geometry. These authors also stated that the behavior found in Figure 26 (copper sliding on copper) "can result only when the hardness of the stationary slider is much greater than the moving specimen," whereas Figure 26 was obtained for two like metals sliding against each other. These completely contradictory findings illustrate that the diversity of different sliding situations currently defies modeling and that any extrapolation of wear and frictional behavior beyond experimental data is questionable. Three other noteworthy findings from this study are shown in Figures 49 and 50. Figure 49a shows results when the test was stopped, the specimens separated (1 hr to 1 day), the specimens returned to contact, and the test resumed. The figure shows that upon resumption of test the friction vs. cycles curves followed the same path. Figure 49b shows results of another variation in test procedure, in which the test was stopped, the specimens separated, the copper contact surfaces moved to make contact on a new portion of the counterface, and the test resumed. In this test the coefficient of friction did not resume the same path upon resumption of test; it dropped to the initial value of the coefficient of friction characteristic of two new specimens placed in contact. The change in coefficient of friction upon resumption of test increased faster, however, than when a fully annealed new sample was employed. These results suggest that the counterface topographical characteristics may be the more significant factor in controlling the coefficient of friction, although a preworn sample can wear and transfer metal, and consequently change the initial counterface topography faster than an unworn sample (at least in the early stage of sliding).

Another variation of test procedure showed the effect of removing loosely adhering wear particles on the coefficient of friction time curves. Results are shown in Figure 50. In this variation the test was stopped, the specimens separated, and contact surfaces were lightly brushed to remove loose [illegible]

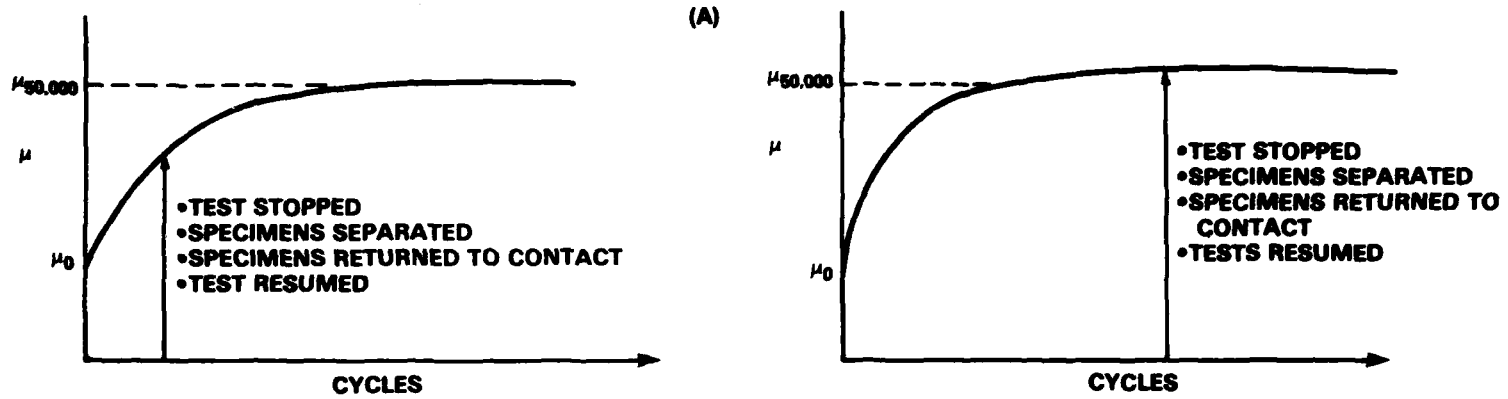


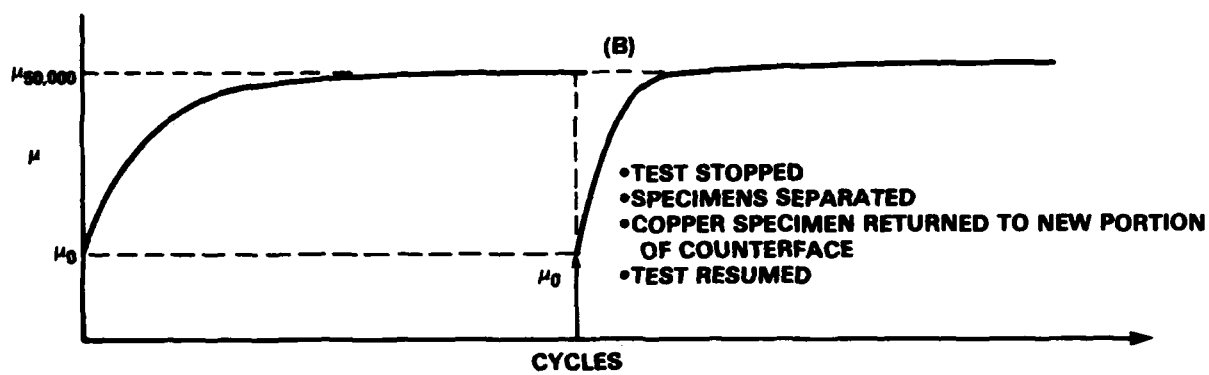


$\mu_0 \approx 0.16 \pm 0.03$

$\mu_{50,000} \approx 0.34$ COPPER SLIDING ON STEEL

$\mu_{50,000} \approx 0.25$ COPPER SLIDING ON INCONEL

Figure 49 - Typical Curves of Coefficient of Friction ($\mu$) vs. Distance of Sliding (Cycles), Showing Effect of (A) Interrupting Test, and (B) Interrupting Test to Move Worn Copper Tip to New Portion of Counterface

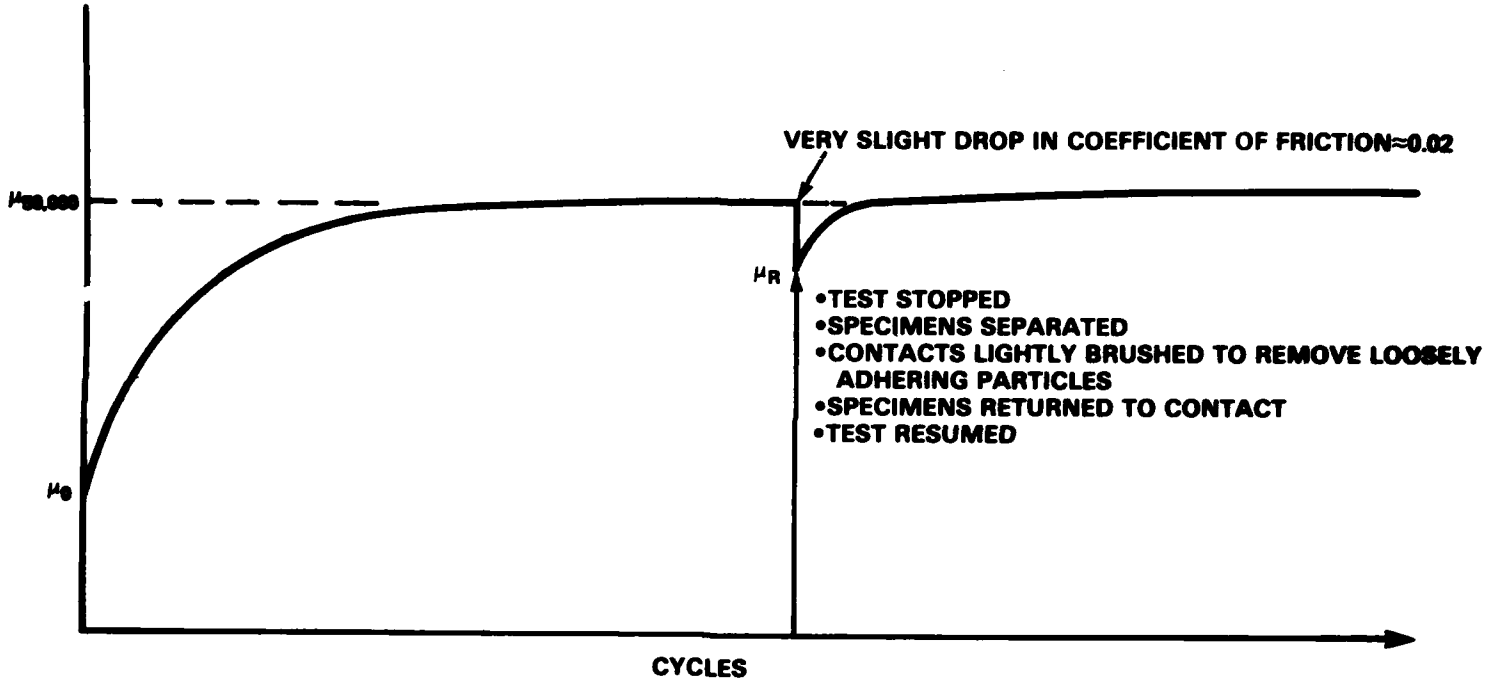


$\mu_0 = 0.16 \pm 0.03$

$\mu_{50,000} = 0.34$ COPPER SLIDING ON STEEL $\mu_R \approx 0.31$

$\mu_{50,000} = 0.24$ COPPER SLIDING ON INCONEL $\mu_R \approx 0.22$

Figure 50 - Typical Curve of Coefficient of Friction ($\mu$) vs. Sliding Distance (Cycles), Showing Effect of Interrupting Test to Remove Loosely Adhering Material by Light Brushing

material, the specimens were returned to contact, and the test was resumed. The figure shows that the coefficient of friction dropped only slightly, suggesting that for these sliding conditions the transfer metal is held together rather strongly, and that the removal of weakly adhering wear particles does not drastically reduce the coefficient on resumption of sliding.

## SUMMARY AND CONCLUSIONS

At least five possible sources of wear particle formation and debris generation sites were identified, but no evidence was found for microchips that would be characteristic of abrasive wear.

Wear particles and metal transfer play a major part in the wear mechanism. The wear particles have great difficulty escaping under conditions of flat, small-amplitude, reciprocating sliding. The decrease in the probability of wear particle removal has two mutually antagonistic effects: (a) the particles can agglomerate and grow, which changes load distribution and increases friction and wear, but (b) the agglomeration and growth of wear particles in the interface may protect the counterface, so that much of the work goes into deforming and fragmenting the existing entrapped debris rather than into producing new wear particles. The second effect is based on comparison with unidirectional tests currently under way, which employed the same sliding conditions and materials used in this study.

The buildup of the transfer patch by accumulation of wear particles leads to severe grooving and substantial roughening of the copper bearing surface. The buildup of the transfer patch and increasing penetration into the bearing surface increases the coefficient of friction, the depth of the deformed layer, and wear. The limiting factor in the buildup of the transfer patch is the strength of the initial attachment of the copper transferred to the hard counterface. This is believed to be dependent upon the size and shape of the surface depressions initially present or created during the rubbing process for copper sliding on steel or Inconel.

Initial transfer of copper to the steel or Inconel counterface takes place not by adhesive (solid-phase welding) transfer but by plastic flow of the copper into the valleys of the harder counterface. In the steel the initial grinding troughs are receptors for transfer, whereas in Inconel holes are formed during the rubbing process in the presumably hard brittle surface layer are receptors. Buildup of the transfer patch by the accumulation of wear particles may occur by an adhesional

process produced by continuous rubbing of the protruding transfer metal (copper) on itself or by mechanical means.

The heavily deformed regions in the copper bearing surface in the intermediate and later stages of sliding may be associated with the high localized load concentrations and surface tractions produced by topographical changes caused by transfer patch growth. The size of this heavily deformed region corresponds to the size of the patch, and in most cases the shape is semicircular. In contrast, the heavily deformed regions in the copper bearing surface that appear during the early stages of sliding may be attributed to the deformation of the asperities on the copper. The depth of this deformed layer takes on the characteristic dimensions of the initial surface relief. Other regions of heavily deformed metal can be produced as the harder counterface's topography plows the softer copper surface. The contribution of the counterface plowing to the formation of heavily deformed metal was minimized in this investigation by the use of a relatively smooth and hard counterface.

These tests also clearly identified the formation of a heavily deformed, fragmented region in the copper tip. These regions of heavy deformation receive stresses that are on the order of the ultimate strength of the copper. They are composed of cells which are subgrains or coherently reflecting domains of the original nondeformed grains. They also contain many voids, groups of voids, and microcracks, which may act as precursors of wear particle formation.

The size and maximum depth of the very highly strained deformed region are highly dependent on the coefficient of friction; they increase with an increase in the coefficient of friction, probably to a power greater than one. Determining the proper functional relationship will require more experimental data, particularly in the low friction region ($\mu<0.1$).

The size and depth of the plastically deformed region depend on both the coefficient of friction and the normal force. The coefficient of friction in the terms of this study is a direct measure of the frictional force, since a constant normal load was employed.

The results of this investigation suggest that the magnitude of the friction force or surface tractive forces may be more important than the normal forces in increasing the size of the zone of deformation.

Changes in the surface traction or coefficient of friction during sliding are probably caused by changes in the surface topography. In copper sliding on steel or Inconel, these changes in friction are dependent on the morphology of the transfer layer, its mechanical properties, and the adherence of the transfer material to the counterface metal. In copper sliding on itself, they are directly dependent on the topographic changes. Topographical changes vary the contact load distribution. A more conforming contact lowers friction and wear, while a nonconforming contact increases both friction and wear. The severity of wear depends not only on metal transfer itself, but also on the morphological and topographical changes developed during transfer. If the transfer is relatively uniform, wear is less severe. However, if the transfer is discontinuous and consists of relatively large particles, wear is more severe.

Wear is highly dependent on the coefficient of friction and is related to the coefficient of friction by a fourth power relationship.

The results of this investigation also suggest that the topographical changes produced by sliding may be more important to wear resistance than is the selection of material properties.

Finally, many conclusions of this study may apply to a variety of other metallic sliding systems. In a given situation a hard metal or a soft metallic film on a hard substrate may perform equally well by preventing topographical change and thus maintaining low friction and wear.

## REFERENCES


1. Tabor, D., "Wear - A Critical Synoptic View," Wear of Materials - 1977, W.A. Glaeser, et al., eds., Am. Soc. Mech. Eng., New York (1977).

2. Archard, J.F., "Contact and Rubbing of Flat Surfaces," Jour. Appl. Phys., Vol. 24, pp. 981-988 (1953).

3. Holm, R., "Electrical Contacts," Almqvist and Wicksells (or Gerbers), Uppsala pp. 214-221 (1964).

4. Burwell, J.T. and C.D. Strang, "Metallic Wear," Proc. Roy. Soc. (London), A 212, pp. 470-477 (1952).

5. Rabinowicz, E., "Friction and Wear of Materials," John Wiley and Sons, Inc., New York (1965).

6. Kerridge, M., "Metal Transfer and Wear Processes," Proc. Phys. Soc. London, B 58, pp. 400-407 (1955).

7. Kerridge, M. and J.K. Lancaster, "The Stages in a Process of Severe Metallic Wear," Proc. Roy. Soc., London, A 236, pp. 250-264 (1956).

8. Rabinowicz, E., "The Dependence of the Adhesive Wear Coefficient on the Surface Energy of Adhesion," Wear of Materials - 1977, W.A. Glaeser, et al., eds., Am. Soc. Mech. Eng., New York (1977) pp. 36-40. Budiansky, F. and McClintock, "Report of the ARPA Materials Research Council," p. 291, Univ. of Mich., Ann Arbor (1975).

9. Halling, J., "Toward a Mechanical Wear Equation," Presented at the Am. Soc. Lubr. Eng.-Am. Soc. Mech. Eng. Joint Lubrication Conference, New Orleans, (4-7 Oct 1981), Am. Soc. Mech. Eng. Paper 81-Lub-5 (in press).

10. Blau, P.J., "Interpretations of the Friction and Wear Break-In Behavior of Metals in Sliding Contact," Wear, Vol. 71, pp. 29-43 (1981).

11. Moore, D.F. "Principles and Applications of Tribology," Pergamon Press, New York (1975) p. 201.

12. Rowe, G.W., "Introductory Survey of Lubrication and Wear," Lubrication and Lubricants, E.R. Braithwaite, ed., Elsevier, New York, p.62 (1967).

13. Buckley, D.H., "The Use of Analytical Surface Tools in the Fundamental Study of Wear," Wear of Materials - 1977, W.A. Glaeser et al., eds., Am. Soc. Mech. Eng., p. 12, New York (1977).

14. Klaus, E.E. and H.E. Bieber, "Effect of Some Physical and Chemical Properties on Lubricants on Boundary Lubrication," Am. Soc. Lubr. Eng. Trans., Vol. 7, pp. 1-10 (1964).

15. Suh, N.P. et al. "The Delamination Theory of Wear," Elsevier, Sequoia, S.A. (1977). Wear, Vol. 44 (1977).

16. Blau, P.J., "The Role of Metallurgical Structure in the Integrity of Sliding Solid Contacts," Solid Contact and Lubrication, S. Cheng and L.M. Keer, eds., Appl. Mech. Div., Vol. 39, pp. 185-191, Am. Soc. Mech. New York, (1980).

17. Litvinov, F.N., and N.M. Mikhin, "The Influence of Surface Roughness on Wear Under Boundary Friction Conditions," Wear of Materials - 1979, K.C. Ludema, et al., eds., Am. Soc. Mech. Eng., pp. 243-245, New York (1979).

18. Stowers, J.F. and E. Rabinowicz, "The Mechanism of Fretting Wear," Jour. Lubr. Tech., Vol. 95F, pp. 65-70 (1972).

19. Ruff, A.W. and P.J. Blau, "Studies of Microscopic Aspects of Wear Processes in Metals, Nat. Bur. Stand. IR 80-2058 (ONR) (June 1980).

20. Kennedy, F.E. and D.A. Voss, "A Re-Examination of the Wear of Leaded Brass on Hardened Steel," Wear of Materials - 1979, Am. Soc. Mech. Eng., pp. 89-96, New York (1979)

21. Suh, N.P. and H.C. Sin, "On the Genesis of Friction and its Effect on Wear," Solid Contact and Lubrication, S. Cheng and L.M. Keer, eds., Appl. Mech. Div., Vol. 39, p. 170, Am. Soc. Mech. Eng., New York (1980).

22. Suh, N.P., "The Delamination Theory of Wear," Wear, Vol. 25, pp. 111-124. (1973).

23. Howell, H.G. et al.,, "Friction in Textiles," Butterworths Scientific Publ., London, or John Wiley and Sons, Inc., New York (1959) Plate I, to Face p. 11.

24. Cocks, M., "Role of Displaced Metal in the Sliding of Flat Metal Surfaces," Jour. Appl. Phys., Vol. 35, pp. 1807-1814 (1964).

25. Cocks, M., "Interaction of Sliding Metal Surfaces," Jour. Appl. Phys., Vol. 33, pp. 2152-2161 (1962).

26. Antler, M., "Processes of Metal Transfer and Wear," Wear, Vol. 7, pp. 181-204 (1964).

27. Antler, M., "Stages in the Wear of a Prow-Forming Metal," Am. Soc. Lubr. Eng. Trans., Vol. 13, pp. 79-86 (1970).

28. Ives, L.K., "Microstructural Changes in Copper Due to Abrasive, Dry and Lubricated Wear," Wear of Materials - 1979, K.C. Ludema et al., eds., Am. Soc. Mech. Eng., pp. 246-256 (1979).

29. Hirth, J.P. and D.A. Rigney, "Microstructural Models for Friction and Wear," Strength of Metals and Alloys, P. Haasen et al., eds., Vol. 3, Pergamon Press, New York,(1979) pp. 1483-1502.

30. VanDijk, J.A.B., "The Direct Observation in the Transmission Electron Microscope of the Heavily Deformed Layer of a Copper Pin After Dry Sliding Against Steel Rings," Wear, Vol 42, pp. 109-117 (1977).

31. Hirth, J.P. and D.A. Rigney, "Crystal Plasticity and the Delamination Theory of Wear," Wear, Vol. 39, p. 133 (1976).

32. Koba, H. and N.H. Cook, "Wear Particle Formation Mechanisms," Final Report - Contract N00014-67-A-0204-0054, NR229-003, Sponsored by Office of Naval Research, MIT, Dept of Mech. Eng., Materials Processing Lab, Cambridge, MA (May 1974).

## INITIAL DISTRIBUTION

Copies

1 ONR/Code 431

1 NRL/Code 6170

6 NAVSEA
- 1/SEA 05D
- 1/SEA 05H
- 1/SEA 05R
- 1/SEA 524
- 2/SEA 99612

12 DTIC

1 National Bureau of Standards

2 Massachusetts Inst. of Tech.
- 1 Prof. E. Rabinowicz/Rm 35-010
- 1 Dr. N. Saka/Rm 35-014

3 Rutgers College of Eng.
- 2 Prof. S. Weissmann
- 1 Prof. T. Tsakalakos

1 Mechanical Eng. Dept.
Columbia University
Prof. Coda Pan

2. Thayer School of Eng.
Dartmouth College
- 1/Prof. F.E. Kennedy, Jr.
- 1/V. Surprenant

CENTER DISTRIBUTION

| Copies | Code | Name |
|---|---|---|
| 1 | 01 | A. Powell |
| 1 | 012.3 | R. Allen |
| 1 | 28 | J.R. Belt |
| 1 | 283 | Dr. G. Bosmajian |
| 10 | 2832 | J.F. Dray |
| 15 | 2832 | S.A. Karpe |
| 10 | 5211.1 | Rept Distribution |
| 1 | 522.1 | Unclass Lib (C) |
| 1 | 522.2 | Unclass Lib (A) |
| 2 | 5231 | Office Services |

DTNSRDC ISSUES THREE TYPES OF REPORTS

1. DTNSRDC REPORTS, A FORMAL SERIES, CONTAIN INFORMATION OF PERMANENT TECHNICAL VALUE. THEY CARRY A CONSECUTIVE NUMERICAL IDENTIFICATION REGARDLESS OF THEIR CLASSIFICATION OR THE ORIGINATING DEPARTMENT.

2. DEPARTMENTAL REPORTS, A SEMIFORMAL SERIES, CONTAIN INFORMATION OF A PRELIMINARY, TEMPORARY, OR PROPRIETARY NATURE OR OF LIMITED INTEREST OR SIGNIFICANCE. THEY CARRY A DEPARTMENTAL ALPHANUMERICAL IDENTIFICATION.

3. TECHNICAL MEMORANDA, AN INFORMAL SERIES, CONTAIN TECHNICAL DOCUMENTATION OF LIMITED USE AND INTEREST. THEY ARE PRIMARILY WORKING PAPERS INTENDED FOR INTERNAL USE. THEY CARRY AN IDENTIFYING NUMBER WHICH INDICATES THEIR TYPE AND THE NUMERICAL CODE OF THE ORIGINATING DEPARTMENT. ANY DISTRIBUTION OUTSIDE DTNSRDC MUST BE APPROVED BY THE HEAD OF THE ORIGINATING DEPARTMENT ON A CASE-BY-CASE BASIS.